NUMERICAL MODELING OF UPHEAVAL BUCKLING OF INITIALLY IMPERFECT SUBMARINE PIPELINES BURIED IN LOOSE AND DENSE SAND

by

© RIYADUL ARMAN

A thesis submitted to the

School of Graduate Studies

in partial fulfillment of the requirements for the degree of

Master of Engineering (Civil)

Faculty of Engineering and Applied Science

Memorial University of Newfoundland

May, 2018

St. John's Newfoundland and Labrador Canada

ABSTRACT

Offshore pipelines are being utilized as one of the most convenient and efficient means of transporting oil and gas. Usually pipelines travel a long distance through a variety of soil conditions. The oil pipelines are operated at high temperature and high pressure to assure the flow and prevent wax formation inside the pipeline. The rise in temperature and internal pressure result in longitudinal expansion of the pipeline, which might cause lateral or upheaval buckling when the longitudinal movement of the pipe is restrained. The pipelines are generally buried to minimize heat loss and interference with other marine activities. For buried pipelines, soil offers resistances to lateral and upheaval buckling. The lateral soil restraint is higher than the uplift resistance and therefore the pipelines are more likely to experience upheaval buckling. Under these circumstances, upheaval buckling may occur that could cause failure in some cases. The resistance to upheaval buckling is provided by submerged weight of the pipe as well as the shearing resistance of the backfill soil. The two most popular burial methods of offshore pipelines, jet trenching and plowing, generally deposit the backfill soil in a loose to medium dense state; however, it could be subsequently densified due to environmental loading. Physical model tests show an increase and post-peak decrease of the uplift resistance with upward displacement of pipelines both for loose and dense sands. In the present study, finite element analysis is conducted to investigate the upheaval buckling behavior of submarine pipelines buried in loose and dense sands. The force–displacement behavior that considers the variation of uplift resistance for a wide range of upward displacement is studied. Different types of buckling (i.e., snap and stable bucking) for various initial imperfection ratios, burial depth and density of sand are thoroughly investigated. The importance of incorporation of the post-peak reduction of uplift soil resistance in the finite element analysis of the upheaval buckling is highlighted.

ACKNOWLEDGEMENTS

All praise to the Almighty, the Most Gracious, the Merciful and the Kind.

I would like to expresses my sincere gratitude to my supervisor Dr. Bipul Hawlader, Professor, Memorial University of Newfoundland (MUN), Newfoundland, Canada and to my co-supervisor Dr. Ashutosh Dhar, Assistant Professor, Memorial University of Newfoundland (MUN), Newfoundland, Canada for their continuous support, excellent guidance, motivation, patience, comments, remarks and engagement through the learning process of this dissertation. Without their guidance, this thesis would not have been possible.

I would also like to sincerely thank my colleagues, Dr. Kshama Roy and Mr. Naveel Islam, for their invaluable advice, suggestion, assistance and time. Thanks to Mr. Diponkar Saha and Mr. MD Anan Morshed for helping me with their printing resources.

I am also indebted to my friends in St. John's, Newfoundland for their support, encouragement and exuberant memories. Special thanks to all the faculty and staff members in the Faculty of Engineering and Applied Science at MUN.

Finally, I would like to express my gratitude to my family for their endless encouragement, strength and support.

This thesis is dedicated to them all.

Table of Contents

List of Tables

List of Figures

List of Symbols

A	cross-sectional area of the pipe
c_f	pipe coating factor
D	external pipe diameter
EI	flexural rigidity of pipe
F_{ap}	peak axial resistance
F_{bp}	peak vertical bearing resistance
f_p	simplified uplift factor
F_v	uplift resistance
F_{vp}	peak uplift resistance
F_{vr}	residual uplift resistance
H	distance of the pipe center from the ground surface (soil cover)
H/D	burial depth
H_t	distance of the pipe crown from the ground surface
K_0	coefficient of earth pressure at rest
K_d	downward stiffness
L	buckling length

L_0	initial imperfection length
M, N	degrees of freedom
N_q, N_γ	bearing capacity factor
q	submerged self-weight of pipe per unit length
R	reduction factor
T_{cr}	critical temperature
T_s	safe temperature
u	axial displacement
UHB	upheaval buckling
u_p	displacement at peak axial resistance
v	vertical displacement
$\tilde{v}$	initial imperfection ratio
v_0	initial imperfection amplitude
v_b	displacement at peak vertical bearing resistance
v_f	buckle amplitude
v_i	initial vertical imperfection distance from the horizontal datum
v_p	displacement at peak uplift resistance

v_r displacement at residual uplift resistance

α coefficient of linear thermal expansion

γ unit weight of the soil

γ' effective unit weight of the soil

θ inclination angle of the slip surface

ϕ angle of internal friction

φ_a axial friction co-efficient

ϕ_μ axial interface friction angle between pipe and soil

ΔT temperature rise

ΔT_a allowable temperature rise

Chapter 1

Introduction

1.1 General

Pipeline network is one of the main means of transporting oil and gas both in offshore and onshore environments. Usually pipelines are buried to prevent any kind of mechanical damage because of third party (e.g., trawling gear) activities and to provide thermal insulation to assure flow at high pressure and high temperature (Schupp 2009). During manufacturing and installation process, pipelines suffer from structural imperfections such as initial out-of-straightness. Moreover, irregularities of the seabed profile also preclude the perfect lie of the pipeline during the laying process (Taylor and Gan 1986). Because of the changes in temperature and internal pressure during operation, compressive loads are typically induced in pipelines by soil resistance to axial extensions. In axially constrained high-pressure and high-temperature pipelines, the initial out-of-straightness (imperfection) causes further upward deformation weakening the resistance of pipeline against the global upheaval buckling (UHB) (Fig. 1.1). Together with temperature and pressure induced expansion, initial out-of-straightness may trigger a global UHB. Therefore, UHB is one of the main considerations in offshore buried pipelines.

The UHB is considered as one of the most common types of instabilities of buried offshore pipelines and a huge concern from the design point of view (Williams 2014). Several field evidences indicate that UHB results in significant vertical upward displacement of the initially buckled section—sometimes even protruding the seabed surface (Palmer et al. 2003). During the first 7 months after it was brought into service, a buried pipeline in the North Sea was displaced

vertically through the soil cover and then protruded a maximum vertical distance of 1.1 m above the seabed (Nielsen et al. 1990) (Fig. 1.2). However, the figure does not show the soil cover and the vertical distance of the pipe from the ground surface since the pipe is exhumed from the field.

The uplift resistance of the buried pipe is provided by the submerged weight of the pipeline, the bending stiffness of the pipeline and the backfill soil cover (Bai and Bai 2014). Since the submerged weight and the bending stiffness of the pipeline remains constant (assuming the cross section of the pipe does not change due to buckling), a proper understanding of the UHB phenomenon and the force–displacement relationship of soil is a prerequisite for analyzing the upheaval buckling. Calculation of the required burial depth to prevent the pipeline from damage due to upheaval buckling is a key design challenge (Bransby et al. 2013). To bury a pipeline, a trench is cut and after the completion of laying operation usually the trench is backfilled with soil cover (Fig. 1.3). Jet trenching and plowing—the two most widely adopted burial methods of offshore pipelines—usually deposit backfill soil in a loose to medium dense state (Williams 2014), although the environmental loadings might eventually densify the soil. Therefore, a pipeline with an initial imperfection and buried in loose and dense sands is the focus of the present study.

1.2 Scope of the research

In practice, the stability of a pipeline against UHB is checked by employing the uplift resistance of the soil in the form of force–displacement curves in the FE model. Following the recommended procedure provided by the design guideline and based on the analysis result, a safe burial depth is determined. It is evident in physical model tests and numerical analysis that post-peak reduction of uplift resistance is a common phenomenon of loose (Wang et al. 2012) and dense sand (Roy et al. 2017 a, b). Most of the design guidelines (e.g., ALA 2005) and previous numerical studies (e.g., Yimsiri et al. 2004) mainly focused on the peak uplift resistance. However, DNV (2007)

recognized the importance of post-peak reduction of uplift resistance for medium to dense sands. For dense sand, DNV (2007) recommended four linear line segments for the force–displacement relation of the uplift soil resistance, in which the uplift resistance reduces linearly from the peak to a residual value with an increase in upward displacement and then remains constant at large displacement. However, for loose sand, a tri-linear model is recommended by DNV (2007) in which the uplift resistance remains constant after the peak. Nevertheless, the force–displacement curve proposed by DNV (2007) is different from the force–displacement curve obtained from the laboratory test results (Chin et al. 2006; Cheuk et al. 2008). Therefore, based on literature review, the effect of post-peak reduction of uplift soil resistance on UHB is investigated in this study.

1.3 Objectives

The main purpose of this study is to perform FE analysis to examine the role of post-peak reduction of uplift soil resistance on UHB of pipelines buried in loose and dense sands. The key temperatures under which a pipeline could be operated without UHB is also examined. The FE model is first validated against analytical solutions, as proposed by Taylor and Gan (1986). FE analyses are then performed for buried pipes with varying initial imperfection ratios, post-peak reduction of uplift resistance, burial depths, seabed stiffness and pipe diameters.

The followings are the main objectives of this research:

- Develop a FE modeling technique to capture different modes of buckling;
- Perform a parametric study to understand the rationale of current industry practice of neglecting the post-peak reduction of uplift soil resistance in the analysis of UHB;
- Find a pragmatic design temperature for different modes of buckling; and

- Provide a simplified a design chart that can be used to find the required burial depth for of a pipeline under given operating conditions.

1.4 Outline of the thesis

The thesis consists of five chapters. The outline is as follows:

- **Chapter 1** highlights the background, scope and objectives of the research work.
- **Chapter 2** contains a comprehensive literature review. However, the review covers the studies mainly related to the upheaval buckling analysis of the offshore pipelines buried in loose and dense sand, which is the focus of the current study.
- **Chapter 3** presents finite element analysis of upheaval buckling of submarine pipelines with initial imperfection. This chapter has been published as a technical paper in the 70th Canadian Geotechnical Conference, GeoOttawa2017, Ottawa, Ontario, Canada, October 1–4, 2017.
- **Chapter 4** presents parametric study on the initially imperfect pipelines buried in loose and dense sand and some design implications.
- **Chapter 5** summarizes the outcomes of the research and recommendations for future studies.

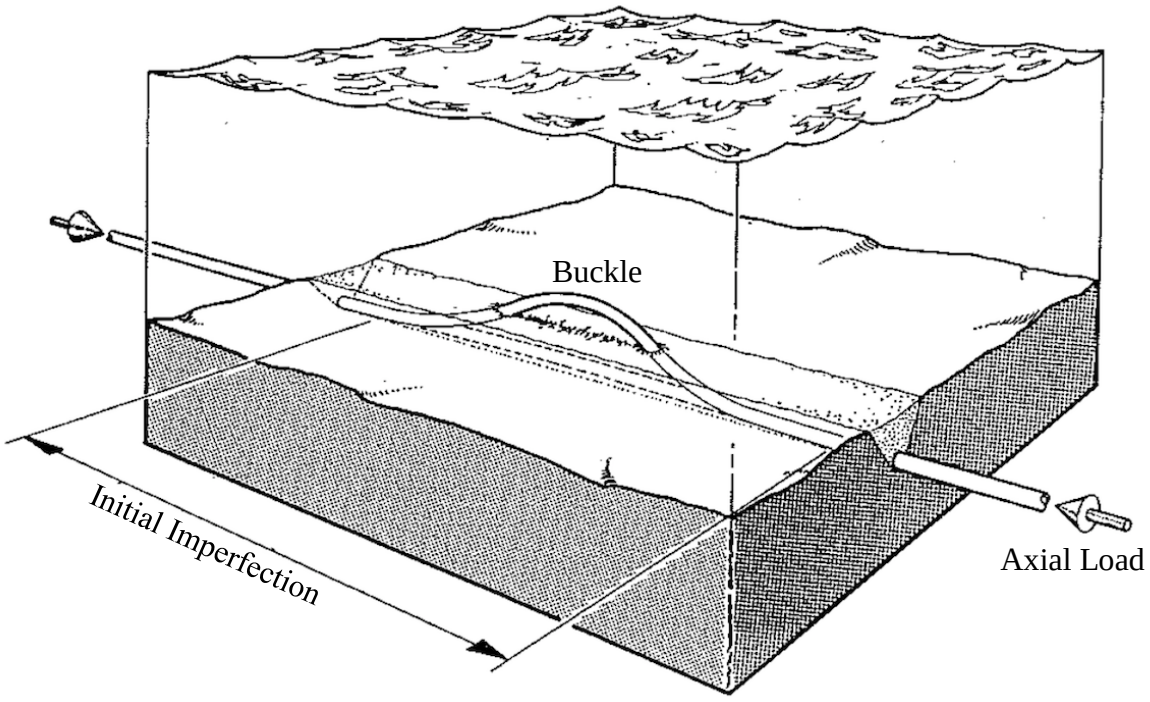

Figure 1.1: Schematic view of upheaval buckling of a buried pipeline (after Pedersen and Michelsen 1988)

Figure 1.2: Pipeline section which has suffered upheaval buckling in the Danish sector of the North Sea (after Nielson et al. 1990)

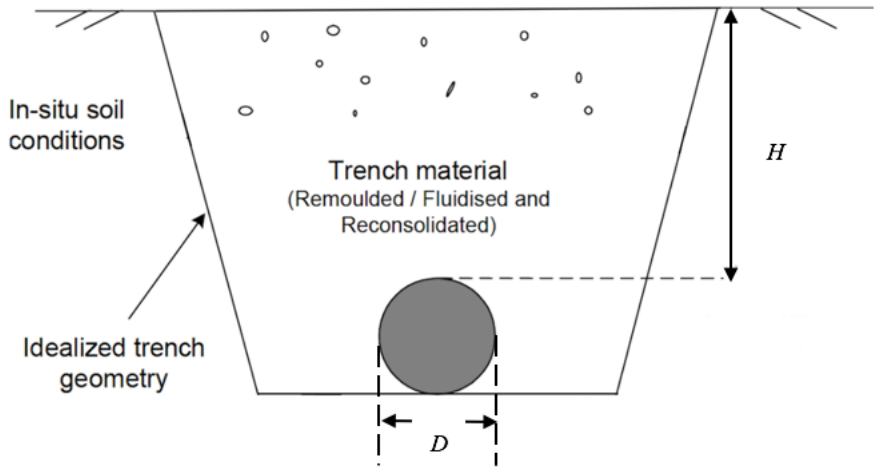

Figure 1.3: Pipeline trenched and backfilled with natural excavated soil

Chapter 2

Literature Review

2.1 Introduction

In the last 40 years, many researchers conducted experimental, analytical and numerical studies on UHB of pipelines. These studies can be categorized into two major categories. One group of researchers is mostly concerned on the structural response of pipeline for the given geotechnical parameters and thermal loading condition, while the other group is interested in geotechnical response when a pipeline is subjected to vertical and axial displacements. The earliest documented UHB of a subsea pipeline is associated with the Maersk Oilog Gas AS'Rolf pipeline and the incident occurred in 1986 (Nielsen et al. 1990) (Fig 2.1). After this incident, UHB became a hot topic and a joint industry study program was carried out by Shell International Petroleum Maatschappij (SIPM) in 1988–1990 in collaboration with other major European oil companies. Summaries of the analysis results were published in the 1990 Offshore Technology Conference (OTC) (e.g., Guijt 1990; Klever et al. 1990; Palmer et al. 1990). Guijt (1990) also mentioned that at least five UHB event took place in the North Sea, three of which happened in 1989, accompanied by remarkable cost penalties. This chapter provides a brief overview of previous research relevant to the present study.

2.2 Analytical and empirical methods

To buckle a straight pin-ended column, which is also known as Euler column, the required compressive stress is inversely proportional to the square of the slenderness of the column. Over adequately large lengths, the pipelines are always very slender. Submarine pipelines often carry

hydrocarbons that have a higher temperature than the surrounding environment. Usually, the prospective thermal expansion is prevented by friction between the surrounding soil of the seabed and the pipeline. As a result, large compressive axial forces develop in the pipeline, which can cause buckling of the pipeline. Allan (1968) carried out analytical studies on UHB of an axially compressed frictionless elastic strip and found that the magnitude of the critical load is profoundly influenced by the degree of initial deflection or imperfection. Similar challenges were experienced by the railway industry for railway tracks. Kerr (1974, 1978) summarized the literatures that are very closely associated with the thermal buckling problems in pipelines. Hobbs (1981, 1984) presented a basic model of buckling (Fig. 2.2) and analyzed both lateral and upheaval buckling problem of a long straight perfectly elastic pipe with a small slope when it reached critical buckling condition and concluded that lateral buckling tends to occur at a lower axial load than UHB unless the pipe is buried. To express the deflected shape of the buckled part of the pipeline, a linear differential equation was proposed by Hobbs (1981). The pipeline is treated as a beam-column under a uniform lateral load. The bending moment at the lift-off point is assumed to be zero. Figure 2.3 illustrates the vertical buckling results for a typical pipeline with a practical range of friction coefficients. Hobbs (1984) made clear that the equilibrium path from A to B is unstable, which is due to the assumption of fully mobilized friction even for vanishingly small displacement. The equilibrium path from B to C shows the relationship between the buckle length and the temperature for a pipeline with small imperfection. To date, the temperatures versus length of buckle and amplitude curves are considered as the classical results in pipeline thermal buckling analysis. However, he did not consider the initial out-of-straightness in the proposed model and recommended to carry out further numerical work on the effects of initial imperfections. It is evident from the field condition that the in situ shape of a buried pipeline is far from being straight.

Taylor and Gan (1986) presented a set of analysis incorporating structural imperfections and deformation dependent axial friction response. They pointed out that initial imperfection ratio v_0/L_0 is an essential parameter which is related to the out-of-straightness of the imperfection (Fig. 2.4). Palmer et al. (1990), based on numerical analysis, proposed a semi-empirical simplified design method and defined two dimensionless parameters for the buckling wavelength and the critical axial force. The parameters are dimensionless maximum download and dimensionless imperfection. They found that the specific shape of an imperfection does not affect the general form of the parameters. It only affects the coefficients of the parameters. The buckle was assumed to be completely symmetric in all the previous studies. For the first time, Ballet and Hobbs (1992) investigated the likelihood of asymmetric buckling in the prop case and pointed out that for asymmetric mode critical temperature is lower than the symmetric mode, which may be significant from the design point of view. Taylor and Tran (1993) proposed a mathematical model, suitable for design application, for a pipe with a prop imperfection which is continuously or discretely buried employing fixed anchorages. Taylor and Tran (1996) summarized three basic types of initial imperfection for subsea buried pipelines (Fig. 2.4). In the first case, which is known as the empathetic model, the pipeline stays in continuous contact with seabed undulations in an otherwise idealized horizontal and straight line. The prop imperfection occurs when an isolated rock is located immediately below the line or another pipeline crosses underneath. The last case occurs when the voids of the prop model get infilled with the soil due to environmental action. The trench step or free span gap or an angularly mismatched field joint can also exist although they are less common. The initial imperfection of the seabed results in initial deformation in the pipeline. When the temperature rises, UHB may take place in the pipeline due to the presence of the initial imperfection. It was assumed that the pipeline was stress-free-when-initially deformed. They also

presented the mathematical models together with the key conceptual and physical problems for each type of initial imperfection. All models assume that the system is symmetric, the seabed is rigid, deformations are relatively small and material properties are linear elastic. Hunt and Blackmore (1997) examined the effects of asymmetric bed imperfections, characterized by a step, and to solve the standard 4th-order linear ordinary differential equation employing a shooting method (Fig. 2.5). After comparing two typical types of imperfections, the prop and the step, they concluded that a more severe destabilizing role can be accredited to the step than the prop. Croll (1997) reinterpreted the classical analysis by Martinet (1936) and extended the approach providing a more direct and simplified model for the UHB analysis of imperfect pipelines. Collberg et al. (2005), as a part of the HotPipe Project, described the procedures and criteria for the pipeline design and covered design scenarios of the DNV-RP (2007), including the pipelines exposed on even seabed, where thermal expansion may be accommodated by lateral snaking; pipelines on uneven seabed corresponding to even seabed; and pipelines on bottom of trenches/covered by natural or artificial backfill. Goplen et al. (2005) implied that the most significant factor in UHB of buried pipelines is the uncertainty in pipeline configuration and uncertainty in pipe–soil interaction. They presented the background of the related uncertainties and the proposed soil capacities and for both uplift resistance and downward resistance in cohesive and non-cohesive soils. They also related these soil models with the design requirements to UHB including functional requirements. Wang et al. (2011) presented a theoretical solution of UHB for different types of initial imperfections. They applied this analytical tool to predict the occurrence of UHB in Bohai Gulf and proposed different protection measures. Liu and Yan (2012) gave an overview of the history of the theoretical and experimental studies of the UHB of the subsea pipelines. Liu et al. (2013) studied the continuous support model of initial imperfection and introduced an

analytical solution for the thermal UHB. Then the analytical methodology was applied to analyze a pipeline in Bohai Gulf, and they concluded that the buckling temperature depends on the amplitude of initial imperfection. Karampour et al. (2013) studied the lateral and upheaval buckling of pipelines and proposed analytical solutions for the UHB and compared the response of three types of localized initial imperfections namely fully contact imperfection, point imperfection and infilled prop. The influence of the shape of initial imperfection on the critical force was pointed out. In addition to the studies above, some researchers put emphasis on the upheaval creep of the subsea buried pipelines; a phenomenon caused by the variations in temperature and pressure loading during operation and results in gradual upward movement of imperfect pipeline sections, which eventually increases the susceptibility to snap buckling. Pedersen and Jensen (1988) and Nielsen et al. (1990) proposed a design criterion for the upheaval creep.

2.3 Physical tests

Usually, all the experimental studies provide essential empirical data along with intuitionistic and visual thermal buckling modes of the subsea pipeline. Besides, theoretical solutions can be verified from different aspects. In addition, the experimental studies reveal the limitations of the available theories and consider some design details of pipeline buckling, which the existing theoretical studies have not taken into account. All the experimental studies demonstrate more vivid and realistic upheaval modes of the pipelines. It is also confirmed that the available theories are applicable and valid to some extent. However, UHB experimentation of pipeline is both costly and complex; thus, in the open literature only a limited number of papers related to UHB experiment can be found. Moreover, it should be noted that the buckle length involved with full-scale testing is considerably high which makes this kind of experiment very difficult. Also, field evidences

show buckle amplitudes of 0.5 m–2 m along with wavelengths of 24 m–70 m (Liu et al. 2013). Allan (1968) carried out an experimental study of buckling of an axially compressed elastic strip. Applying a uniformly distributed force, it was held down against a flat, rigid base. He introduced a "prop" imperfection deliberately underneath the initially straight elastic strip and observed that the height of the deliberately introduced "prop" imperfection influences the buckling load of the initially straight elastic strip. The experimental setup is shown schematically in Figure 2.6(a). He also solved the governing equations of an elastic strip with appropriate boundary conditions, which was loaded simultaneously by transverse and axial forces, and then proposed a simple buckling formula. Allan (1968) observed good agreement between the predictions of the formula and experimental test results (Fig. 2.6(b)). Baldry (1973) undertook a set of experiments of a similar type where he also introduced small "prop" imperfections between the flat base and the strip to commence buckling. By supporting the strips on many uniform rollers, he eradicated friction between the flat base and the strips. Moreover, for imperfections as small as 3% of the thickness of the strip, he found experimental reconfirmation of Allan's buckling formula. Maltby and Calladine (1995a, b) conducted small-scale experimental studies and described several aspects of UHB for a thin-walled steel pipe of 6 mm diameter and 5 m length, buried in artificial soil and suggested some critical axial force formulas for the initially imperfect pipelines. Using an electrical remote-sensing device, the vertical and horizontal profiles of the pipe were determined. Axial load was applied to the pipe through internal oil pressure and a screw arrangement, and the transverse horizontal load was imparted by a string and pulley. Unlike Allan (1968) and Baldry (1973), they used a slender tube rather than strips. Several tests were performed under both transverse and axial loading and cyclic axial loading, and the results demonstrate that the UHB is sensitive to the small imperfections and the force–displacement relation of the soil is nonlinear.

The first paper on pipeline thermo-mechanical buckling published in 1993. Raoof and Maschner (1993) carried out a small-scale test in a rig which was capable of testing both lateral and vertical buckling of 7 m long pipelines heated up to 100°C. For various magnitudes of initial point imperfection, they presented the findings of buckling tests in the vertical mode which was carried out on 16-mm-diameter copper/nickel pipes. Based on the comparisons between theoretical results and the test data, several conclusions are made demonstrating the limitations of the existing theories (Fig. 2.7). Taylor and Tran (1996) designed and constructed a complex and novel experimental rig with regards to the crucial upheaval state which can test both isolated prop and contact undulation imperfection topology. A 6-m long seamless ferritic stainless steel pipe of 9.53-mm O.D. with fixed anchor restraints was used in test and the necessary thermal action was provided by the heated water. The water heater/cooler allowed to set the discrete thermal increments to 0.1 °C accuracy. Prop imperfection was replicated by a single blade and in-filled imperfection was simulated by infilling the voids of the prop with a sand-coated balsa framework (Fig. 2.8 (a)). After comparing the experimental data with theoretical models (Fig. 2.8(b)), satisfactory theoretical/experimental correlation was obtained concerning the definition of the crucial UHB state under adequate imperfection. Experimental data suggests that while the empathetic model is robust, the other models afford more economic, yet conservative, data for the larger imperfection cases. Therefore, designers should avert the infilling of prop voids wherever possible because they play an important role during the pre-upheaval flexural energy release in the isolated prop case (Taylor and Tran 1996).

Usually, vertical buckling mode, the inertial loading, and the axial friction force coefficient along with the geotechnical parameters are related to the UHB. Thus, for the axial friction force and the uplift resistance, it is necessary to develop physically relevant pipe–soil interaction characteristics.

According to many researchers, the pipe–soil interaction characteristics also have a significant effect on the UHB behavior of submarine pipeline. In 1981, the first work in the field of pipe–soil interaction was published (Hobbs 1981). Anand and Agarwal (1980) undertook small-scale model and large-scale prototype experimental studies. They calculated the frictional resistance between concrete-coated pipes and surrounding soil in the longitudinal as well as the lateral directions and to design the pipeline for lateral stability. Since 1985, several papers have been surfaced on submarine pipeline frictional characteristics which are also related to buckling. Taylor et al. (1985) performed a small-scale test on the sand using 48.3-mm outer diameter (O.D.) steel pipe with 3.2-mm wall thickness in view of North Sea conditions. They conducted pull-out tests and axial friction tests and proposed a semi-empirical design formula based on the force–displacement relationship of the pipe for different burial depths. Friedmann (1986) undertook horizontal and vertical pull-out tests for pipeline buried in sand and soft clay and presented the force–displacement relationships of the pipe for different outside diameter and length with varying burial depth. Schaminee et al. (1990) conducted a full-scale laboratory test on a 10.2 cm (4-in.) pipe buried in cohesive and cohesionless soil and presented the results of the uplift and axial resistance. They pointed out that the uplift resistance includes the friction or shear force component and the weight, for cohesionless soils.

2.3.1 Model tests for uplift resistance

Trautmann et al. (1985) carried out an experimental study on 1.2-m long and 102-mm diameter steel pipe buried in the Cornell filter sand (dense, medium and loose conditions) to observe the effects of soil density and depth of burial on the peak force imposed on the pipe and the displacements at which they are mobilized. They compared the results with several published models and found that, while the results of medium and dense sand comply well, the measured

values of uplift resistance are much lower than predicted for loose sand. Finally, they presented a simplified procedure that can be employed to the design of buried pipelines. Based on the test results, Friedmann and Debouvry (1993) presented empirical formulas to calculate the maximum axial resistance and vertical resistance. Dickin (1994) performed centrifuge tests on 213-mm long stainless steel pipes with 25-mm diameter and 213-mm long steel strip anchors with 25-mm width buried in dry Erith sand (Fig. 2.9). The tests were carried out in both loose and dense sand packing under 40 times of gravitational acceleration. He observed the influence of pipe diameter, burial depth and backfill density on uplift resistance. However, no significant difference between the behavior of buried pipes and strip anchors was found, which justifies the application of anchor theory to the buried pipe. Bransby et al. (2002) conducted laboratory and centrifuge tests using 32-mm and 48-mm diameters and 498-mm long pipes, buried in loose and dense Silica sand and gravel, to observe the uplift behavior of buried offshore pipelines. However, though loose sand tests were carried out both in the laboratory and the centrifuge, dense sand tests were only performed in the laboratory. From the test results they found that due to shear induced volumetric response, dense and loose sand undergo different deformation mechanisms after the mobilization of peak uplift resistance. Bai and Bai (2005) presented a summary of the calculation method of the maximum breakout force of pipe in the lateral and axial direction of soil. According to ALA (2005), soil loading on the pipeline can be represented by discrete nonlinear springs (e.g., elastic-plastic, multilinear). Based on pipeline response from the field experimental investigations and laboratory tests for shallow buried pipelines with uniform soil conditions, this guideline recommend how to define the maximum soil spring forces and associated relative displacement required to develop these forces. Nevertheless, the accuracy of the results calculated relies highly on empirical value since design conditions of the buried pipeline are quite different, mostly for

changeable soil conditions. Thus, to predict the soil resistance with pipeline movement experimental studies are still essential. Chin et al. (2006) undertook centrifuge uplift tests on a 305-mm long smooth pipe with 19-mm diameter which was buried in uniform Congleton sand at different depths ranging from H/D = 3–7.7, where H is the depth of pipe measured from ground surface to the center of the pipe and D is the diameter of the pipe, and examined the uplift behavior of pipelines both in loose and dense soil condition. They also performed a comprehensive literature survey to review analytical models used to predict the peak uplift resistance. Based on the test results they reported that peak uplift resistances are mobilized within small pipe displacements and increases with embedment and soil density. By comparing the test results with analytical models and other test results they demonstrated that there is no one model that can be used to predict uplift resistance (Fig. 2.10). Cheuk et al. (2008), employing a novel image-based deformation measurement technique, described the mechanisms by which uplift resistance is mobilized in Silica sand both in loose and dense conditions. They showed that the peak uplift resistance is mobilized through the formation of an inverted trapezoidal block, bounded by a pair of shear bands, exhibiting strain-softening behavior. They found that the shear band inclination is dependent on the soil density, and thus dilatancy. Shear bands form after the peak resistance and revealing strain-softening behavior. At large pipe displacements, depending on the soil density and particle size, either a combination of a flow-around mechanism and a vertical sliding block mechanism near the pipe or a localized flow-around mechanism without surface heave was observed (Fig. 2.11). Wijewickreme et al. (2009) performed full-scale axial pullout tests to investigate the performance of steel pipelines subjected to relative soil movements, which were buried in loose and dense sands. The test results show that, in case of loose dry sand, the measured axial loads are comparable to those predicted using guidelines commonly used in practice (e.g., ASCE 1984). However, in dense

dry sand, the peak values are several-fold higher than the predictions from guidelines. They suggested that for pipes embedded in soils that are prone to significant shear-induced dilation, the use of the coefficient of lateral earth pressure at rest (K_0) to measure axial soil loads, using equations recommended in guidelines, should be dealt with caution. Wang et al. (2010) carried out a series of full-scale and centrifuge tests on 100-mm and 258-mm diameter pipes buried in loose and saturated dense Fraction E sand to investigate the necessity of discounting the shear contribution from the uplift resistance for *H/D* ratios less than 1. From the test results, they did not find any rationale behind this industry practice of neglecting shear contribution of uplift resistance for lower *H/D* ratios. They also examined the uplift mechanism through Particle Image Velocimetry (PIV) method which illustrates the deformation mechanism in an intuitively visible manner. Gao et al. (2011) carried out a series of large-scale model tests on fine sand to obtain the force–displacement relationships under different test conditions. For different burial depths, the pipe segments were pulled out in uplift and axial directions. For loose sand, the effect of post-peak reduction of the uplift soil resistance on UHB is analyzed using FE modeling. Saboya et al. (2012) performed small-scale pullout tests in centrifuge at 10g for different sand densities, two geogrid widths and three burial depths, and demonstrated that the post-peak behavior is highly improved for pipes anchored in geogrid that allows the pipe to withstand considerable displacements without loss of resistance.

Though parameters vary, based on the tests results, Fig. 2.12 depicts the curves that schematically represent the force–displacement relationship of the pipe buried in loose and dense sand, respectively.

2.4 Numerical analyses

Because of the substantial cost involved with physical model tests and taking the advantages of recent advancement of computing facilities, the application of numerical simulations (e.g., FE analysis) on UHB has been well documented in several studies. Sophisticated finite element methods have been used to model pipeline buckling taking into account many important features. Moreover, the numerical analysis also has the advantage to be very quick in computer time and inexpensive and can be done over and over again at will, to simulate pipeline along its route with varying soil conditions and operating temperatures. The soil around the pipeline influences the response of pipelines and therefore pipe–soil interaction has caught special attention. Lyons (1973) carried out small- and large-scale tests on sand and large-scale tests on soft clay. To predict the resistance to sliding, he developed a FE model. The results illustrate that pipelines do not settle into sand but do settle into clay, causing different sliding behavior in different soil. Afterwards, in the literature, researchers presented many computational programs on soil–pipe interaction problems. The FE methods have been widely used, including the 1-D beam model (Zhou and Murray 1993, 1996; Lim et al. 2001) and 3-D shell model (Selvadurai and Pang 1988). In numerical models, the boundary element models are also applied (Mandolini et al. 2001). Various material models have been employed for simulating the soil behavior. Among those, the most popular models are elastic and elastoplastic models. Nowadays, commercial FE packages such as PLAXIS, Abaqus, ADINA and ANSYS are being used to analyze the effects of non-linearity in soil–pipe interaction, soil properties, pipeline material behavior and and large displacements. Different numerical tools, such as PIPLIN-III, PlusOne, PIPSOL, ABP, and UPBUCK (Klever et al. 1990), have been utilized for various situations in the last 20 years for pipeline UHB analysis. For instance, one can model quickly (computational time) a considerable length of pipeline and

examine the overall structural behavior for different load conditions using Abaqus (Hibbitt et al. 2000; Gao et al. 2011). Considering both nonlinear geometry and material effects, Shaw and Bomba (1994) developed a FE analysis method to study the pipeline response under UHB conditions. Case study results illustrate that the temperature rise corresponding to the pipeline buckling is much lower for nonlinear material behavior than linear material behavior. According to Zhang and Tuohy (2002), the simplified approaches can be not only overly conservative but also may fail to identify the vulnerable features and the underlying risk of UHB in some cases. This can lead to dreadful economic consequences. They investigated a case study of a trenched but unburied 152-mm (6.0-in.) diameter pipeline for UHB using static FE analysis. It demonstrates that FE methods can be employed for more realistic evaluation of the behavior of offshore flowline UHB potential. Yimsiri et al. (2004) conducted FE analysis of lateral and upward pipe movements using the Mohr-Coulomb and Nor-Sand models to calculate the peak force and also to investigate the transition from shallow to deep failure mechanisms. Finally, based on FE analysis results, a design chart for deeply buried pipelines has been constructed. Villarraga et al. (2004) presented a method for analyzing buried pipelines with initial imperfections and analyzed a problem idealizing it as a 2-D problem. During buckling analysis, they addressed pipeline imperfections only as perturbations. However, for analyzing the UHB of high-temperature and high-pressure pipelines, the use of simplified analytical models has been a standard approach for a long time. FE analysis of pipeline uplift was conducted by Vanden Berghe et al. (2005) and Newson and Deljoui (2006). Vanden Berghe et al. (2005) employed PLAXIS, a 2-D FE software, to study the soil behavior during upward displacement of a pipe buried in loose sand and presented the comparison between FE results and theoretical (White method) results (Fig. 2.13). The results depict that pipeline uplift in loose sand is governed by “local” failure and a “flow around” mechanism, and the wedge failure

mechanism, which is basis of simplified methods, are not suitable. For soil–pipe interaction, a numerical methodology is presented by Rubio et al. (2007), which not only contemplates the full 3-D geometry and elastoplastic material behavior but also considers the effect of large displacements. Using a penalty formulation, the contact conditions are imposed, which is found very effective in a case studied. Jukes et al. (2009) gave an overview of the latest advancement of the numerical tools and implied that for the design and simulation of pipelines under extreme conditions advanced numerical tools are very suitable. A highly nonlinear FE program named SIMULATOR is developed, which uses Abaqus as the FE engine. The SIMULATOR analysis is a static large deflection analysis and includes all relevant non-linearities such as large deflection and large rotations, elasto-plastic pipe materials interpolated over relevant temperature ranges, and non-linear pipe-soil interactions. Project example demonstrates that the developed program can be utilized to carry out complex design cases such as local modeling of pipelines, global analysis, and selection of pipeline route. Wang et al. (2009) described the FE tool that was created as part of the SIMULATOR, J. P. Kenny's in-house pipeline analysis package, developed over the Abaqus platform, which can simulate pipeline UHB for different pipeline configurations under various conditions. Gao et al. (2011) used Abaqus for analyzing the foregoing case in Bohai gulf which was based on a large displacement formulation for the pipe. They adopted nonlinear soil spring based on experimental test data. The length of the model was taken as 500 m with a small vertical imperfection, and the ends were fully fixed. The temperature and internal pressure along the wall acted as loads on the pipeline. They showed that pipeline capacity against thermal buckling decreases with increase in initial imperfection height and increases with burial depth. Zeng et al. (2014), based on dimensional and FE analysis, proposed some formulas for the critical axial forces which include the out-of-straightness directly and integrally unlike traditional formulas. They also

illustrated the application of these formulas. Wang et al. (2015) studied the UHB of the unburied subsea pipeline using FE analysis and compared the results of 2-D and 3-D static and dynamic analysis. Zhang and Duan (2015), using FE analysis, studied the UHB behaviors of eight groups of pipeline segments with different imperfection shapes and out-of-straightness and defined a new parameter to express different imperfection shapes. Finally, they proposed a universal formula to calculate the critical axial force. Jung et al. (2016) presented a methodology to evaluate multidirectional force-displacement relationships for soil–pipeline interaction analysis and design by employing FE model.

Literature reviews insinuate that though FE analysis for the UHB of offshore pipelines has progressed rapidly over the last few years, a FE analysis for pipeline thermal buckling, which can simulate the pipe initial imperfections, realistic soil-pipe interaction, the temperature field and the stress field at the same time, is underdeveloped.

2.5 Summary

The prediction of UHB resistance for buried pipelines has been a challenge since huge uncertainty and randomness in the cover material is involved because of many factors. Most of the previous analytical and empirical techniques for UHB analyses have been developed for idealized and simplified conditions. Moreover, most of the researchers only examined the peak uplift resistance of buried pipelines and did not consider the effect post-peak reduction of uplift resistance for thermal UHB. Therefore, in this study, the numerical modeling technique is developed to get better insight into the effect of strain-softening and post-peak reduction of uplift resistance on structural response of pipelines.

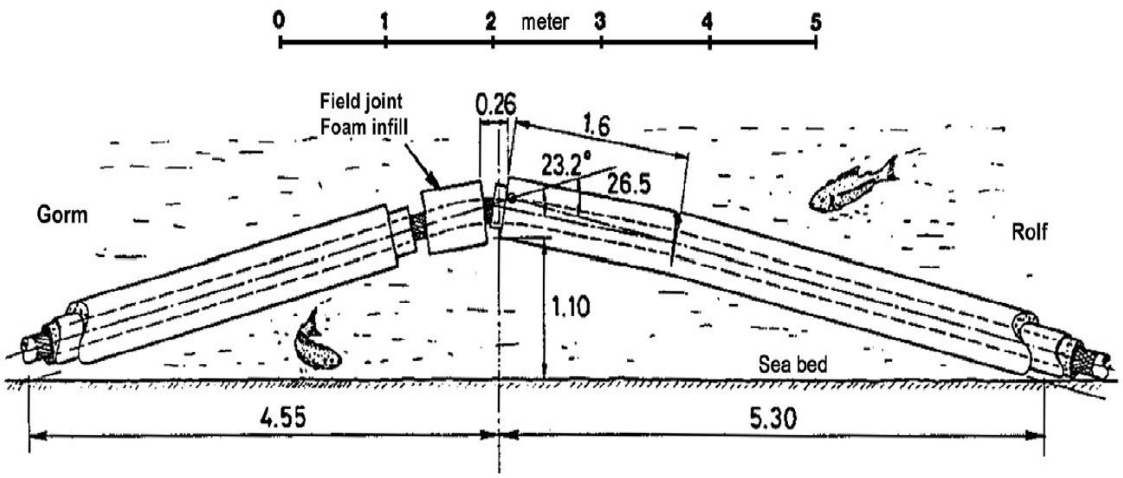

Figure 2.1: Geometry of the exposed Rolf A/Gorm E pipeline (after Neilsen et al. 1990)

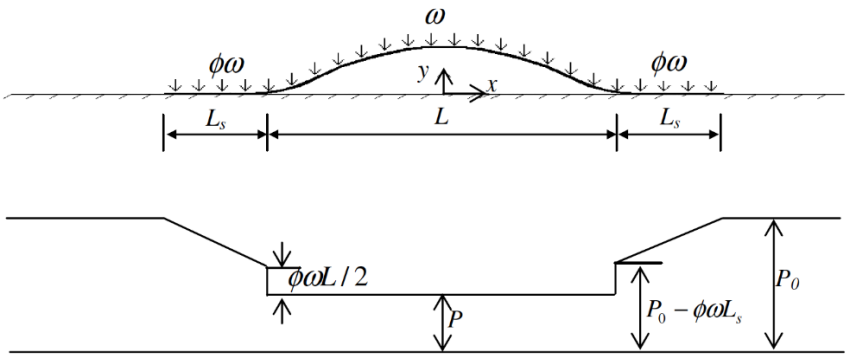

Figure 2.2: Force analysis of a pipeline section with vertical buckling (after Hobbs 1981)

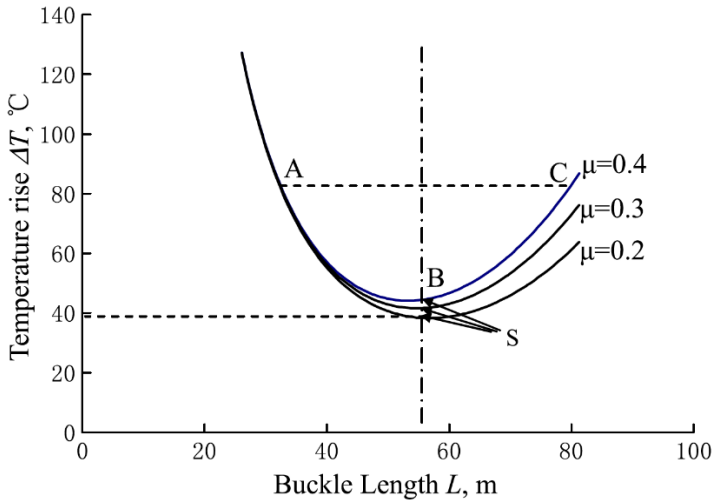

Figure 2.3: Buckle wavelength versus friction coefficient of foundation (after Hobbs 1984)

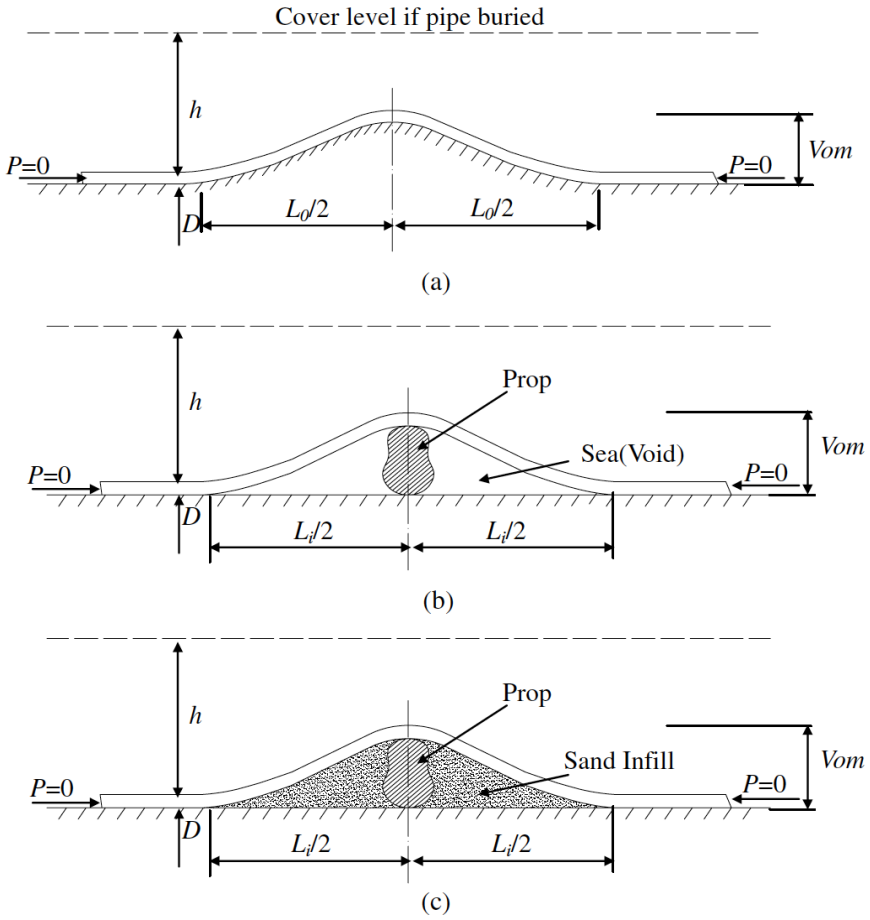

Figure 2.4: Typical imperfection configurations (after Taylor and Tran 1996)

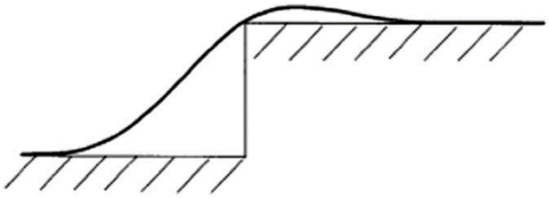

Figure 2.5: Step imperfection (after Hunt and Blackmore 1997)

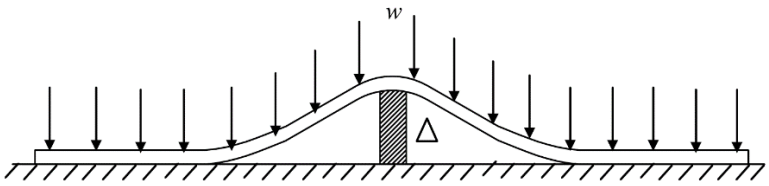

(a)

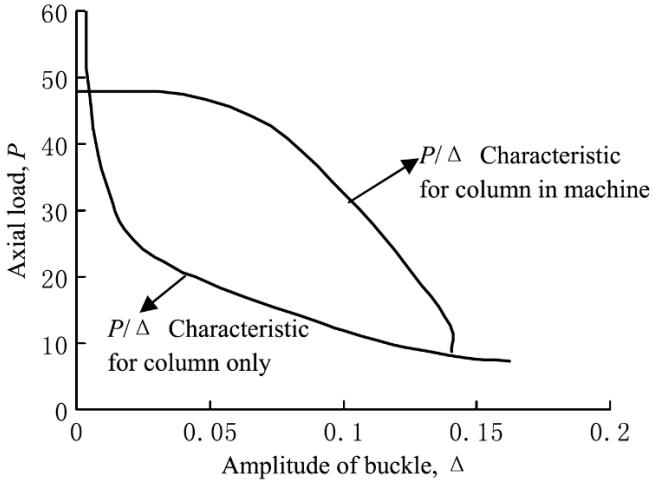

(b)

Figure 2.6: Experimental study of buckling of an axially compressed strip: (a) strip with initial imperfection; (b) column behavior (after Allan 1968)

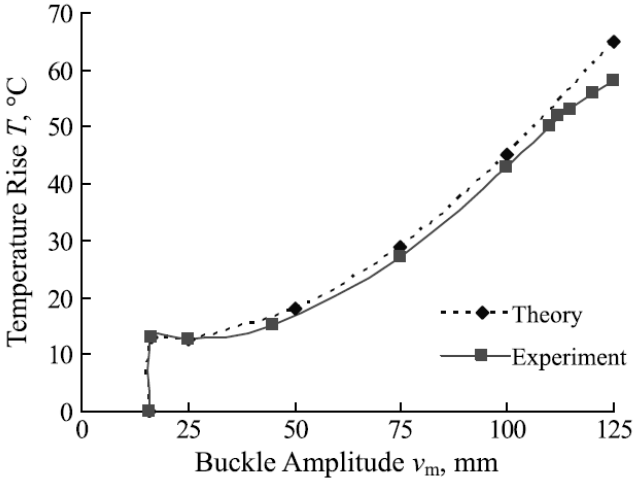

Figure 2.7: Comparison of test data with theory (after Raoof and Maschner 1993)

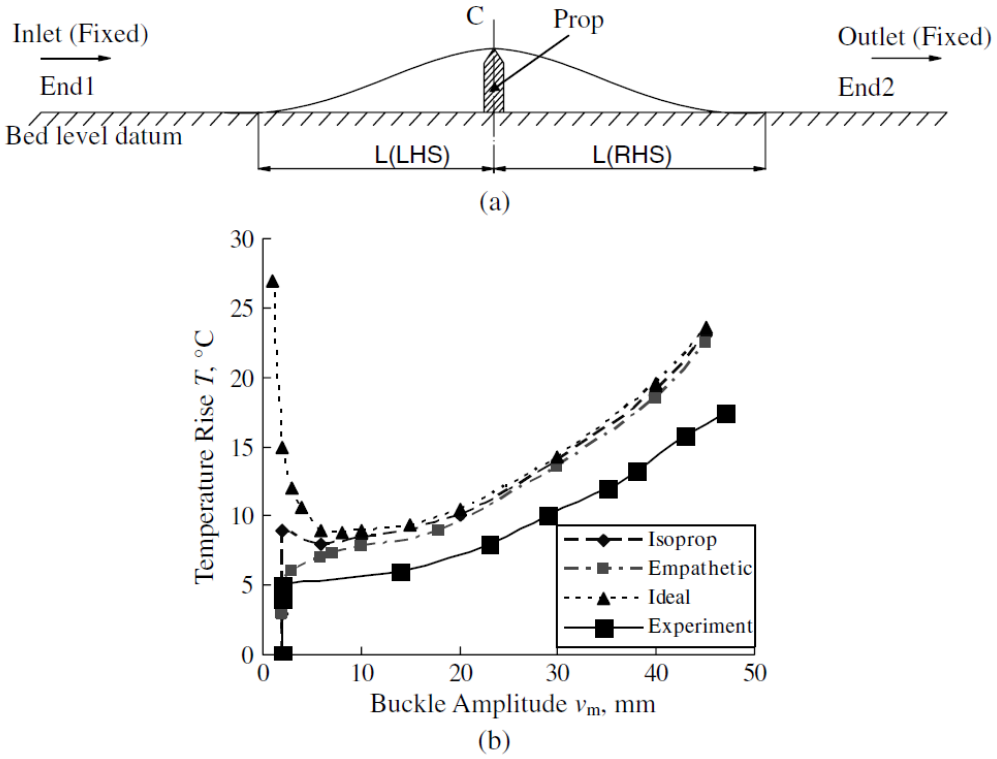

Figure 2.8: Pipe experimentation: (a) elevation from the east side of the laboratory; (b) results comparison of the isolated prop mode (after Taylor and Tran 1996)

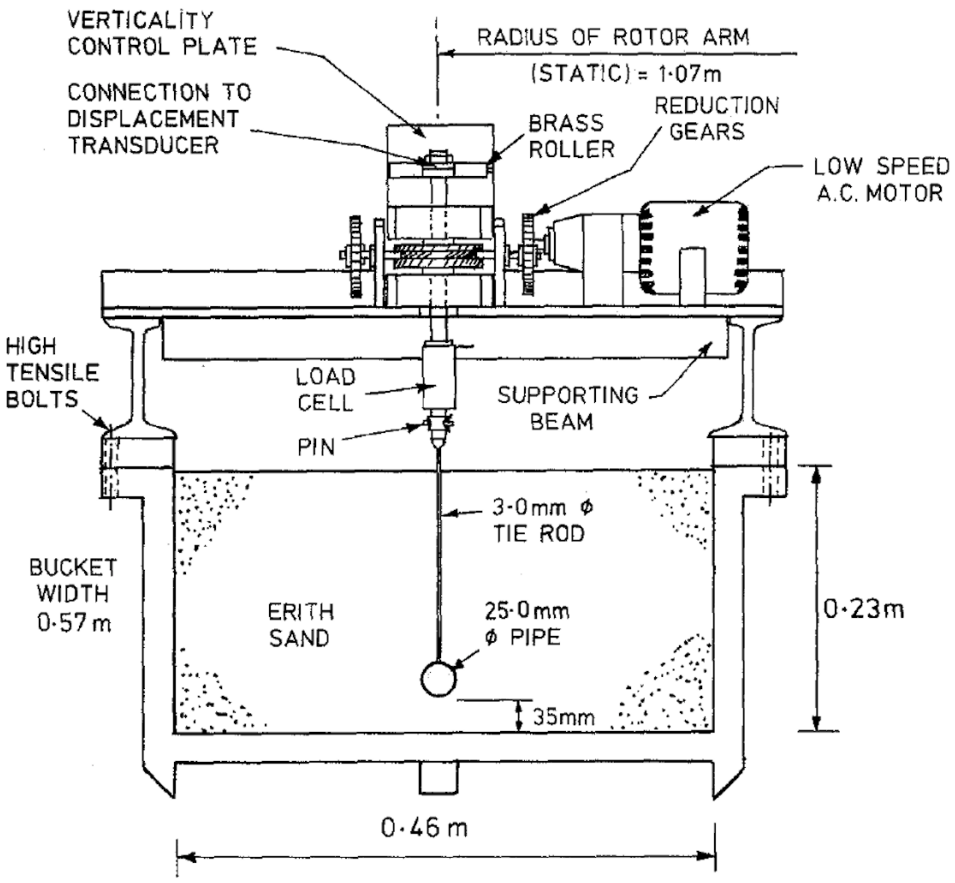

Figure 2.9: Arrangement for uplift test on buried pipes in centrifuge (after Dickin 1994)

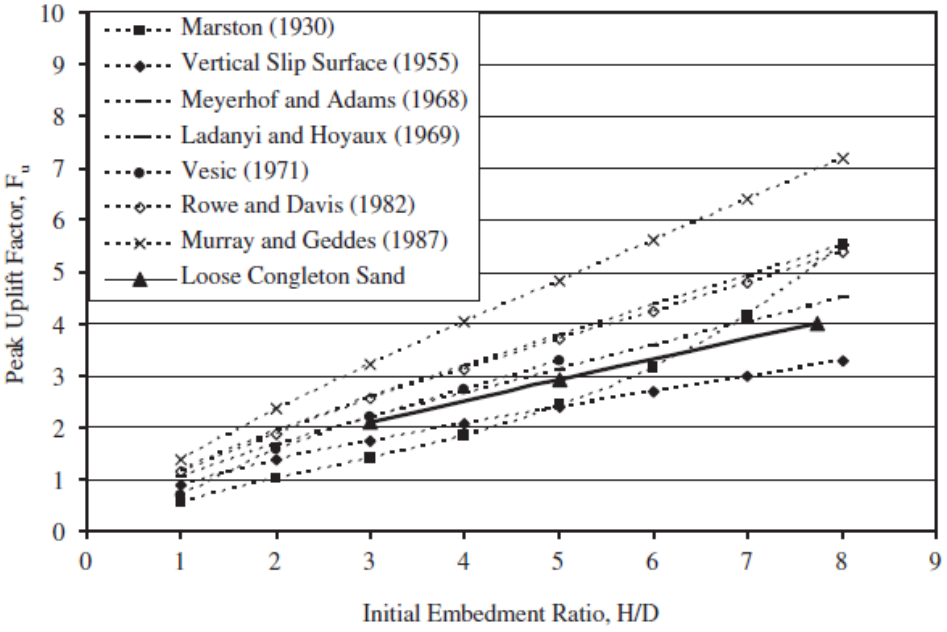
Marston (1930)
Vertical Slip Surface (1955)
Meyerhof and Adams (1968)
Ladanyi and Hoyaux (1969)
Vesic (1971)
Rowe and Davis (1982)
Murray and Geddes (1987)
Loose Congleton Sand
Peak Uplift Factor, F_u
Initial Embedment Ratio, H/D
0
1
2
3
4
5
6
7
8
9
10

(a)

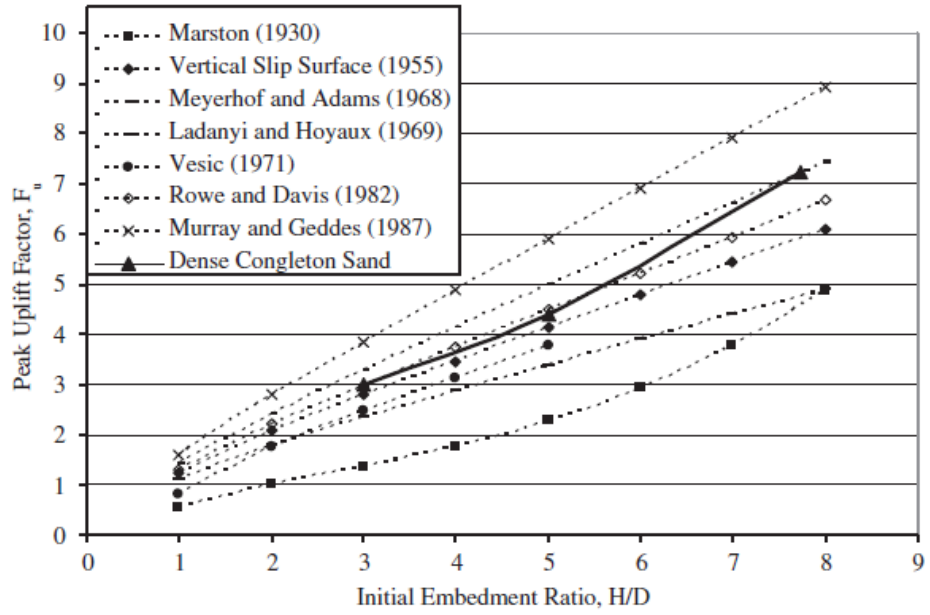
Marston (1930)
Vertical Slip Surface (1955)
Meyerhof and Adams (1968)
Ladanyi and Hoyaux (1969)
Vesic (1971)
Rowe and Davis (1982)
Murray and Geddes (1987)
Dense Congleton Sand
Peak Uplift Factor, F_u
Initial Embedment Ratio, H/D
0
1
2
3
4
5
6
7
8
9
10

(b)

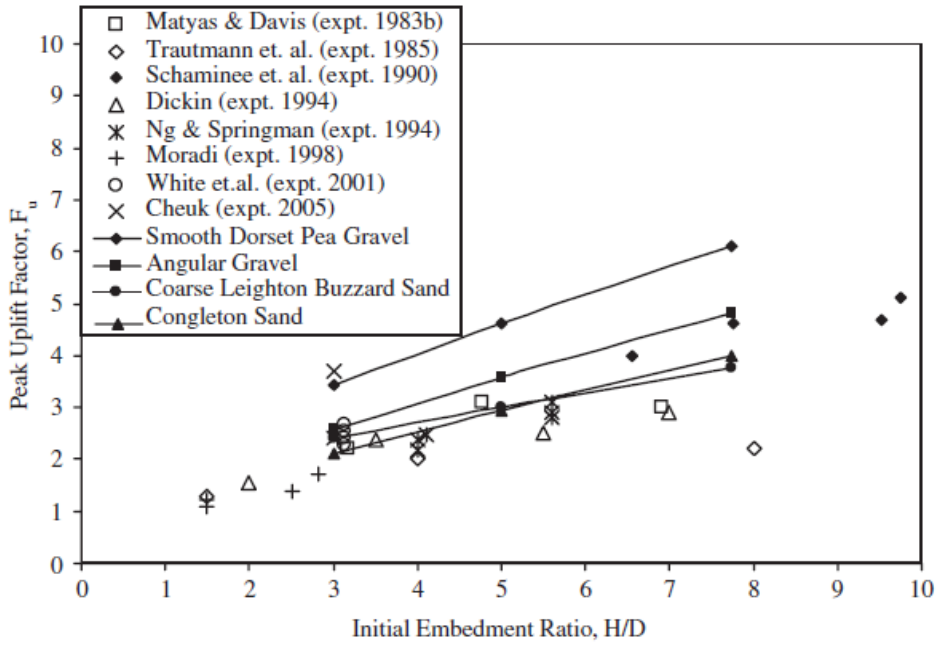

(c)

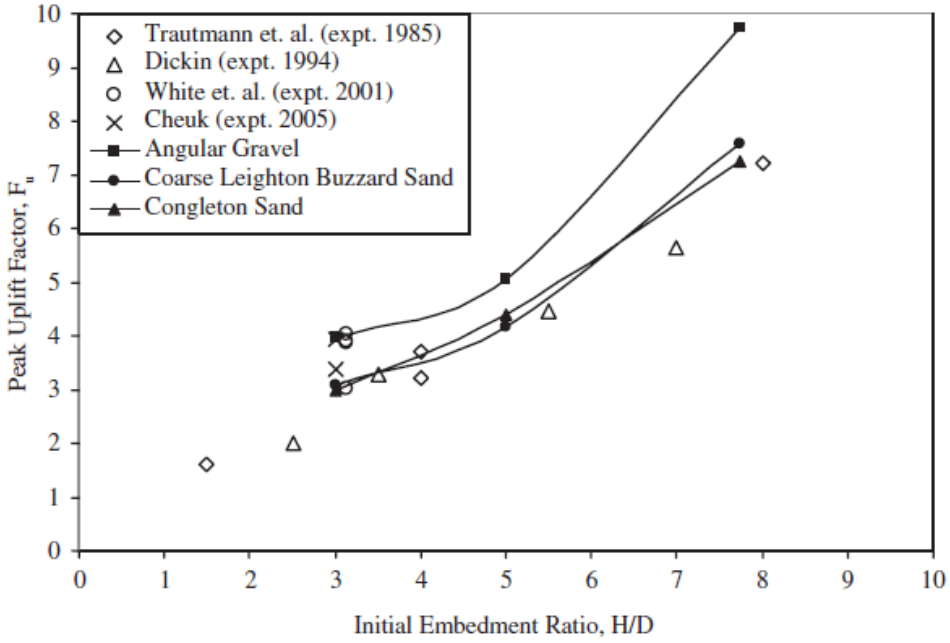

(d)

Figure 2.10: Comparison (a) with analytical model (loose condition); (b) with analytical model (dense condition); (c) test data (loose condition); (d) test data (dense condition) (after Chin et al. 2006)

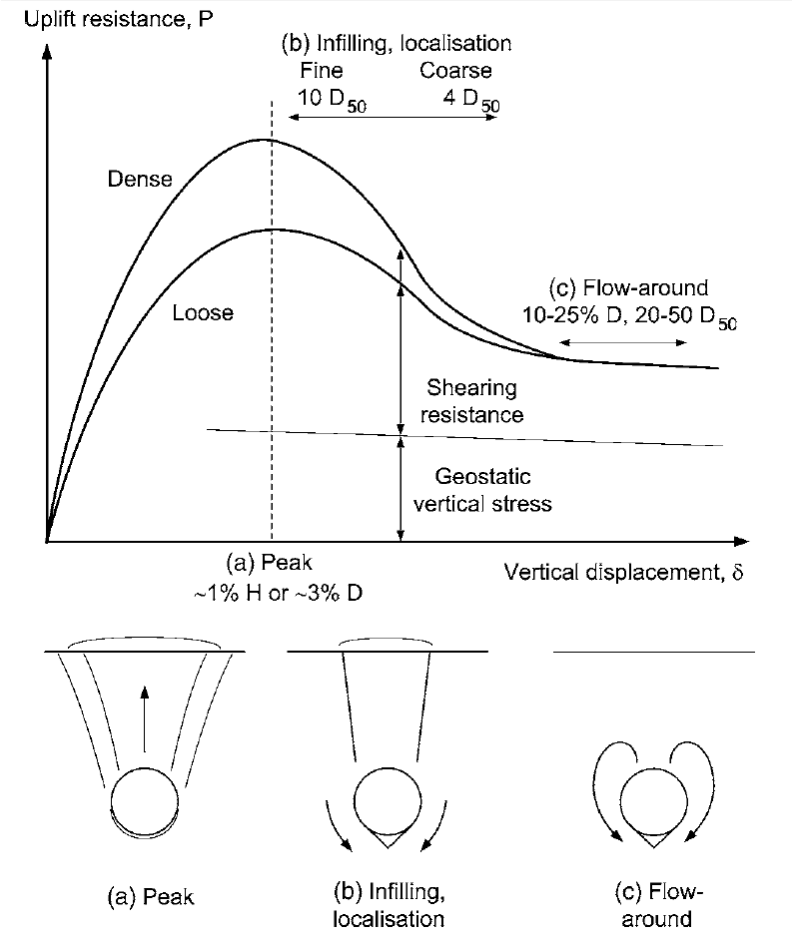

Figure 2.11: Summary of uplift load-displacement response and the corresponding deformation mechanisms (after Cheuk et al. 2008)

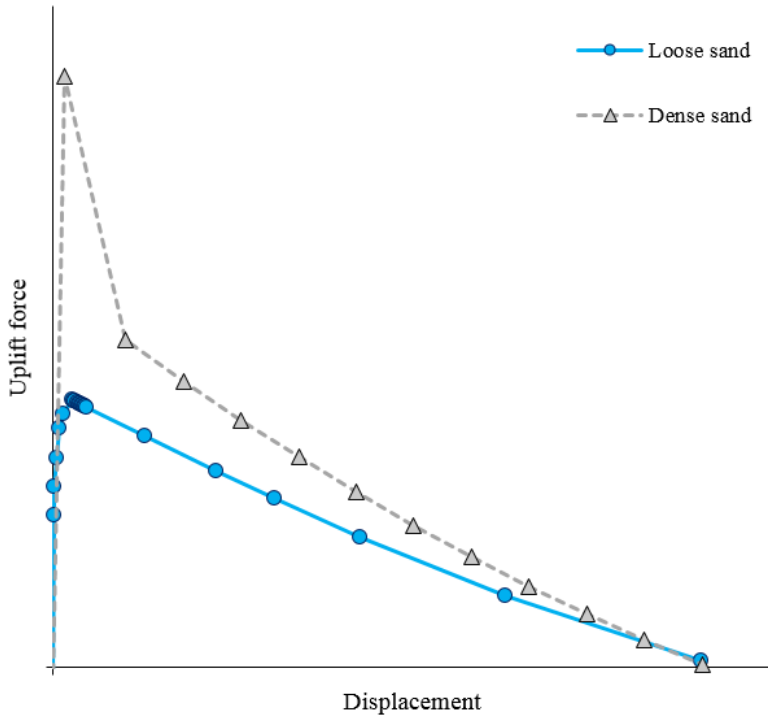

Figure 2.12: Typical uplift resistance/displacement curve for a buried pipe

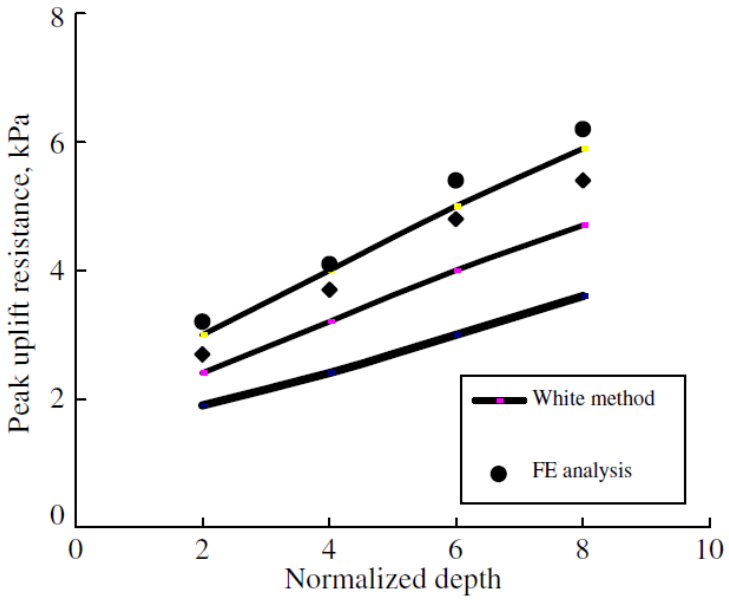

Figure 2.13: Comparison between FE results and theoretical results (after Vanden Berghe et al. 2005)

Chapter 3

Finite Element Analysis of Upheaval Buckling of Submarine Pipelines with Initial Imperfection

3.1 General

Offshore pipelines are considered to be one of the most effective and efficient systems for transporting hydrocarbons. Pipelines are often buried and generally travel long distances through a variety of soil conditions. During operation, the rise in temperature and internal pressure result in longitudinal expansion of the pipeline, which might cause upheaval buckling and failure in some cases. Finite element analysis of upheaval buckling of submarine pipelines is presented in this chapter. Both surface laid and buried pipes are considered in the present study. An initial imperfection, which could have occurred during the manufacturing or installation process, is considered in the numerical modelling of pipes. Soil is modelled using a set of nonlinear springs. The FE model is validated with the analytical solution available in the literature. A parametric study is performed for various burial depths and soil stiffness. The role of post-peak degradation of uplift soil resistance on upheaval buckling of pipe is highlighted. The work presented in this chapter has been published in Arman et al. (2017).

3.2 Introduction

Subsea oil and gas production facilities generally comprise an extensive network of offshore pipelines that transport hydrocarbons from a production facility to a receiving terminal. Although pipeline burial is associated with high installation costs, offshore pipelines are often required to be buried to avoid mechanical damage due to extensive trawling and to assure hydrocarbon flow at

high pressure and temperature (Schupp 2009). Temperature induced expansion, together with vertical out-of-straightness, might cause global upheaval buckling (UHB), which is one of the main types of instabilities that must be addressed in the design of buried offshore pipelines (Williams 2014). Field evidence suggests that UHB might result in significant large vertical upward displacement of the buckled section and in the worst cases, it might protrude above the ground surface (Palmer et al. 2003). For example, Nielsen et al. (1990) reported that a 219-mm diameter (D) buried pipeline in the North Sea displaced ~ 1.5 m (i.e., 6.8D) vertically through the soil and then protruded a maximum vertical distance of 1.1 m (i.e., 5D) above the seabed during the first 7 months after it was brought into service. The uplift resistance offered by the backfill soil over the pipe is the only resistance against the UHB (neglecting the weight of the pipe and suction force below the pipe for a drained loading condition), and therefore, proper understanding of the UHB phenomenon, including the appropriate soil resistance, is necessary for the selection of required burial depth– typically expressed as the H/D ratio, where H is the distance of the center of the pipe from the ground surface. The two most popular burial methods of offshore pipelines, jet trenching and ploughing, generally deposit backfill soil in a loose to medium dense state (Williams 2014); however, it could be subsequently densified due to environmental loading. For example, Clukey et al. (2005) observed a continual natural densification of sandy backfill soil (relative density (DR) less than ~ 57% to ~ 85 – 90% in 5 months) over a mechanically trenched and buried pipeline, which has been attributed to the wave action at the test site in the Gulf of Mexico.

Offshore pipelines generally suffer structural imperfections (e.g., initial out-of-straightness) either during the manufacturing process or during the laying operation. The uneven seabed condition might also preclude the perfect lie of the pipeline during the laying process (Taylor and Gan 1986).

The initial out-of-straightness (imperfection) will result in further deformation in axially constrained high pressure and temperature pipelines and will weaken the pipeline resistance against the UHB. Therefore, offshore pipelines with an initial vertical imperfection are most critical for UHB.

Several experimental (Maltby and Calladine 1995a, b; Taylor and Tran 1993, 1996; Liu et al. 2015) and theoretical studies (Hobbs 1981, 1984; Ballet and Hobbs 1992; Croll 1997; Hunt and Blackmore 1997; Villaraga et al. 2004) have been conducted in the past on the UHB behavior of offshore pipelines with different initial imperfections. Most of these studies considered surface laid pipelines (Hobbs 1981, 1984; Taylor and Tran 1993, 1996), while a few considered buried pipelines (Villaraga et al. 2004; Liu et al. 2013). Due to the large cost associated with the physical tests and due to the recent advancement of computing facilities, the application of numerical simulations (e.g., finite element (FE) analysis) on UHB has been well documented (Shaw and Bomba 1994; Zhang and Tuohy 2002; Newson and Deljoui 2006; Gao et al. 2011; Liu et al. 2013, 2015). In order to assess pipeline stability against the UHB, the uplift resistance of the soil is typically used as an input for FE modelling to determine a safe burial depth (H/D), following the procedures recommended in design guidelines (i.e., ALA 2005; DNV 2007). Although post-peak reduction of the uplift resistance is a common feature of dense sand (Roy et al. 2017a,b), most of the design guidelines (e.g., ALA 2005) and previous numerical studies (e.g., Yimsiri et al. 2004; Liu et al. 2013) did not consider the post- peak resistance of dense sand for modelling the UHB. However, DNV (2007) recognized the post-peak reduction of the uplift resistance for medium to dense sand and recommended a force-displacement relation using four linear line segments in which the uplift resistance reduces linearly from the peak to a residual value with uplift displacement and then remains constant.

The effect of post-peak reduction of the uplift soil resistance on the UHB is analyzed here using FE modeling. Taylor and Tran (1996) characterized the initial imperfection of offshore pipelines in three categories—empathetic, isolated prop and infilled prop. A pipe with an initial imperfection (empathetic configuration) buried in dense sand is the focus of the present study. The FE model is first validated with the analytical solution for surface laid pipe proposed by Taylor and Gan (1986). The analysis is then extended to the buried pipes considering different values (0 – 50%) of post-peak reduction of uplift soil resistance. Finally, the role of post-peak reduction of uplift soil resistance on the UHB behavior is highlighted.

3.3 Problem statement

Figure 3.1 shows the typical topology and the essential features of the pipe considered in the present study. The pipe is in continuous contact with the soil beneath the pipe, which is termed as the 'empathetic configuration' by Taylor and Gan (1986). The initial vertical imperfection distance from the horizontal datum (v_i) is determined using Eq. (3.1) proposed by Taylor and Tran (1996) for the empathetic model.

$$v_i = v_0 \left\{0.707 - 0.26176\pi^2 \frac{x^2}{L_0^2} + 0.293\cos\left(2.86\frac{\pi x}{L_0}\right)\right\} \tag{3.1}$$

where v_0 denotes the maximum vertical imperfection distance (amplitude) from the horizontal datum and L_0 is the initial imperfection length (Fig. 3.1).

The initial imperfection ratio ($\tilde{v} = v_0/L_0$) controls the types of buckling and therefore plays a unique role in the UHB of pipelines (Taylor and Gan 1986). For a certain value of $\tilde{v}$, v_0 and L_0 can be obtained from Eq. (3.2) as proposed by Taylor and Gan (1986):

$$\frac{v_0}{L_0^4} = 2.407 \times 10^{-3} \frac{q}{EI} \tag{3.2}$$

where q is the submerged self-weight of pipe per unit length, EI is the flexural rigidity of pipe; v_f and L are the maximum vertical displacement (buckling amplitude) and maximum buckling length, respectively (Fig. 3.1). The pipe is assumed to be perfectly elastic and stress free with the initial imperfection. To be consistent with the analytical solution, a 650-mm diameter surface laid pipe with a submerged weight of q = 3.8kN/m is used for model verification. For parametric study, q ~ 1.6kN/m is used for a 300-mm diameter buried pipe with a concrete coating of 50 mm considering the densities of steel, concrete, water and oil are 7850, 2800, 1025 and 800 kg/m3, respectively.

The soil resistance on the pipe is modeled by discrete nonlinear (e.g., elastic-plastic, multi-linear) springs as illustrated in Fig. 3.1. The maximum axial and vertical soil spring forces and the associated relative displacements necessary to develop these forces are computed using Eqs. (3.3) and (3.4), respectively, proposed by ALA (2005).

$$F_{\mathrm{ap}} = 0.5\pi\gamma HD(1 + K_0)\tan\phi_{\mu}\,, u_{\mathrm{p}} = 3\ \mathrm{mm} \tag{3.3}$$

$$F_{\mathrm{vp}} = \gamma\phi H^2/44,\ \ v_{\mathrm{p}} = 0.01H \tag{3.4}$$

where F_{ap} and F_{vp} are maximum axial and uplift force per unit length of pipe, respectively, γ is the unit weight of the soil, K_0 is the coefficient of earth pressure at rest, ϕ_{μ} is the axial interface friction angle between pipe and soil, ϕ is angle of internal friction of sand and u_p and v_p are displacements necessary to develop F_{ap} and F_{vp}, respectively.

3.4 Finite element formulation

FE analyses are performed using Abaqus/Standard FE software (Dassault Systèmes 2014). The pipe parameters used in the present FE analyses are listed in Table 3.1. A two-node two-

dimensional linear beam element (B21) is used for modelling the pipe while the soil is modelled as nonlinear springs (SPRING1) in both axial and vertical directions (Fig. 3.1). An element size of 0.5 m is used for the pipe. However, a mesh sensitivity analysis with 0.1 and 0.3 m element sizes is also conducted and no significant difference in temperature rise is found. For example, for a surface laid pipe with $\tilde{v}$ = 0.003, maximum temperature rises of 87.3 °C and 87.4 °C were found for pipe element sizes of 0.1m and 0.3m respectively. The seabed is assumed to be rigid and therefore, a high spring stiffness is used in the downward vertical direction. The length of the pipeline considered in the present study is 3,500 m, which is sufficiently higher than the virtual anchor length. Therefore, no effect of the end constraints is expected in the FE model.

The modified Riks method also known as the Arc-length method, which considers an algorithm to obtain nonlinear static equilibrium solutions for unstable problems, is used in the present study. The modified Riks method was successfully used by previous researchers for FE analysis of UHB of pipes (Liu et al. 2013).

The numerical analysis is conducted in two steps. In the first step, a gravitational load is applied while keeping the initial temperature of the pipe fixed at zero degree Celsius. In the second step, the temperature is increased using the predefined field option available in Abaqus/Standard.

3.5 Model verification

FE analyses are first performed for surface laid pipes to compare the results with analytical solutions proposed by Taylor and Gan (1986). Two initial imperfection ratios, $\tilde{v}$ = 0.003 and 0.01, are considered to capture both snap buckling and stable buckling. In snap buckling, the pipeline suffers an unstable deformation causing a dynamic snap; however, in stable buckling, buckling amplitude gradually increases with temperature until the pipeline eventually goes into failure mode

(Fig. 3.2). Figure 3.2 shows the temperature rise (ΔT) against buckle amplitude (v_f) for $\tilde{v}$ = 0.003 and 0.01. The parameters used for this FE analysis are shown in the first column of Table 3.1. To be consistent with the results of the analytical solutions, the maximum axial soil spring force (F_{ap}) is calculated using $F_{ap} = q\varphi_a(1 - e^{-25u/u_p})$ (see the inset of Fig. 3.2), as proposed by Taylor and Gan (1986), where φ_a is the axial friction co-efficient, and u is the axial displacement. For model verification, $u_p \sim 0.005$m and $\varphi_a \sim 0.7$ are used following the analytical solution of Taylor and Gan (1986).

As shown in Fig. 3.2, the initial imperfection ratio ($\tilde{v}$) has a significant effect on the UHB of a pipeline. For $\tilde{v}$ = 0.003, T increases to the peak value (critical buckling temperature, T_{cr}, point A) until the pipeline suffers an unstable deformation and a dynamic snap occurs (zone ABC in Fig. 3.2). The analytical results for $\tilde{v}$ = 0.003 and 0.01 proposed by Taylor and Gan (1986) are also included in Fig. 3.2. The present FE analysis can successfully capture the dynamic snap, as compared to the analytical solution proposed by Taylor and Gan (1986) (Fig. 3.2). For $\tilde{v}$ = 0.01, the buckle amplitude continues to increase from v_0 with T and no snap behavior is evident (Fig. 3.2). Such buckling behavior is known as "stable buckling." Similar stable buckling behavior was also found by Taylor and Gan (1986) in their analytical solution, as shown in Fig. 3.2. The critical buckling temperature (T_{cr}) for this case is defined by the intersection of the two tangent lines drawn from the initial and final slopes of the curve (Fig. 3.2). There is a slight difference in the temperature rise (ΔT) between the FE results and analytical solutions, which might be attributed to the approximation of the non-linear solver technique of the Modified Riks method and to the assumptions of the analytical solutions, where the large structural deflection was not considered. In the Modified Riks algorithm the size increment is determined by the automatic increase in convergence speed. It does not require to restrict the size increment artificially in the computation

process. Similar relationships between T and v_f, as shown in Fig. 3.2, are also obtained for other initial imperfection ratios; however, those results are not presented here for clarity.

A high T_{cr} (~ 87 °C at point A) is required to initiate the UHB for a lower initial imperfection ratio ($\tilde{v}$ = 0.003) as compared to T_{cr} ~ 50 °C for $\tilde{v}$ = 0.01 (Fig. 3.2). Similar results were also found by Liu et al (2013) from their FE analyses with a 0.323-m diameter surface laid pipeline on Bohai Gulf clay. The present FE analysis thus successfully modeled both snap and stable buckling behavior.

3.6 Parametric study

3.6.1 Effect of burial depth

Six FE analyses are performed for three burial depths (H/D = 1, 2 and 3) and two initial imperfection ratios, $\tilde{v}$ = 0.003 and 0.01. Note that, in this study, the effects of burial depth are incorporated using Eqs. (3) and (4), which define the spring constants. The temperature rise (ΔT) vs buckle amplitude (v_f) curves for $\tilde{v}$ = 0.003 and 0.01 are shown in Figs. 3.3(a) and 4.3(b), respectively.

Figure 3.3 shows that T_{cr} increases with burial depth. For example, T_{cr} ~ 120 °C for H/D = 3 is required for snap buckling as compared to T_{cr} ~ 60 °C for H/D = 1 (Fig. 3.3(a)). Similar results—a higher T_{cr} for higher H/D ratio—are also found for stable buckling, as shown in Fig. 3.3(b). For a given pipe diameter, as the soil cover (H) above the pipe increases with the H/D ratio, the uplift resistance of the pipe (F_v) also increases with H/D (Eq. 3.4) and therefore, higher T_{cr} is required for the UHB of pipe. Similar conclusions (i.e., higher T_{cr} for higher H/D) for a 0.323-m pipe buried at H/D ~ 1–9 in Bohai Gulf sand were also drawn by Gao et al. (2011) from their FE analyses.

3.6.2 Effect of post-peak reduction of uplift soil resistance

Physical model test results (Trautmann 1983; Chin et al. 2006; Cheuk et al. 2008) on pipes buried in dense sand show that vertical resistance (F_v) increases quickly with vertical displacement (v) and reaches the peak value (F_{vp}) at a small v. A quick reduction of F_v occurs after the peak, followed by a gradual reduction of F_v at large v. Similar post-peak reduction of F_v has also been found by Roy et al. (2017a) in their FE analysis of pipes buried in dense sand. The ALA (2005) design guidelines do not explicitly consider the post-peak reduction of F_v (Eq. 3.4). However, DNV (2007) recognized the importance of post-peak reduction of F_v and recommended a tri-linear force-displacement curve, as shown in the inset of Fig. 3.4(a).

According to DNV (2007), the upward resistance reduces linearly from the peak value (F_{vp}) to a residual value (F_{vr}) at an upward displacement of three times the displacement required to mobilize the peak resistance. After that, the upward resistance remains constant at F_{vr}. Therefore, the effect of the post-peak reduction of uplift resistance offered by the backfill soil on UHB of pipeline is further examined in this section.

Physical model test results (Trautmann 1983; Chin et al. 2006; Cheuk et al. 2008) and FE analyses (Jung et al. 2013; Roy et al. 2017a & b) show a wide variation of post- peak reduction of uplift resistance. For example, Cheuk et al. (2008) showed ~ 40% reduction of uplift resistance from the peak for a 100-mm diameter pipe buried in dense Leighton Buzzard sand, while Chin et al. (2006) showed ~ 50% reduction for a 190-mm diameter pipe buried in dense Congleton sand. Therefore, analyses are performed for 0%, 15%, 25%, and 50% post-peak reduction of uplift resistance, as shown in the inset of Fig. 3.4(a). Again, two initial imperfection ratios, $\tilde{v}$ = 0.003 and 0.01, are considered. The axial spring stiffness is calculated using Eq. (3.3) without post-peak reduction (see the inset of Fig. 3.4(b)). Three burial depths (H/D = 1–3) are considered for both cases.

Following DNV (2007), the upward displacement required to reach the residual uplift resistance is calculated as $v_r = 3v_p$.

Figures 3.4(a) and 3.4(b) show the effect of post-peak reduction of uplift soil resistance on the buckling response of a buried pipe (H/D = 3) for $\tilde{v}$ = 0.003 and 0.01 respectively. For $\tilde{v}$ = 0.003, the critical buckling temperature (T_{cr}) decreases with an increase in post-peak reduction of uplift soil resistance (Fig. 3.4(a)). For example, T_{cr} ~ 123 °C for a 0% reduction (curve a) while T_{cr} ~ 106 °C for a 50% reduction (curve d) (Fig. 3.4(a)). Similarly, for $\tilde{v}$ = 0.01, T_{cr} ~ 77 °C for a 0% reduction (curve a), while T_{cr} ~ 63 °C for a 50% reduction (curve d) (Fig. 3.4(b)). As the available uplift resistance is less for curve (d) than curve (a) (see the insets of Fig. 3.4(a)), T_{cr} is also lower for the latter case (Fig. 3.4).

The critical buckling temperature is plotted against burial depth in Fig. 3.5. As shown, T_{cr} increases with burial depth for both $\tilde{v}$ = 0.003 and 0.01. Similar results—higher T_{cr} for higher H/D ratios—have also been found by Gao et al. (2011) from FE analysis with a 0.323-m diameter pipeline buried in Bohai Gulf sand. The present study shows that T_{cr} is also influenced by the post- peak uplift resistance. As an example, for H/D = 2, T_{cr} is ~88 °C for 0% reduction while T_{cr} ~ 76 °C for 50% reduction (Fig. 3.5). Moreover, the difference between T_{cr} for 0% and 50% post-peak reduction increases with H/D for both $\tilde{v}$ = 0.003 and 0.01. Figure 3.5 also shows that the post-peak reduction of uplift resistance has a significant effect on T_{cr} for large H/D and $\tilde{v}$.

3.7 Summary

Thermal expansion of buried pipelines may cause upheaval buckling if the uplift resistance offered by the backfill soil is not sufficient to prevent upward displacement. Finite element (FE) analyses of upheaval buckling of pipeline with an initial imperfection are conducted using Abaqus/Standard

FE software. The FE model is first validated using analytical solutions for a surface laid pipeline. The FE models are then extended to buried pipelines to show the effect of post-peak reduction of uplift soil resistance on the UHB of pipelines. The following conclusions can be drawn from this study:

(i) The present FE modeling technique can successfully capture both snap and stable buckling.

(ii) The critical buckling temperature increases with burial depth (H/D) for both snap and stable buckling.

(iii) The critical buckling temperature decreases with an increase in post-peak reduction of uplift soil resistance.

(iv) The difference of the critical buckling temperatures for 0% and 50% post-peak reduction of uplift soil resistance increases with burial depth.

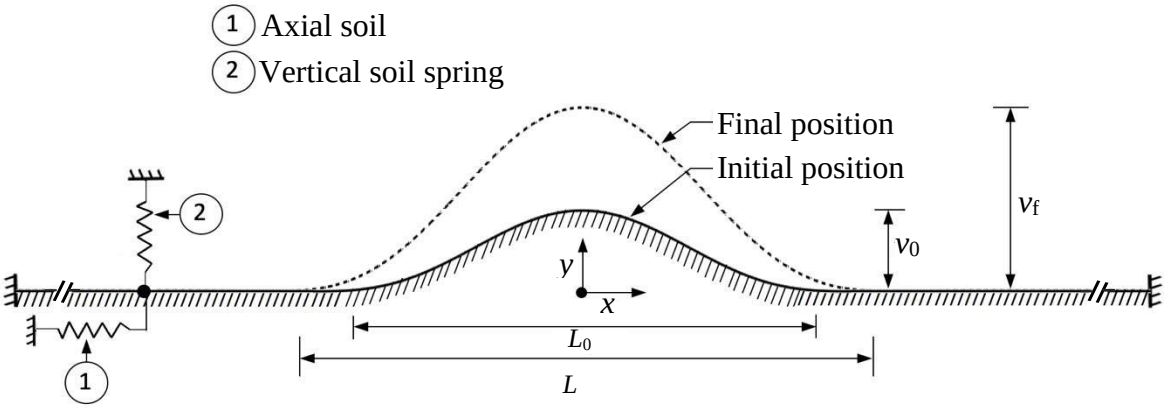

Figure 3.1 Problem definition and geometry of the pipe with initial imperfection

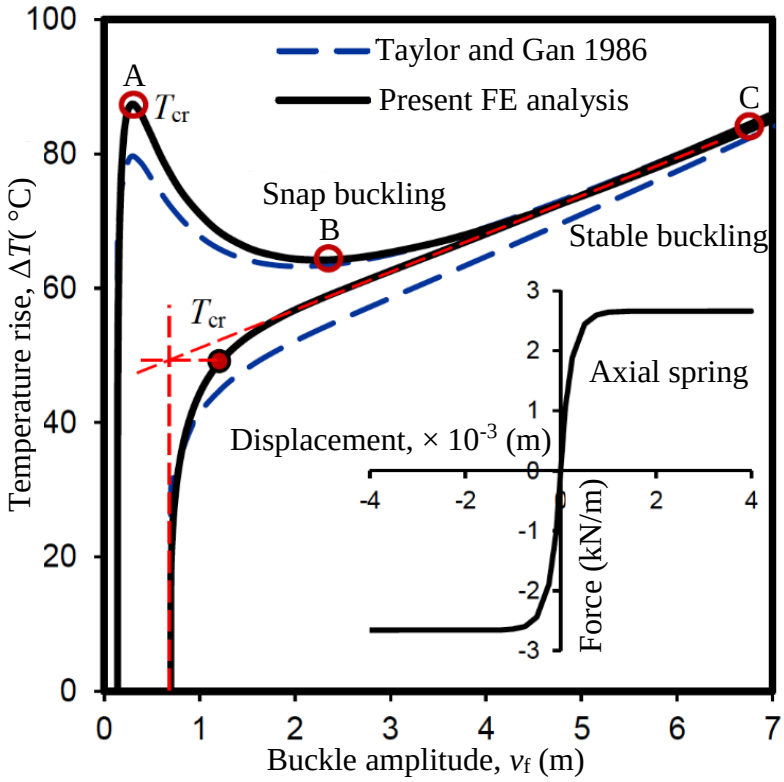

Figure 3.2: Comparison of present FE analyses with the analytical solution

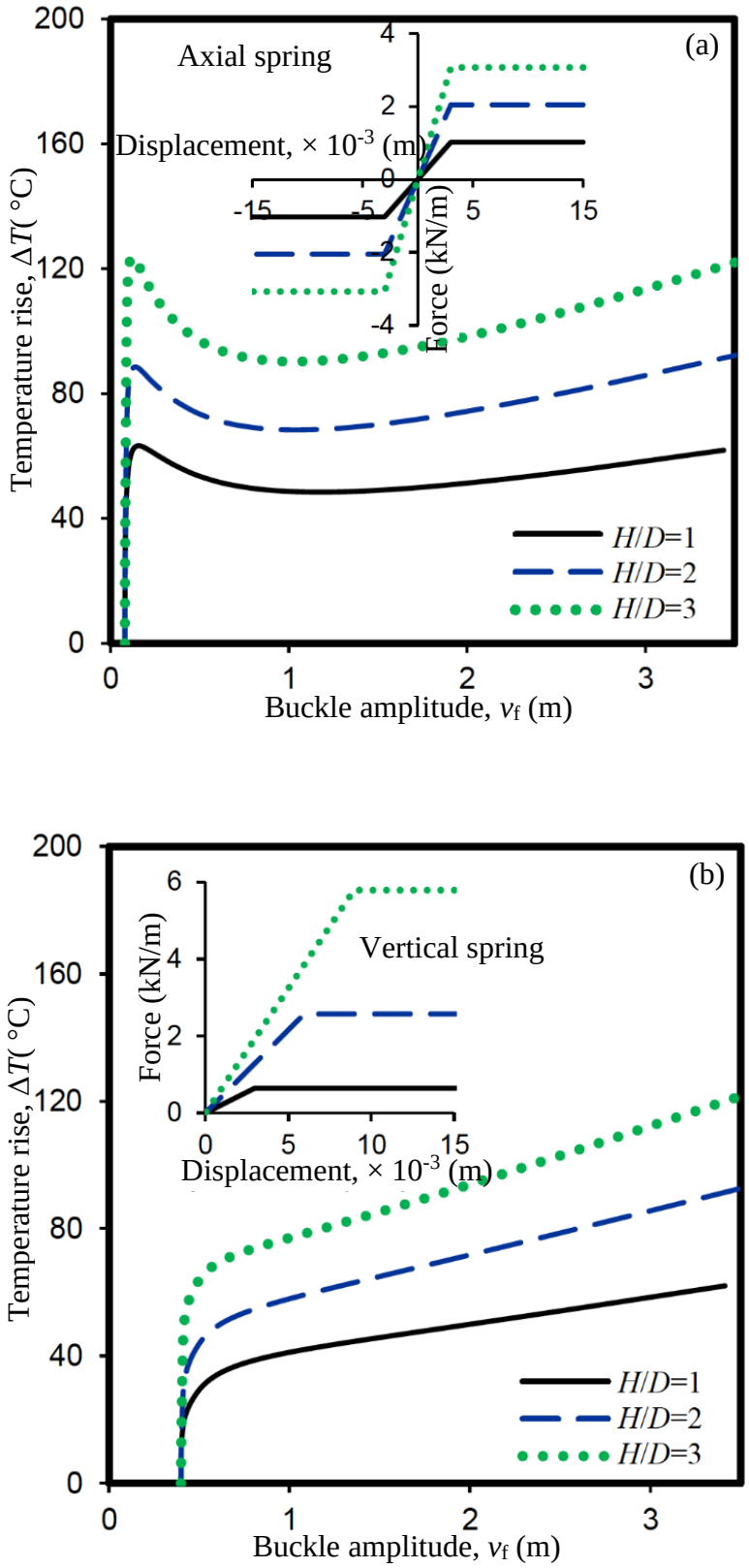

Figure 3.3: Effect of burial depth (a) for $\tilde{v}$ = 0.003; (b) for $\tilde{v}$ = 0.01

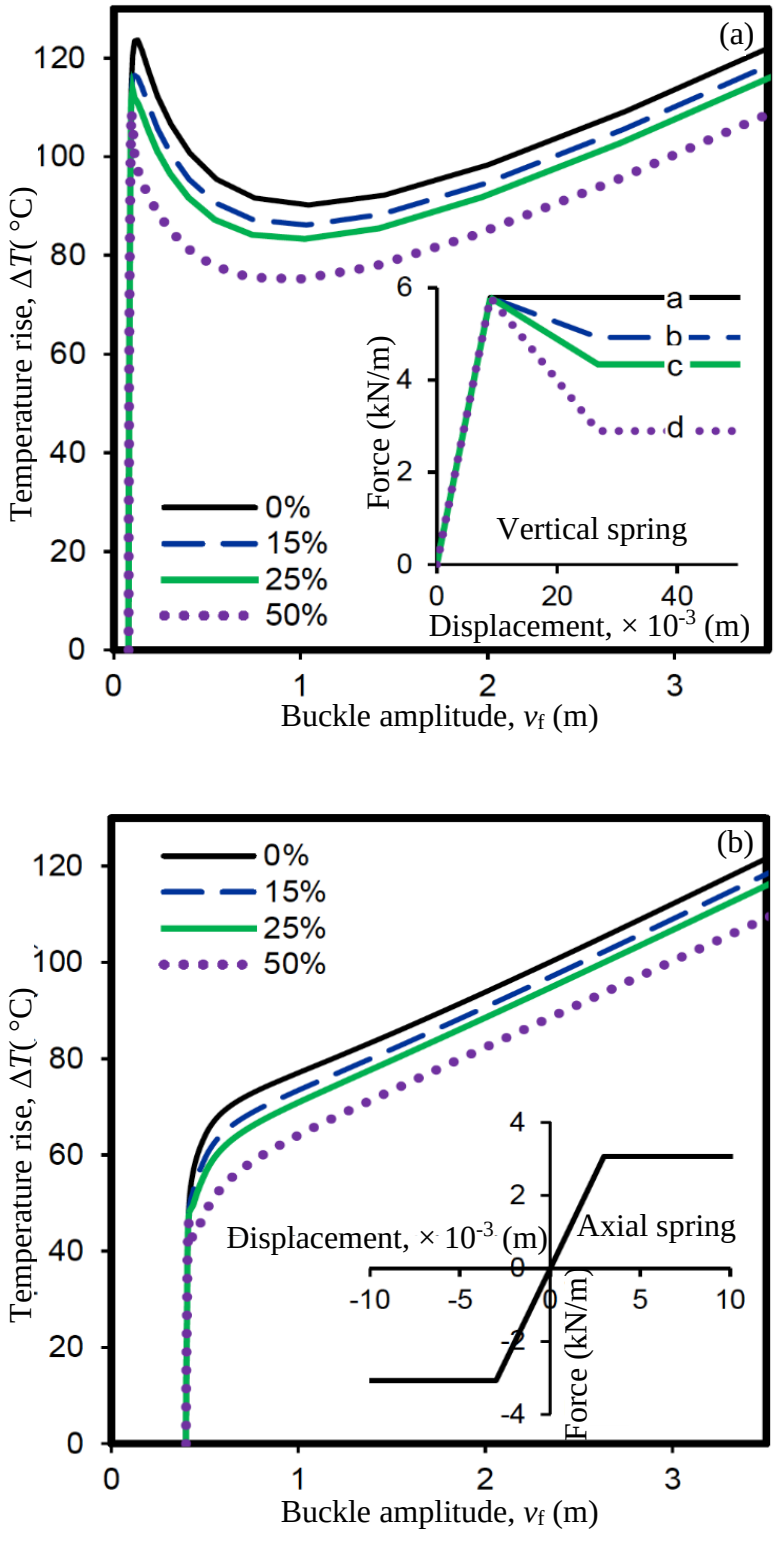

Figure 3.4: Effect of post-peak reduction of uplift soil resistance (a) for $\tilde{v}$ = 0.003; (b) for $\tilde{v}$ = 0.01

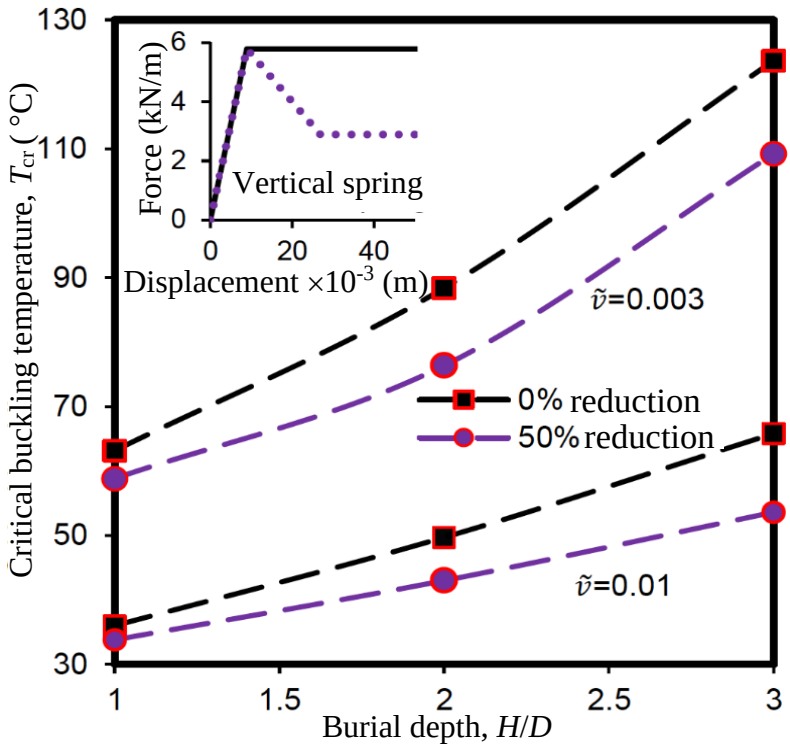

Figure 3.5: Effect of post-peak reduction of uplift soil resistance on critical buckling temperature (T_{cr})

Table 3.1: Parameters of pipe used in FE analysis

Parameters	**Model verification**	**Parametric study**
External diameter, *D* (m)	0.65	0.3
Wall thickness, *t* (m)	0.015	0.0127
Cross sectional area, *A* (m^2)	29.92×10^{-3}	11.4×10^{-3}
Young's modulus pipeline, *E* (GPa)	206	206
Sectional moment, *I* (m^4)	1.509×10^{-3}	1.17×10^{-4}
Pipe self-weight, *q* (N⁄m)	3800	1588
Yield stress, σ_y (MPa)	448	448
Thermal expansion coefficient, α ($°C^{-1}$)	11×10^{-6}	11×10^{-6}

Chapter 4

Factors Affecting Upheaval Buckling of Initially Imperfect Pipelines Buried in Sand and Some Design Implications

4.1 General

Upheaval buckling (UHB) is one of the design considerations for high temperature and high pressure buried pipelines. Offshore buried pipelines travel a very long distance through a wide range of soil conditions while delivering hydrocarbon from the production end to the receiving end. Although experimental evidences show that both loose and dense sand exhibit a post-peak reduction of uplift soil resistance, the current design guidelines, such as ALA (2005) and DNV (2007), do not take into account the effect of such behavior in the design against UHB. To investigate the rationale behind the current design practice, parametric studies on the effects of post-peak reduction of uplift soil resistance, burial depth, soil density, pipe diameter and coefficient of earth pressure at rest on UHB are carried out. An initially imperfect pipeline, which may result from the manufacturing or installation process, is considered in this study. The soil resistance is modelled using a series of independent discrete nonlinear springs. Based on the results obtained from finite element (FE) analyses, some key issues are presented that may affect the design of pipeline against UHB.

4.2 Introduction

Pipeline network has become the primary means of transporting hydrocarbon from the production end to the receiving end in many parts of the world. Albeit high capital expenditure involved, offshore pipelines are often buried to provide safeguard against mechanical damage due to the

third party (e.g., trawling gear) activities and to ensure hydrocarbon flow at high pressure and high temperature (Schupp 2009). Structural imperfections (e.g., initial out-of-straightness) are part and parcel of the offshore pipelines, which result from the manufacturing process or due to laying operation. During the laying process, irregularities of the seabed profile also preclude the perfect lie of the pipeline (Taylor and Gan 1986). Compressive stress is typically induced in pipelines by the frictional resistance to axial extensions. Axial extensions occur due to temperature or internal pressure changes. In an axially constrained high-pressure (HP) and high-temperature (HT) pipelines, the initial out-of-straightness (imperfection) calls forth further deformation weakening the resistance of the pipeline against the global upheaval buckling (UHB). In conjunction with temperature and pressure induced expansion, initial out-of-straightness may trigger global upheaval UHB. Therefore, offshore buried pipelines with an initial imperfection should be designed against UHB. It is one of the most common types of instabilities of buried offshore pipelines and a major concern from the design point of view (Williams 2014). It is apparent from several field evidences that UHB causes remarkable vertical upward displacement of the initially buckled section. Sometimes even jutting out the ground surface (Palmer et al. 2003). Clukey et al. (2005) observed a continual natural densification of sandy backfill soil— the relative density (D_R) increases from ~ 57% to ~ 85–90% in 5 months—in a mechanically trenched buried pipeline. This has been attributed to the wave action at the test site in the Gulf of Mexico. Therefore, to capture both the long-term and short-term field conditions, a pipe with an initial imperfection and buried in loose and dense sand is considered in the present study.

4.3 Previous Research and Current Practice

In the last 40 years, researchers conducted experimental, analytical and numerical studies on the UHB of pipelines which are briefly presented in this chapter. The literature review implies that studies on UHB of offshore pipelines has progressed rapidly over the last few years.

4.3.1 Analytical studies

Allan (1968) carried out analytical studies on UHB of an axially compressed frictionless strip and found that buckling problem is sensitive to initial imperfections. Hobbs (1981, 1984) analyzed both lateral and upheaval buckling problem of a long straight perfectly elastic pipe with a small slope when it reached the critical buckling condition and concluded that lateral buckling tends to occur at a lower axial load than UHB unless the pipe is buried. Taylor and Gan (1986) presented a set of analysis incorporating structural imperfections and deformation dependent axial friction response. They pointed out that the initial imperfection ratio v_0/L_0 is an essential parameter which is related to the out-of-straightness of the imperfection. Wang et al. (2011) presented a theoretical solution of UHB for different types of initial imperfections. They applied this analytical tool to predict the occurrence of UHB in the Bohai Gulf and proposed different protection measures. Liu et al. (2013) studied the continuous support model of initial imperfection and introduced an analytical solution for thermal UHB. Then the analytical methodology was applied to analyze a practice in Bohai Gulf, and they concluded that the buckling temperature depends on the amplitude of the initial imperfection. Karampour et al. (2013) studied the lateral and upheaval buckling of pipelines and proposed some analytical solutions for the UHB and compared the response of the three types of localized initial imperfections. The influence of the shape of initial imperfection on the critical force was pointed out.

4.3.2 Laboratory and centrifuge tests

According to many researchers, the pipe/soil interaction characteristics also have a significant effect on the UHB behavior of submarine pipeline. Taylor et al. (1985) performed a small-scale test on the medium to fine sand in view of North Sea conditions. They conducted pullout tests and axial friction tests and proposed a semi-empirical design formula based on the force-displacement relationship of the pipe for different burial depths. Schaminee et al. (1990) conducted a full-scale laboratory test on a buried pipe and presented the results of the uplift and axial resistance. Dickin (1994) performed centrifuge tests to study the influence of pipe diameter, burial depth and backfill density on the resistance of pipes in the sand and did not find any significant differences between the behavior of buried pipes and strip anchors which justifies the application of anchor theory to the buried pipe. Taylor and Tran (1996) designed and constructed a complex and novel experimental rig with regards to the crucial upheaval state which can test both isolated prop and contact undulation imperfection topology. They also summarized three basic types of initial imperfection for the subsea buried pipeline. Bransby et al. (2002) conducted laboratory and centrifuge tests using loose sand, dense sand and gravel to observe the uplift behavior of buried offshore pipelines and found that due to volumetric response, dense and loose sand undergo different deformation mechanisms after the mobilization of peak uplift resistance. Chin et al. (2006) undertook centrifuge uplift tests to examine the uplift behavior of pipelines buried in a range of cohesionless soils and reported that peak uplift resistances are mobilized within small pipe displacements and increases with embedment and soil density. Cheuk et al. (2008), employing a novel image-based deformation measurement technique, described the mechanisms by which uplift resistance is mobilized in silica sand. They showed that peak uplift resistance is mobilized through the formation of an inverted trapezoidal block, bounded by a pair of shear bands,

exhibiting softening behavior. Wang et al. (2010) carried out a series of full-scale and centrifuge tests in loose sand, saturated dense sand and dry gravel to investigate the necessity of discounting the shear contribution from the uplift resistance for H/D ratios less than 1. From the test data, they did not find any rationale behind this industry practice. Gao et al. (2011) carried out a series of large-scale model tests in fine sand to obtain the force-displacement relationships under different test conditions. For different burial depth, the pipe segments were pulled out in uplift and axial directions. For loose sand, the effect of post-peak reduction of the uplift soil resistance on the UHB is analyzed here using FE modeling.

4.3.3 FE analyses

Because of the substantial cost involved with the physical tests and due to the recent advancement of computing facilities, the application of numerical simulations (e.g., FE analysis) on UHB has been well documented in several studies. Zhang and Tuohy (2002) performed upheaval buckling analysis on a trenched unburied production flowline using ANSYS which is an FE analysis program package. Yimsiri et al. (2004) conducted FE analysis of lateral and upward pipe movements using the Mohr-Coulomb and Nor-Sand soil models to find the solution for the peak force and investigate the transition from shallow to deep failure mechanism. Finally, based on the FE analysis results, a design chart for deeply buried pipelines is constructed. Gao et al. (2011) adopted nonlinear soil spring based on experimental test data and performed FE analysis using Abaqus package program which showed that pipeline capacity against thermal buckling decreases with increase in initial imperfection height and increases with burial depth. Zhang and Duan (2015), using FE analysis, studied the UHB behaviors of eight groups of pipeline segments with different imperfection shapes and out-of-straightness and defined a new parameter to express

different imperfection shapes. Finally, they proposed a universal formula to calculate the critical axial force.

4.3.4 Studies on post-peak reduction of uplift resistance of soil

Physical model test results (Trautmann 1983; Chin et al. 2006; Cheuk et al. 2008) and FE analyses (Jung et al. 2013; Roy et al. 2017a & b) show a wide variation of post-peak reduction of uplift resistance. For example, Cheuk et al. (2008) showed ~ 40% reduction of uplift resistance from the peak for a 100-mm diameter pipe buried in dense Leighton Buzzard sand, while Chin et al. (2006) showed ~ 50% reduction for a 190-mm diameter pipe buried in dense Congleton sand. Moreover, modeling of post-peak degradation of uplift resistance has some important practical implications, as recognized in previous studies. For example, Klever et al. (1990) showed that classical "effective weight" method of calculating upward resistance is unconservative. They showed that, when a complete force-displacement curve is considered, it gives significantly lower permissible temperatures than classical solutions based on the effective weight method. A similar conclusion has been drawn by Goplen et al. (2005), who suggested linear soil stiffness model for preliminary analysis and full model (with post-peak degradation) to determine the failure temperature due to upheaval buckling. Wang et al. (2009) also recognized this and conducted buckling analysis using a soil resistance model with post-peak degradation. They also mentioned that "for no pipe uplift, the uplift resistance involves only the weight of pipe and soil. Upon starting of pipe uplift, soil resistance increases linearly with the uplift resistance to a peak, followed by a decrease until it reaches nil upon pipe breakout."

4.3.5 Current practice

To assess pipeline stability against the UHB, the uplift resistance of the soil is typically used as an input for FE modeling to determine a safe burial depth (H/D), following the procedures

recommended in design guidelines (i.e., ALA 2005; DNV 2007). Although post-peak reduction of the uplift resistance is a common feature of loose and dense sands (Roy et al. 2017 a,b; Wang et al. 2011), most of the design guidelines (e.g., ALA 2005) and previous numerical studies (e.g., Yimsiri et al. 2004) did not consider the post-peak reduction of the uplift resistance of loose and dense sand while modelling the UHB. However, DNV (2007) recognizes the post-peak reduction of the uplift resistance for medium to dense sand but recommends a force-displacement curve using tri-linear segments in which no post-peak reduction of uplift resistance is considered. Another approach is also suggested by DNV (2007) in which four linear line segments are used and the uplift resistance reduces linearly from the peak to a residual value with the increase in uplift displacement and then remains constant. Nevertheless, the force-displacement curve proposed by DNV (2007) is different from the force-displacement curve obtained from the laboratory test results. Comparison of force-displacement relationship proposed by different design guidelines and previous authors are illustrated in Fig. 4.1 and the insets show the initial part of the curve in an enlarged scale. DNV (2007) not only initially overestimates the stiffness of force-displacement curve for both loose and dense sand but also overshoots the peak uplift displacement for loose sand. Moreover, DNV (2007) undershoots the post-peak reduction of the uplift soil resistance for dense sand whereas, for loose sand, DNV (2007) does not consider the post-peak reduction of the uplift soil resistance at all. So, based on laboratory test results of loose and dense sand, the effect of post-peak reduction of uplift soil resistance on UHB behavior of pipeline is investigated in this chapter. The FE model is first validated with the analytical solution for surface laid pipe proposed by Taylor and Gan (1986) which is shown elsewhere (Arman et al. 2017). To investigate the rationale behind the current design practice, parametric studies on the effect of post-peak reduction of uplift soil resistance, burial depth, soil density, pipe diameter and

coefficient of earth pressure at rest on UHB are carried out. Finally, the importance of incorporating the post-peak reduction of uplift soil resistance while analyzing the UHB of an offshore buried pipeline is highlighted.

4.4 Problem statement

In this chapter, a similar problem to Chapter 3 is considered regarding imperfection configuration. Figure 4.2 illustrates the model layout and key features of the pipeline used in this study. The initial imperfection height is denoted by v_i which is the distance of the pipe from the horizontal datum and can be obtained by using Eq. (3.1) proposed by Taylor and Tran (1996) for the empathetic model. Equation (3.2) shows the relationship between v_0 and L_0, as proposed by Taylor and Gan (1986). It is assumed that the pipeline is stress-free when initially deformed and the pipe material is elastic-perfectly plastic. Steel, concrete, water, and oil densities are considered as 7,850 kg/m^3, 2,800 kg/m^3, 1,025 kg/m^3 and 800 kg/m^3, respectively. A 298.5-mm diameter buried pipe with submerged weight (filled with oil) of $q \sim 0.63$ kN/m is used as a base case whereas, for parametric study, buried pipes of 141.3-mm diameter, 406.4-mm diameter, and 508-mm diameter are also used, which have submerged self-weight of 0.32 kN/m, 0.8 kN/m, and 0.92 kN/m, respectively. For modeling the soil resistance, a series of discrete nonlinear spring (e.g., elastic-plastic, multi-linear) is used for both in the axial and vertical directions, as shown in Fig.4.2. The maximum axial soil spring force and the associated relative displacement necessary to develop this force is computed using Eq. (4.1), as proposed by ALA (2005).

$$F_{ap} = \pi\gamma' HD\frac{1+K_0}{2}\tan\phi_\mu \, , u_p = 3 \text{ mm (dense sand); } 5 \text{ mm (loose sand)} \qquad (4.1)$$

where F_{ap}, K_0, γ' and ϕ_μ are the maximum axial force per unit length of pipe, the coefficient of earth pressure at rest, the effective unit weight of soil and the axial interface friction angle between pipe and soil, respectively, u_p is the displacement necessary to develop F_{ap}.

In the present study, γ' of 10 kN/m^3 and 8.7 kN/m^3 are used for dense and loose sands, respectively, and the corresponding K_0 are 0.5 and 0.4. For dense sand, ϕ=45° is used while for loose sand it is considered as 35°. Pipe coating is assumed to be rough for which the coating factor (c_f) is 0.8 according to ALA (2005) and ϕ and c_f are used to calculate ϕ_μ ($\phi_\mu = \phi \times c_f$).

Again, the maximum vertical bearing soil spring force and the corresponding relative displacement at which this force develops is calculated using the Eqs. (4.2 – 4.4), as proposed by ALA (2005).

$$F_{bp} = N_q \gamma' HD + N_\gamma \gamma \frac{D^2}{2}, v_b = 0.1D \quad (4.2)$$

$$N_q = \exp(\pi tan\phi)\, tan^2(45 + \frac{\phi}{2}) \quad (4.3)$$

$$N_\gamma = e^{(0.18\phi - 2.5)} \quad (4.4)$$

where F_{bp}, ϕ, γ' and γ are the maximum vertical bearing force per unit length of pipe, the angle of internal friction of soil, the effective unit weight of soil and the unit weight of soil, respectively, v_b is the displacement necessary to develop F_{bp}. N_q and N_γ are the bearing capacity factors. The peak uplift resistance on the pipeline in the sand is heavily affected by burial depth and soil density (Dickin 1994). In practice, burial depth is expressed as H/D ratio which is also popularly known as embedment ratio. Traditionally this parameter is used to define whether burial depth is shallow or deep. According to most of the authors, a pipeline is shallowly buried if $H/D \leq 5$ (Chin et al. 2006). Burial depth of most of the offshore pipelines are shallow and hence the focus of this chapter. From previous studies, it is evident that the peak uplift resistance (F_{vp}) mobilizes not only

very quickly but also rapidly drops by half to a residual value (F_{vr}) in case of dense sand. After F_{vp}, two types of soil displacement mechanism occur which is discussed in detail elsewhere (Bransby et al. 2001). However, for loose sand, no such quick drop is observed (Wang et al. 2011). Pipe-soil interaction is a complex phenomenon, and it can be captured properly if soil parameters are well defined, and pipe-soil loading is chosen in such a way that it complies with physical model test results (Bransby et al. 2013).

In this chapter, for loose sand, the vertical spring in the upward direction is formulated based on the equations proposed by Wang et al. (2011). The peak uplift resistance is estimated employing the following equation:

$$\frac{F_{\mathrm{vp}}}{\gamma' H_{\mathrm{t}} D} = 1\left(0.5 - \frac{\pi}{8}\right)\frac{D}{H_{\mathrm{t}}} + f_{\mathrm{p}}\left[\frac{D}{H_{\mathrm{t}}}\left(\frac{H_{\mathrm{t}}}{D} + 0.5\right)^2\right] \tag{4.5}$$

where F_{vp}, H_t, and f_p are the peak uplift resistance, burial depth measured from the ground surface to pipe crown and simplified uplift factor.

The corresponding peak uplift displacement, as well as different threshold values of peak uplift resistance, is calculated using the following equation:

$$v_{\mathrm{p}} = D\left(M \times \frac{H_t}{D} + N\right) \tag{4.6}$$

where *M* and *N* are the coefficients for different threshold level, as discussed in Wang et al. (2011).

Finally, to develop the backbone curve for different uplift displacements, the residual uplift resistance is calculated employing the following equation:

$$\frac{F_{\mathrm{vr}}}{\gamma'(H_{\mathrm{t0}} - v)D} = 1\left(0.5 - \frac{\pi}{8}\right)\frac{D}{(H_{\mathrm{t0}} - v)} + f_{\mathrm{r}}\left[\frac{D}{(H_{\mathrm{t0}} - v)}\left(\frac{(H_{\mathrm{t0}} - v)}{D} + 0.5\right)^2\right] \tag{4.7}$$

where F_{vr}, H_{t0}, and f_r are the residual uplift resistance, initial burial depth measured from the ground surface to pipe crown and residual uplift factor.

Again, for dense sand, vertical spring in the upward direction is formulated employing the equations developed by Roy et al. (2017). The peak uplift resistance is calculated using the following equations:

$$F_{vp} = R\gamma' D^2 \left[\left\{\left(\frac{H}{D} - v_p\right) - \frac{\pi}{8} + \left(\frac{H}{D} - v_p\right)^2 \tan\theta\right\} + F_A \left(\frac{H}{D} - v_p\right)^2\right] \quad (4.8)$$

$$F_A = (\tan\phi - \tan\theta)\left[\frac{1+K_0}{2} - \frac{(1-K_0)\cos 2\theta}{2}\right] \quad (4.9)$$

where R, ϕ and θ are the reduction factor, the peak representative inclination angle of internal friction, and the inclination angle of the slip planes to the vertical, respectively.

The corresponding peak uplift displacement is:

$$v_p = 0.002\frac{H}{D} + 0.025 \quad (4.10)$$

In Eq. (4.8), R varies from 0.95–0.8 for H/D = 1–4 whereas ϕ and θ are constant (55° and 25°, respectively).

Again, the residual uplift resistance and the corresponding displacement are estimated using Eqs. (4.11) and (4.12), respectively.

$$F_{vr} = \gamma' D^2 \left[\left\{\left(\frac{H}{D} - v_r\right) - \frac{\pi}{8} + \left(\frac{H}{D} - v_r\right)^2 \tan\theta\right\} + \left\{F_A \left(\frac{H}{D} - v_r\right)^2\right\}\right] \quad (4.11)$$

$$v_r = 0.0035\frac{H}{D} + 0.1 \quad (4.12)$$

To calculate the residual uplift resistance as per Eq. (4.11), ϕ= 35° and θ = 8° are used.

4.5 Force-displacement behavior of the pipeline buried in loose and dense sand

It is quite difficult to predict the upheaval buckling resistance of the buried pipe since soil cover characteristic depends on many factors like burying techniques, the time interval between burial and commissioning, the rate of the pullout, environmental load and so on. These result in uncertainty and randomness of the cover created (Bai and Bai 2014). Figure 4.3 illustrates a typical force-displacement curve of a buried pipe in loose and dense sand. Using four discrete points, the force-displacement relationship can be described rationally for the dense sand whereas only three discrete point is sufficient for the loose sand. Point 'a' indicates the uplift resistance at the beginning. Since this is at the initial stage, the corresponding displacement is also considered as zero. With an increase in displacement, the uplift resistance of the pipe gradually increases from point 'a' to 'b' in case of dense sand and from point 'a' to 'b'' in case of loose sand mobilizing the peak uplift resistance (F_{vp}) at a certain displacement v_p. This rise of uplift resistance is caused by the activation of the shear stress in the soil. For the dense sand, the upward movement beyond v_p results in post-peak softening and this residual uplift resistance and corresponding displacement are denoted by F_{vr} and v_r respectively, at point 'c'. However, for the loose sand, no such behavior is observed. With further upward movement, the uplift resistance of the pipe falls from point 'c' to point 'd' for the dense sand and from point 'b'' to point 'd' for the loose sand and the pipe eventually reaches zero at the seabed. At this point, the only resistance remains for further upward displacement is the submerged weight of the pipe. This reduction of uplift resistance from point 'b' to 'd' essentially indicates the shear failure of the soil and loss of soil cover (Nielsen et al. 1990). It should be noted that in addition to the soil resistance, the submerged unit weight of the pipeline will also contribute to the uplift resistance.

4.6 FE formulation

Abaqus/Standard (Dassault Systemes 2014) is used to perform FE analyses. Table 4.1 shows the pipe parameters used in this chapter for FE analysis. In Abaqus/Standard, a beam element is a one-dimensional line element in three-dimensional space. The main advantage of beam elements is that they are geometrically simple and have few degrees of freedom. These elements are well suited for cases involving contact, such as the laying of a pipeline in a trench or on the seabed. Hybrid beam element types (B21H, B33H, etc.) are also provided in Abaqus/Standard for use in cases where it is numerically difficult to compute the axial and shear forces in the beam by the usual finite element displacement method. This problem arises most commonly in the geometrically nonlinear analysis when the beam undergoes large rotations and is very rigid in axial and transverse shear deformation, such as a flexing long pipe or cable. The problem in such cases is that slight differences in nodal positions can cause very large forces, which, in turn, cause large motions in other directions. The hybrid elements overcome this difficulty by using a more general formulation in which the axial and transverse shear forces in the elements are included, along with the nodal displacements and rotations, as primary variables. Although this formulation makes these elements more expensive, they generally converge much faster when the beam's rotations are large and, therefore, are more efficient overall in such cases (Dassault Systemes 2014). In this study, a 2-D FE model is adopted since it simplifies the problem while providing a reliable solution for global buckling (Liu et al. 2014). A two-node 2-D linear beam element (B21H) is used for modeling the pipe and soil is modeled as nonlinear springs (SPRING1) in both axial and vertical directions (Fig. 4.2). A mesh sensitivity analysis is performed for an element size ranging from 0.1 m to 0.5 m. Finally, an element size of 0.5 m is used for optimizing speed since no significant difference in result is found. A 3,500-m long pipeline is used in the current study so that effect of end constraints

can be avoided. Therefore, a fixed boundary condition is used for both ends of the pipeline. The lateral displacement of the model is not allowed. In the FE analysis, the load is applied to the pipeline by changing the temperature. But in practice, the combination of a rise in temperature and internal pressure induces the UHB in the pipeline. However, the internal pressure can be converted into an equivalent temperature rise (Hobbs 1984). To simulate the UHB, material nonlinearity and geometric nonlinearity are considered in FE analysis. The modified Riks method (arc length method) is employed to find the temperature-uplift response, as this method considers an algorithm to obtain nonlinear static equilibrium solution and is highly suitable for the unstable problem. Previous authors also successfully utilized the arc length method for UHB analysis of pipe (e.g., Klever et al. 1990; Liu et al. 2013; and Liu et al. 2014). The FE analysis is performed in two steps. First, only gravitational load is applied and the initial temperature value is set to zero. Finally, using the predefined field option available in Abaqus/Standard the temperature is increased to the desired value. Thus, thermal stress along with Poisson effect cause the pipeline to expand longitudinally and eventually resulting in UHB.

4.7 Buckling characteristics

Numerical analysis results for different initial imperfection ratios ($\tilde{v}$) imply that snap bucking and stable buckling are the two basic configurations of UHB which occur for relatively lower and higher initial imperfection ranges, respectively. The former one usually happens when a pipeline is first put into operation and is considered as the classical upheaval buckling by most of the pipeline designers (Finch 1999). For a series of $\tilde{v}$ (0.003 – 0.011), FE analyses are performed for pipe 1 buried in dense sand and H/D = 2, as illustrated in Fig. 4.4. Results for only three $\tilde{v}$ (0.003, 0.006, and 0.011) are presented for better visualization. Fig. 4.4 illustrates that, for the low $\tilde{v}$ range, an apex appears on the curve which indicates the "critical buckling temperature" associated with

snap buckling; pointing out that the pipeline will suffer from unstable deformation and will yield by the time snap through is completed. With the increase in $\tilde{v}$, this apex tends to disappear gradually indicating that pipeline with high $\tilde{v}$ will undergo the most stable and predictable buckling. Also, there exists a $\tilde{v}$ range which lies in between the above mentioned two cases but can be considered as a subcase of the snap buckling since snap is still involved with medium $\tilde{v}$ range. But in that case, the pipe will not yield after the snap. Again, it can be a problem because pipeline may protrude and become vulnerable to the third party (e.g., trawling gear) activities. However, it should be noted that the $\tilde{v}$ range associated with this classification will vary depending on individual pipeline parameters (Taylor and Gan 1986).

With a view to preventing UHB, different authors proposed different threshold temperatures as a design criterion, as shown in Fig. 4.5. However, the safe temperature (T_s) and the critical temperature (T_{cr}) are mentioned as a possible design criterion most frequently in the literature (e.g., Hobbs 1984, Taylor and Gan 1986, Nielson et al. 1990, Palmer et al. 1990, Wang et al. 2011). For instance, according to Palmer et al. (1990), the burial depth should be chosen in such a way that there remains an adequate temperature increase margin between the operating temperature of the pipeline and the critical temperature. The maximum temperature (apex) is termed as the critical temperature (T_{cr}) since snap through occurs at this temperature. The minimum temperature after the apex is commonly known as the safe temperature (T_s). It is accepted generally to use the through of the U-shape curve as the design criterion to avoid vertical buckling and conservative approach to prevent UHB (Hobbs 1984). However, this concept is introduced based on a linear analysis which does not reflect the correct displacement history during uplift (Nielson et al. 1990).Taylor and Gan (1986) proposed a yield based criterion and argued that it is deemed appropriate to use critical temperature rather than a ‘vague’ safe temperature which is not related

to the material property. A few authors (e.g., Palmer et al. 1990) mentioned about the uplift temperature in their studies. It is defined as the temperature at which pipe just starts to move. Again, creep temperature is the temperature corresponding to the peak uplift resistance of the soil and usually used to prevent ratcheting problem (e.g., Nielson et al. 1990). However, most of the previous studies were done on snap buckling, and design temperature is well defined. But this is not the case for stable bucking. For stable buckling, Taylor and Gan (1986) suggested that yield temperature can be a design criterion. But at this large displacement pipeline might get exposed to the trawling gear activity and soil cover fails to serve one of the main purposes. As there is no minimum value, in this case, the temperature at which the slope of the post-buckling curve becomes nearly constant is termed as safe by (Liu et al. 2014).

4.8 Results and discussion: Base case

DNV (2007) recommends designing the buried pipeline to remain in place. To do so, DNV (2007) follows the approach to find an applied temperature from the FE analysis of UHB where the pipeline-soil interaction fails. In this case, the pipeline fails when the mobilization of the soil exceeds the peak uplift displacement v_p. Moreover, DNV (2007) states that UHB is only acceptable if pipeline integrity in the post-buckled condition is ensured. However, no guidance on the pipe integrity check in the post-buckled condition is given, and UHB is therefore considered as an Ultimate Limit State (ULS) failure. Wang et al. (2009) also recommended that keeping a few degrees of temperature margin, and design temperature should be selected in such a way that pipeline only reaches to v_p at the operating temperature. Palmer et al. (1990) also adopted same design approach as mentioned earlier. Pedersen and Jensen (1988) proposed a limit on the amount of allowable uplift to maintain the elastic recovery properties of the soil cover which is imposed to avoid the upward creep of the pipeline. Thus, at first glance, engineers may think to adopt the

full force-displacement curve in the analysis is redundant. To demonstrate the necessity of adopting the soil softening behavior in FE model for loose and dense sand, four cases are considered in this study as illustrated in Fig. 4.6(a) and the results from the FE analysis reveal some interesting aspects. In order to compare the results between case I and case II, FE analyses are first carried out for Pipe 2. Two initial imperfection ratios of 0.005 and 0.011 are considered to capture both snap buckling and stable buckling. It is evident from Figs. 4.6(b) and 4.6(c) that, in snap buckling, the pipeline undergoes an unstable deformation accompanied by a dynamic snap. But in stable buckling, with the increase in temperature, a gradual increase in buckling amplitude is observed until the pipeline eventually yields. Figure 4.6(b) illustrates the temperature rise (ΔT) against buckle amplitude (v_f) for $\tilde{v}$ = 0.005 and H/D = 3 which manifests the significant effect of soil softening not only on critical temperature but also on safe temperature. Critical temperatures (T_{cr}) for case I and case II are ~ 118 °C and ~ 125 °C, respectively. Safe temperatures (T_s) are ~ 62.5 °C and ~ 92 °C for case I and case II, respectively. This apparent decay of the temperature value is attributed to the differential uplift resistance of case I and case II, which occurs after the peak uplift resistance. DNV (2007) recommends using the temperature corresponding to the peak uplift displacement as the design criterion, which is 111 °C for both case I and case II. So, at this point, it seems like not considering the full force-displacement curve is pragmatic. But it is evident from the Fig. 4.6(b) that the safety margin with respect to critical temperature reduces to ~ 50% if the post-peak reduction of uplift soil resistance is considered. Another point is worthy of getting attention here; the remarkable shift of the displacement at which the snap takes place if full force-displacement curve is considered. Inset (ii) of Fig. 4.6(b) shows the force-displacement curve used in this analysis, and it shows that peak mobilization displacement is ~ 9.3 mm, whereas snap occurs at 15 mm and 36.5 mm for case I and case II, respectively, which is shown as the inset (i) of Fig.

4.6(b) on an enlarged scale. If case II is adopted during the FE analysis of UHB, it gives higher uplift resistance and fails to capture the actual global buckling response of the pipeline since at 36.5 mm uplift displacement a significant segment of the soil in the buckled region of the pipeline actually reaches the post-peak softening zone. Again, some of the analysis results demonstrate that the displacement at which snap occurs get even closer to the peak mobilization displacement with the increase in burial depth. For instance, for H/D = 2, the peak mobilization displacement is 8.7 mm and snap occurs at 19.2 mm for case I. The difference between these two displacements is 10.5 mm, which shrinks to only 5.7 mm for H/D = 3, as mentioned earlier. Usually, offshore pipelines are designed for 25 years. A typical loading scenario of a pipeline may include hydrostatic test, initial start-up, various numbers of partial shutdowns of different magnitudes and a number of full shutdowns (Jin et al. 2010). Since soil cover characteristics are dependent on numerous factors and very random in nature, it implies that in reality snap may still take place, putting the integrity of the pipeline in jeopardy. Hence, applying a displacement based criterion without adopting the full force-displacement curve may offer little help. Similarly, Fig. 4.6(c) shows the temperature rise (ΔT) against buckle amplitude (v_f) for $\tilde{v}$ = 0.011 and H/D = 1 and the safe temperatures (T_s) are found to be ~ 19 °C and ~ 30.5 °C for case I and case II, respectively. The safe temperature (T_s) for this case is defined by the intersection of the two tangent lines drawn from the initial slope and the slope of the curve when first tends to become constant to restrict the vertical displacement to a reasonably small value. Otherwise the pipe may protrude eventually.

Figure 4.6(d) shows the temperature rise (ΔT) against buckle amplitude (v_f) for loose sand where $\tilde{v}$ = 0.003 and H/D = 2. Inset of Fig. 4.6(d) shows the force-displacement curve used in this analysis. The difference between T_{cr} for case III and case VI is very small compared to dense sand and T_{cr} are ~ 66.5 °C and ~ 68 °C, respectively. However, since T_s occurs at relatively large

displacement, the difference between T_s is still significant. T_s is ~ 39 °C and ~ 56 °C for case III and case IV, respectively. The temperature corresponding to the peak uplift displacement is found to be ~ 63 °C, for both case III and case IV. At first, it seems like the effect of soil softening on T_{cr} is negligible for loose sand. But Fig. 4.6(d) implies that if the temperature corresponding to the peak uplift displacement is considered, safety margin with respect to critical temperature reduces to ~ 30% for case III compared to case IV. For this particular analysis, the peak mobilization displacement is 13 mm whereas snap occurs at 29 mm and 42 mm for case III and case IV, respectively. Like dense sand, the displacement at which snap occurs get closer to the peak mobilization displacement with the increase in burial depth. Similarly, Fig. 4.6(e) shows the temperature rise (ΔT) against buckle amplitude (v_f) for $\tilde{v}$ = 0.011 and H/D = 1 and the safe temperatures (T_s) are found to be ~ 14.5 °C and ~ 23 °C for case III and case IV, respectively. The force-displacement curve used in this analysis is provided as the inset of Fig. 4.6(e).

4.9 Parametric study

Typically, small to medium diameter pipelines, ranging from 100 to 500 mm, are used in offshore to transport hydrocarbon, and during operation, the temperature rises at around 140°C (Wang et al. 2011). Albeit according to most of the authors the temperature may go up to 100°C (e.g., Hobbs 1984, Taylor and Gan 1986). Therefore, in this parametric study 141.3-mm, 298.5-mm, 406.4-mm and 508-mm diameter pipes are considered with initial imperfection heights of 60 – 940 mm (i.e., initial imperfection ratio = 0.003 – 0.011). Finally, analyses are performed for the temperature rise (ΔT) of 150 °C using the FE model described above. The critical and safe temperatures which lie within 150 °C, are presented in Table 4.2 – 4.9. Since the equations for force–displacement behavior of loose sand proposed by Wang et al. (2011) are only valid for soil cover not exceeding

0.6 m, analyses are performed for H/D = 1 and 2 for 298.5-mm diameter pipe and H/D = 1 only for larger pipes of 406.4-mm and 508-mm diameters.

4.9.1 Effect of burial depth

Sixteen FE analyses are performed for case I and case III, four burial depths (H/D = 1, 2, 3 and 4) and two initial imperfection ratios, $\tilde{v}$ = 0.003 and 0.011. In this study, soil cover (H) is measured from the pipe center to the ground surface and external diameter is considered as the pipe diameter (D). For case I, the temperature rise (ΔT) vs. buckle amplitude (v_f) curves for $\tilde{v}$ = 0.003 and 0.011 are shown in Figs. 4.7(a) and 4.7(b), respectively. Figure 4.7 shows that T_{cr} and T_s increase with burial depth. For example, T_{cr} ~ 80 °C for H/D = 4 is required for snap buckling as compared to T_{cr} ~ 26 °C for H/D = 1 (Fig. 4.7(a)). Similar results—a higher T_{cr} and T_s for higher H/D ratio—are also found for stable buckling, as shown in Fig. 4.7(b). For a given pipe diameter, as the soil cover (H) above the pipe increases with embedment ratio, the uplift resistance of the pipe (F_v) also increases and therefore, a higher T_{cr} is required for UHB of the pipe. Figure 4.7(b) indicates that, with the increase in burial depth, buckling characteristic tends to shift from the stable buckling to the snap buckling. For lower H/D (H/D = 1, 2) no snap is observed but for H/D = 3 snap starts to take place which becomes even clearer for H/D = 4. A similar effect is observed for loose sand.

4.9.2 Effect of pipe diameter

To investigate the effect of pipe diameter, FE analyses are performed for all the four cases (case I, case II, case III and case IV), two soil covers (H = 0.5 m and 1 m), nine initial imperfection ratios ranging from $\tilde{v}$ = 0.003 to 0.011 and for four different pipe sizes. The temperature rise (ΔT) vs. buckle amplitude (v_f) curves for $\tilde{v}$ = 0.003, 0.011 and case III, case IV are presented in Fig. 4.8. All the pipes are at 0.5 m depth. It is evident from Fig. 4.8(a) that T_{cr} and T_s increase with pipe

diameter for the same burial depth. For example, T_{cr} ~ 66.5 °C for pipe 4 is required for snap buckling as compared to only T_{cr} ~ 44 °C for pipe 1 (Fig. 4.8(a)). 4.8(b) shows the effect of post-peak reduction of uplift soil resistance for different pipe diameters. The force-displacement curves used in these analyses are provided in the inset of Fig. 4.8(a) and Fig. 4.8(b). It is apparent that, as the pipe diameter increases, the effect of post-peak reduction of uplift soil resistance becomes more significant. For instance, for pipe 1, T_{cr} is ~ 43.5 °C and ~ 44.3 °C for case III and case IV, respectively, whereas for pipe 4 T_{cr} is ~ 66.5 °C and ~ 70.7 °C for case III and case IV, respectively. In case of stable buckling, T_s also increases with the increase in pipe diameter (Fig. 4.8(c)) and similar results—a higher difference in T_s for larger diameter pipe—are found for snap and stable buckling, as shown in Figs. 4.8(b) and 4.8(d). This is mainly because, for a certain burial depth, a larger diameter pipe has wider soil column on it than a smaller diameter pipe. Hence, the uplift resistance of the pipe also increases with D and therefore, higher T_{cr} and T_s are required for the UHB. Fig. 4.8(d) also reveals that for larger pipe diameter buckling characteristic leans towards the snap buckling.

4.9.3 Effect of soil density

Since in the field soil can exist in loose to dense condition, a parametric study is conducted to study the effect of soil density. Figure 4.9 shows the temperature rise (ΔT) vs. buckle amplitude (v_f) curves for case I, case II, while all the other parameters are kept same as Fig. 4.8. For same pipe diameter, soil cover and initial imperfection ratio T_{cr} and T_s increase with soil density, which becomes clear from Fig. 4.8(a) and Fig. 4.9(a). For example, T_{cr} ~ 66.5 °C for pipe 4 in loose soil condition (Fig. 4.8(a)) whereas T_{cr} increases to ~ 87.3 for dense soil condition (Fig. 4.9(a)). For a higher $\tilde{v}$, soil density should exhibit a similar effect on T_s. Comparison of Figs. 4.8(c) and 4.9(c) reveals that with the increase in soil density buckling characteristics inclines towards snap through.

It becomes more apparent in Fig. 4.9(d) which shows that, for dense soil condition, the pipeline still suffers snap buckling, unlike loose soil condition. Moreover, Figs. 4.8(b) and 4.9(b) illustrate that the difference between T_{cr} is larger for case I and case II (~ 6.2 °C for pipe 4) than the difference between T_{cr} for case III and case IV (~ 4 °C for pipe 4). Same statement is applicable for T_s (Figs. 4.8(d) and 4.9(d)). The corresponding magnified force-displacement curves are provided in the insets of Fig. 4.9.

4.9.4 Effect of the coefficient of earth pressure at rest

For dense sand, the angle of internal friction varies with the displacement of the soil. Hence, the coefficient of earth pressure at rest (K_0) also changes which is an essential parameter for computing soil loads on a buried pipeline. Different authors proposed different K_0 values. For instance, according to Jefferies and Been (2006), $K_0 = 0.5$ should be used while Gramm (1983) proposed $K_0 = 0.7–0.85$ for dense sand. Again, Achmus (1995) suggested $K_0 = 0.9$ for dense sand. Therefore, to capture the influence of K_0 on UHB, six FE analyses are performed for $K_0 = 0.5–0.9$, and the results are shown in Fig. 4.10. As shown, both T_{cr} and T_s increase with an increase in K_0 value. For case I, T_{cr} increases from ~ 97.8 °C to ~ 112 °C when K_0 is increased from 0.5 to 0.9, whereas T_s rises from ~ 45.6 °C to ~ 49.5 °C. Difference in T_{cr} for case I and case II remains almost constant for different K_0. A similar effect is also observed on T_s. When $K_0 = 0.5$, T_{cr} is ~ 97.8 °C and ~104.1 °C for case I and case II, respectively, resulting in ~6.3 °C difference. Again, when $K_0 = 0.9$, T_{cr} is ~ 111.9 °C and ~ 118.4 °C for case I and case II, respectively, resulting in ~6.5 °C deviation.

4.9.5 Effect of the downward stiffness of the soil

Previous studies show that the downward stiffness may be important for UHB (Goplen et al. 2005; Shi et al. 2013). To examine the influence of downward stiffness (K_d) on key temperatures, six FE

analyses are performed for three K_d values, pipe 2 and $\tilde{v}$ = 0.005, and the results are presented in Fig. 4.11. Goplen et al. (2005) shows that when the uplift resistance reaches a certain magnitude, the downward deformation increases, causing the change in failure mode. Below this point, the result is less dependent on the downward stiffness. With a view to finding this threshold uplift resistance, H/D = 1 and 3 are chosen for dense sand. Analyses results show no significant effect of K_d on T_{cr} and T_s which implies that for shallow burial depth downward stiffness maybe less significant parameter. For example, for H/D = 1, T_{cr} rises from ~ 32.9 °C to only ~33 °C (inset of Fig. 4.11(a)) when K_d is increased tenfold (from 5E6 N/m/m to 5E7 N/m/m), whereas for H/D = 3, T_{cr} increases from ~ 117.1 °C to ~ 118.2 °C (inset of Fig. 4.11(b)) for the same increment of K_d. Although the effect is not significant for the cases analyzed, analyses results reconfirm that with the increase in uplift resistance influence of K_d becomes prominent (Goplen et al. 2005).

4.10 Practical implication

Figure 4.12 elucidates the effect of soil softening on the UHB characteristics of the pipeline buried in dense sand (case I and case II). Initial imperfection ratios are shown here together with the allowable temperature rise ΔT_a values for Pipe 2 and H/D = 2. It should be noted that ΔT_a for snap buckling is taken as the critical temperature and for stable buckling is taken as the safe temperature. It is apparent from Fig. 4.12 that the incorporation of the full force-displacement curve in the FE analysis can improve the pipeline design process in two ways. The current design practice not only overpredicts the ΔT_a but also gives lower $\tilde{v}$ at which stable buckling occurs. For instance, for case II stable UHB takes place at initial imperfection height of 214.3 mm ($\tilde{v}$ = 0.005) or higher whereas for case I pipeline experience snap buckling over the whole range of $\tilde{v}$; even at initial imperfection height of 613 mm ($\tilde{v}$ = 0.011). This finding can be very crucial from the design point of view and to date no other studies shed light on this aspect of UHB. Though DNV (2007) suggests using the

temperature corresponding to the peak uplift displacement, a lower temperature than the critical temperature, if UHB takes place, it fails to portray the actual scenario for the designer. Knowing about the actual UHB characteristics, the protective measures can be taken beforehand. Finally, FE analyses are carried out for various pipe diameters, burial depths, and initial imperfection ratios to produce design charts for loose and dense sand and can be used in thermal submarine pipeline buckling which is shown in Fig. 4.13. In most of the cases, a designer can obtain approximate initial imperfection height from the field survey and operating temperature at which hydrocarbon will flow through the pipeline. Based on these two parameters, a suitable burial depth can be chosen easily. For example, for an initial imperfection height of 0.2 m, according to Eq. (4.2) $\tilde{v}$ = 0.005 and 0.004 for pipe 2 and pipe 3, respectively. In this case, required soil covers to prevent UHB are ~ 0.9 m (H/D = 3) and ~ 0.8 m (H/D = 2) for pipe 2 and pipe 3, respectively, if the pipeline is expected to be operated at 120 °C (Fig. 4.13(a)). Required burial depth is lower for larger diameter pipe and vice versa. Hence, a designer can tradeoff burial depth with pipe diameter for a particular project condition, depending on capital and operating expenditures. It should be noted that the allowable temperature rise value is shown in Fig. 4.13 is subjected to the imposition of a safety factor.

4.11 Summary

The numerical simulations presented in this chapter shows that in FE analyses nonlinear soil springs can be employed to model the soil behavior during the pipeline movement. For modeling uplift resistance of the soil, a force-displacement curve with post-peak reduction of uplift soil resistance is recommended. Along the pipeline, axial direction soil resistance can be modeled by elastic-perfectly plastic springs. For a pipeline subjected to axial compression, two major buckling mechanisms are analyzed. The effects of initial imperfection, post-peak reduction of uplift soil

resistance, burial depth, pipe diameter, soil density and coefficient of earth pressure at rest are discussed.

Based on the finite element analyses, the following conclusions can be drawn:

i. Force-displacement curve plays a major role in UHB phenomenon. The critical buckling temperature as well as the safe temperature significantly decreases with an increase in post-peak reduction of uplift soil resistance. The effect of post-peak reduction of uplift soil resistance becomes more prominent for higher burial depth.

ii. It is evident that the critical buckling temperature and the safe temperature increase with the increase in the burial depth, pipe diameter, soil density, coefficient of earth pressure at rest and downward soil stiffness.

iii. Though force-displacement curve proposed by current design guidelines are based on reduced internal friction angle, they over predict the pipeline resistance against UHB. It is noteworthy that for the model with soil softening the pipeline tends to undergo snap through at a higher imperfection height. This finding can be very helpful to choosing pipeline protection measure in practice.

iv. Finally, a simple design chart for use in thermal offshore pipeline buckling is produced. Considering the pipeline initial imperfection and operation conditions, required burial depth can be determined from the chart. However, similar charts can be prepared for other pipeline and soil parameters.

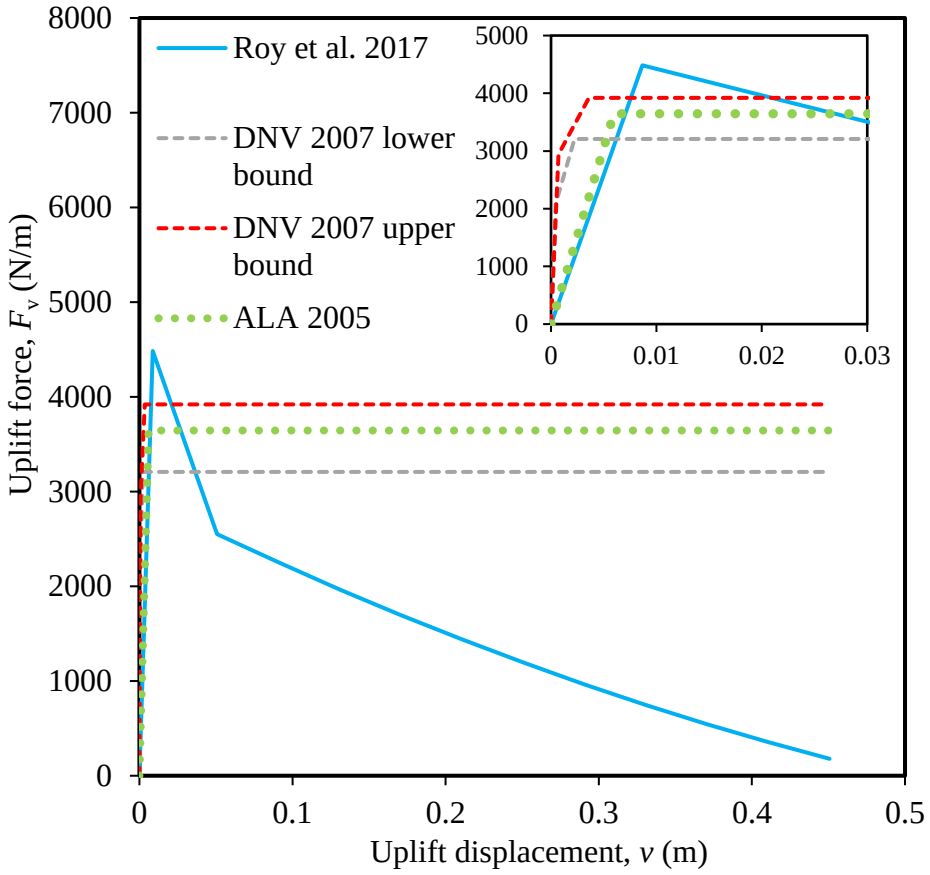
Roy et al. 2017
DNV 2007 lower bound
DNV 2007 upper bound
ALA 2005
Uplift force, F_v (N/m)
Uplift displacement, v (m)
0
1000
2000
3000
4000
5000
6000
7000
8000
0.1
0.2
0.3
0.4
0.5
0.01
0.02
0.03

(a)

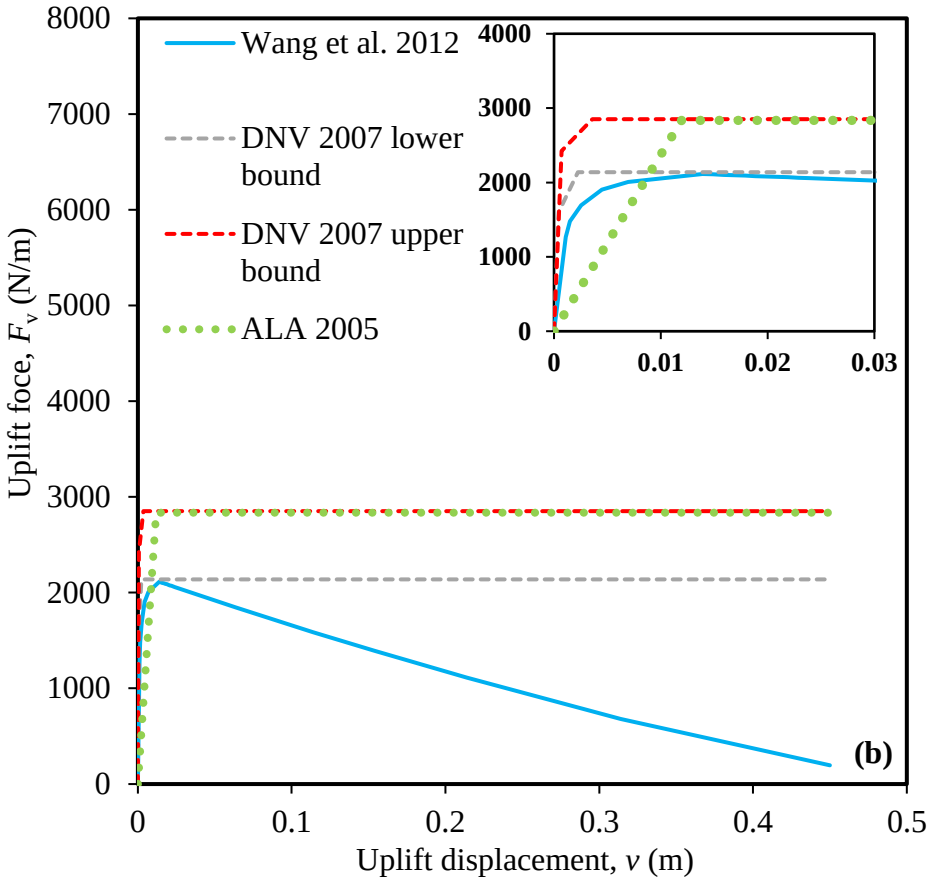

(b)

Figure 4.1: Comparison of uplift force versus uplift displacement curve (a) dense sand; (b) loose sand

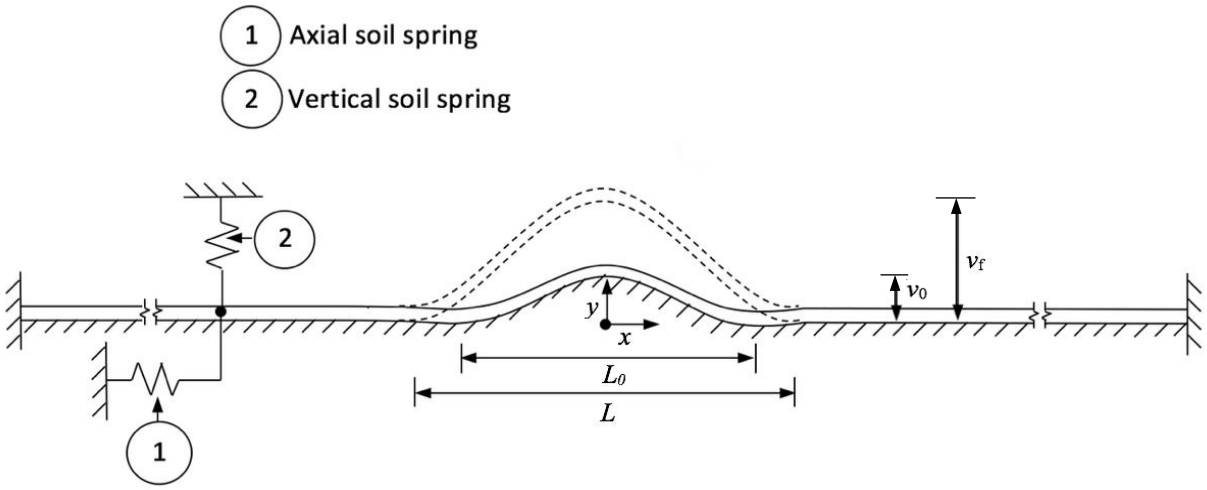

Figure 4.2: Geometry of the pipeline with empathetic configuration

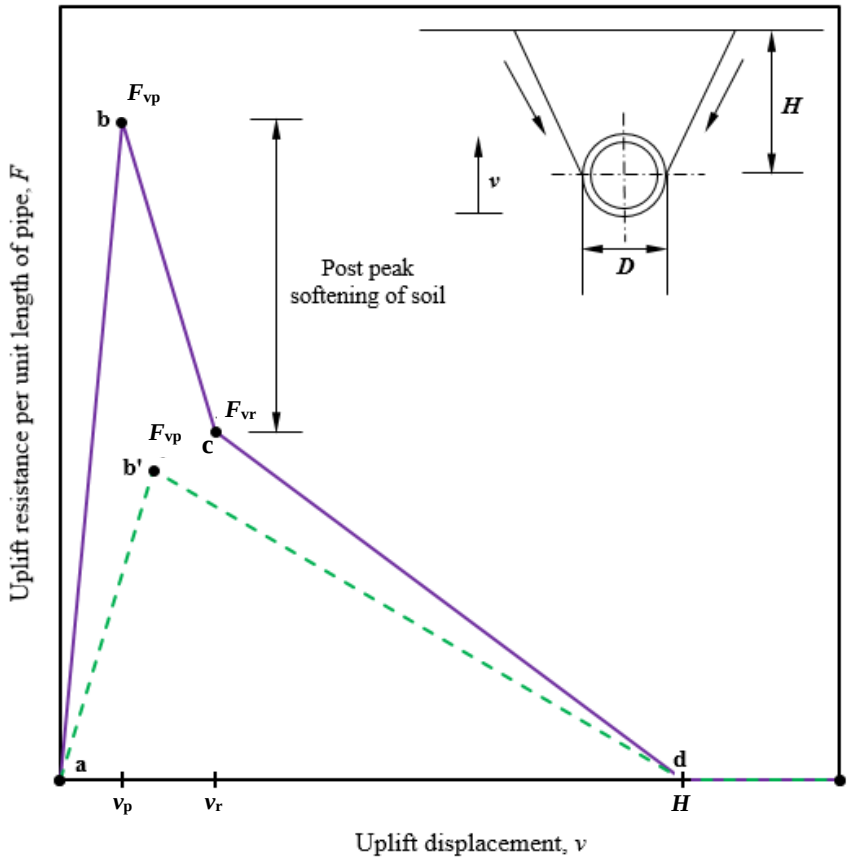

Figure 4.3: Typical force-displacement curves of a pipe buried in dense and loose sand

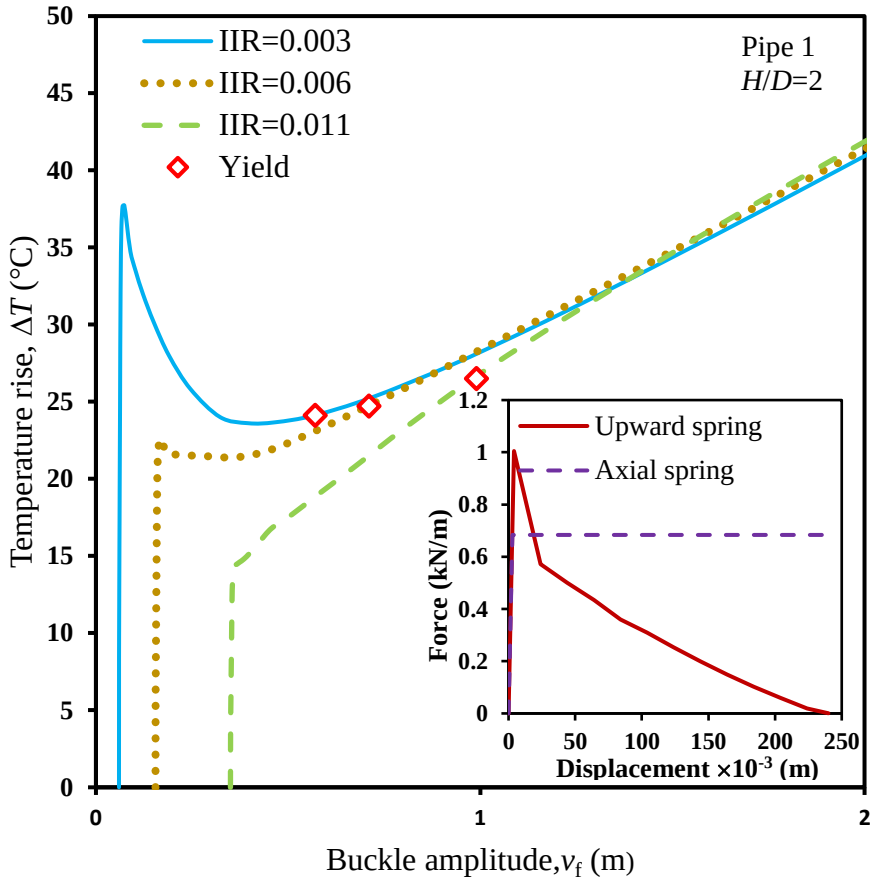

Figure 4.4: Buckling characteristics for different initial imperfection ratios ($\tilde{v}$)

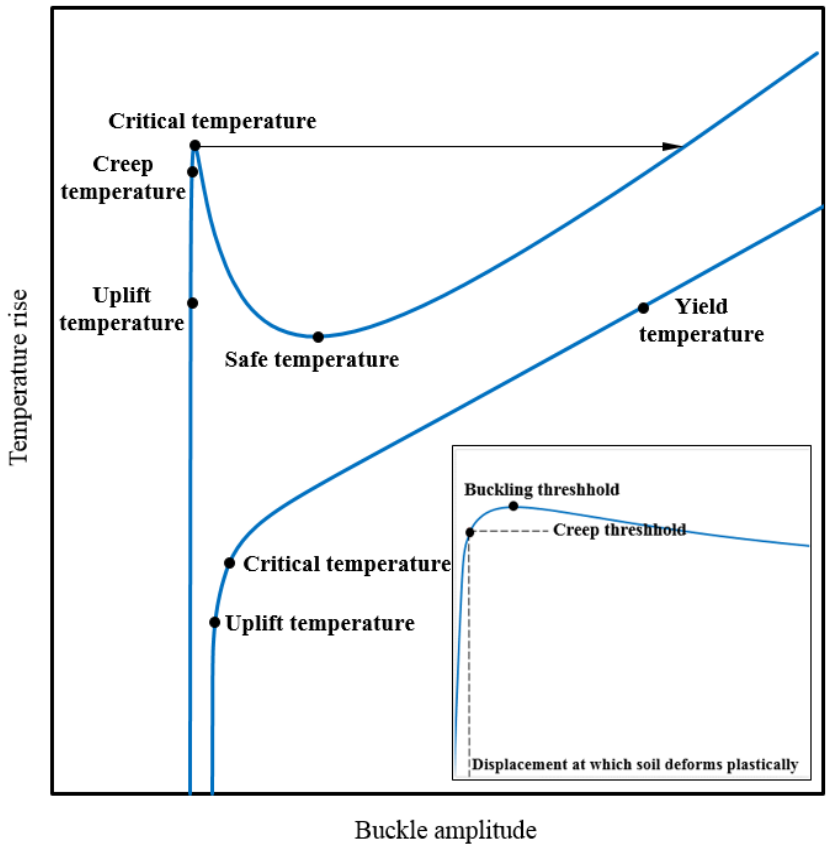

Figure 4.5: Different threshold temperatures mentioned in the literature

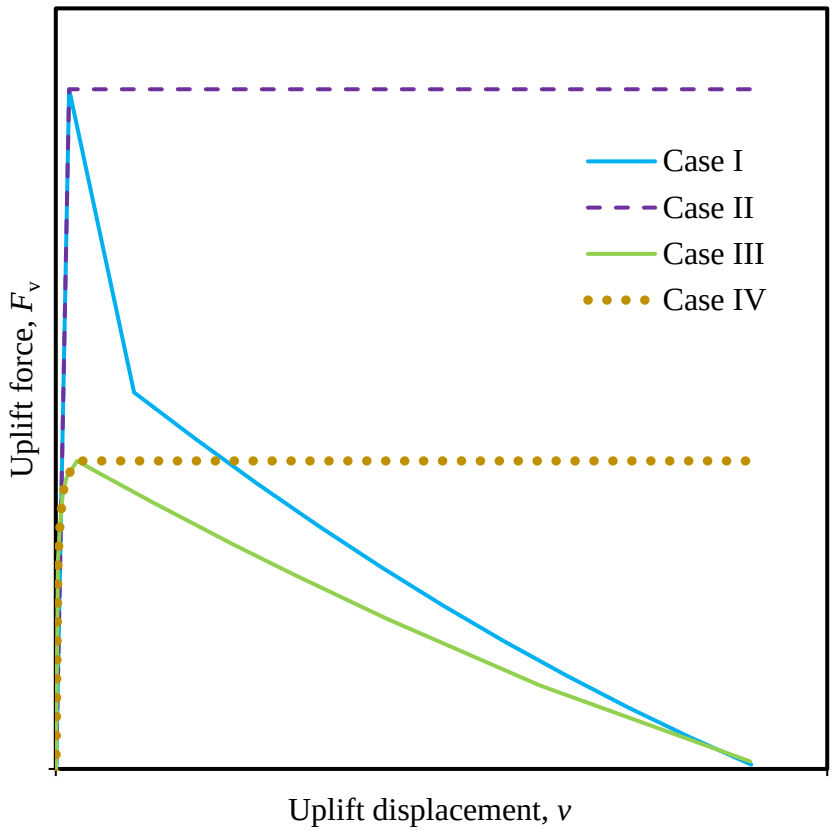
Case I
Case II
Case III
Case IV
Uplift force, F_v
Uplift displacement, v

(a)

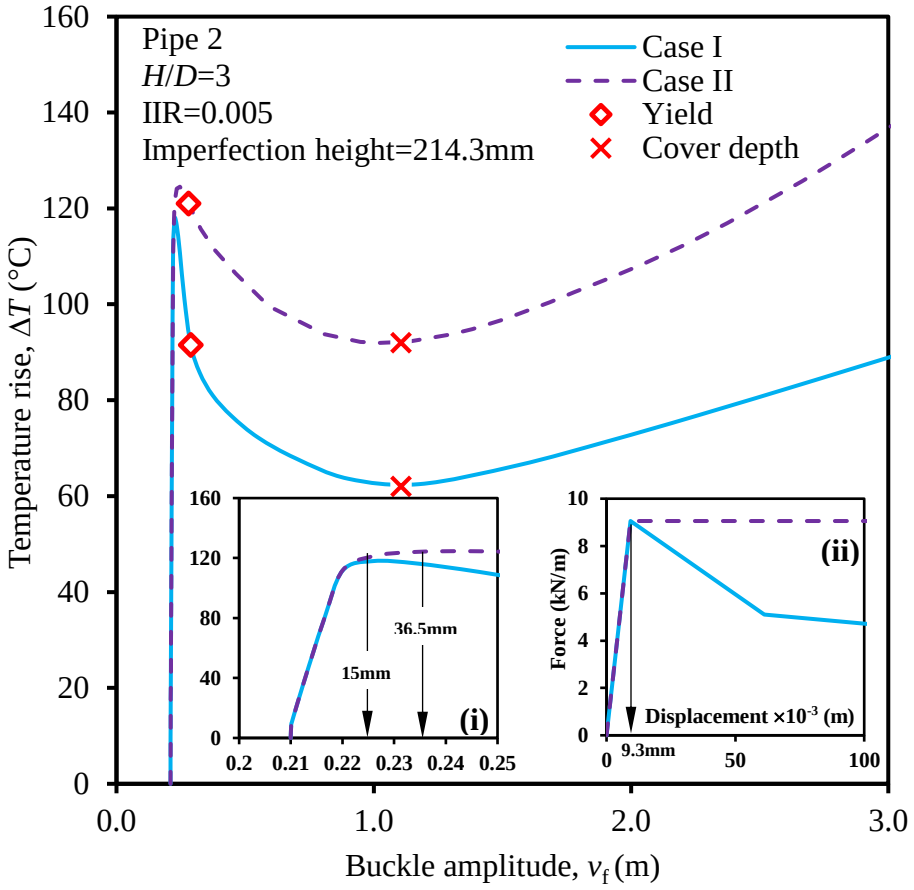
Pipe 2
H/D=3
IIR=0.005
Imperfection height=214.3mm
Case I
Case II
Yield
Cover depth
Temperature rise, ΔT (°C)
Buckle amplitude, v_f (m)
160
140
120
100
80
60
40
20
0
0.0
1.0
2.0
3.0
(i)
36.5mm
15mm
0.2
0.21
0.22
0.23
0.24
0.25
(ii)
Force (kN/m)
Displacement ×10^-3 (m)
9.3mm
10
8
6
4
2
0
50
100

(b)

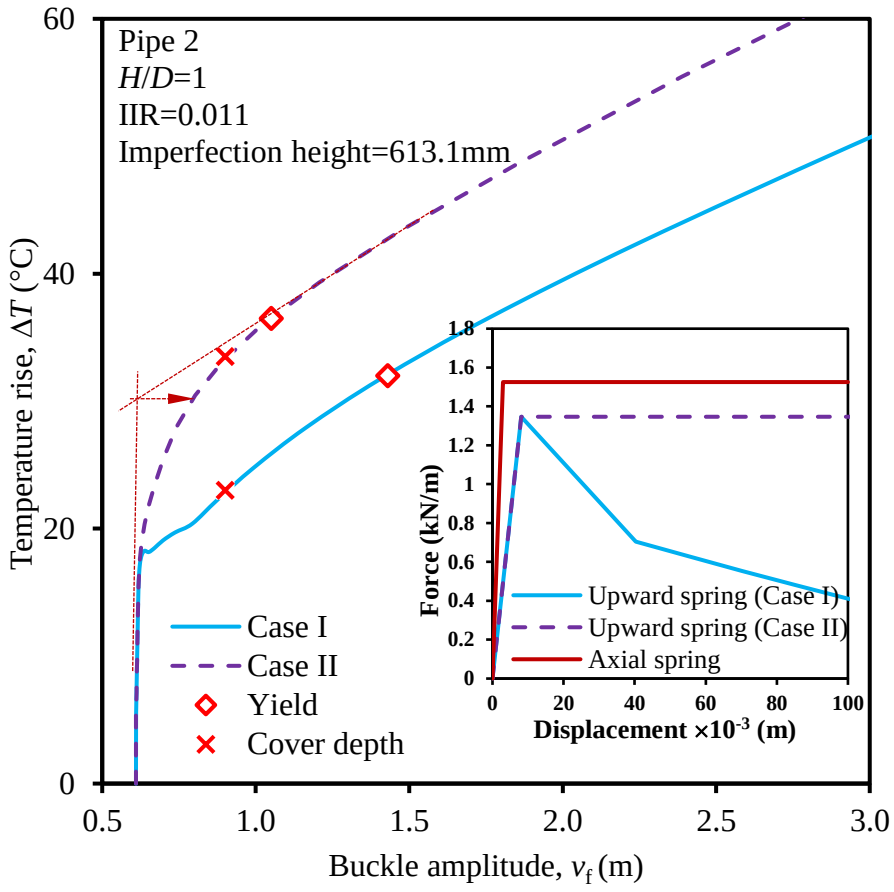
Pipe 2
H/D=1
IIR=0.011
Imperfection height=613.1mm
Temperature rise, ΔT (°C)
Buckle amplitude, v_f (m)
Case I
Case II
Yield
Cover depth
Force (kN/m)
Displacement ×10^-3 (m)
Upward spring (Case I)
Upward spring (Case II)
Axial spring

(c)

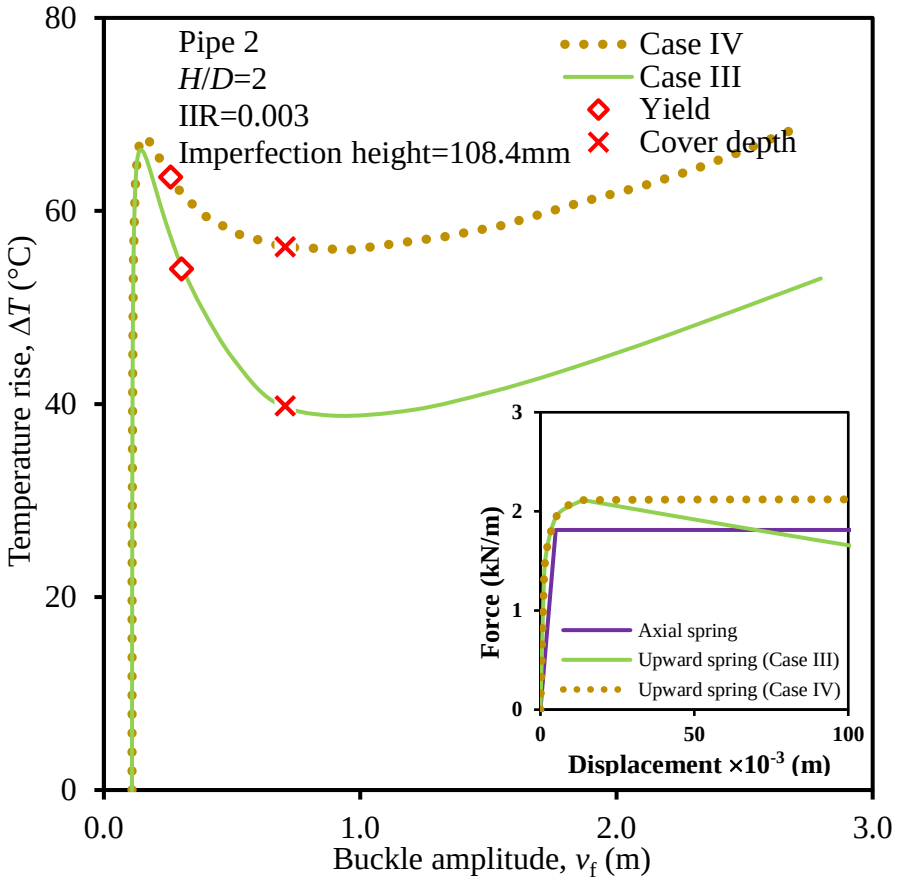
Pipe 2
H/D=2
IIR=0.003
Imperfection height=108.4mm
Case IV
Case III
Yield
Cover depth
Temperature rise, ΔT (°C)
Buckle amplitude, v_f (m)
Force (kN/m)
Displacement ×10^-3 (m)
Axial spring
Upward spring (Case III)
Upward spring (Case IV)

(d)

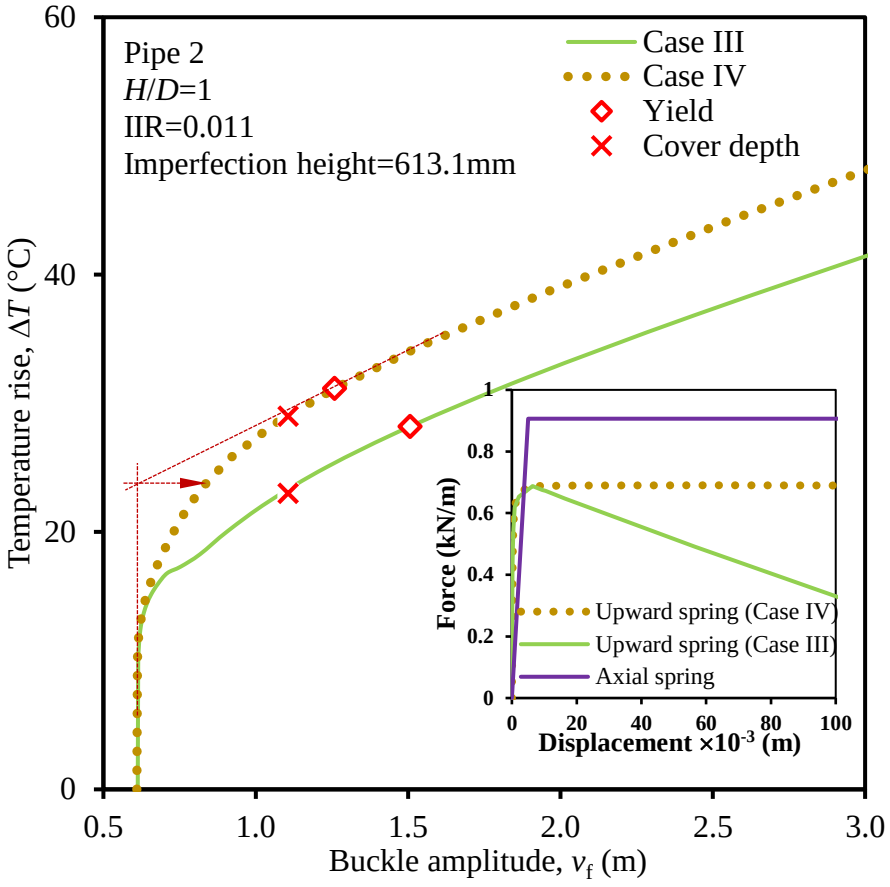

(e)

Figure 4.6: Effect of post-peak reduction of uplift soil resistance on key temperatures (a) Cases considered; (b) dense sand and $\tilde{v}$ = 0.005; (c) dense sand and $\tilde{v}$ = 0.011; (d) loose sand and $\tilde{v}$ = 0.003; (e) loose sand and $\tilde{v}$ = 0.011

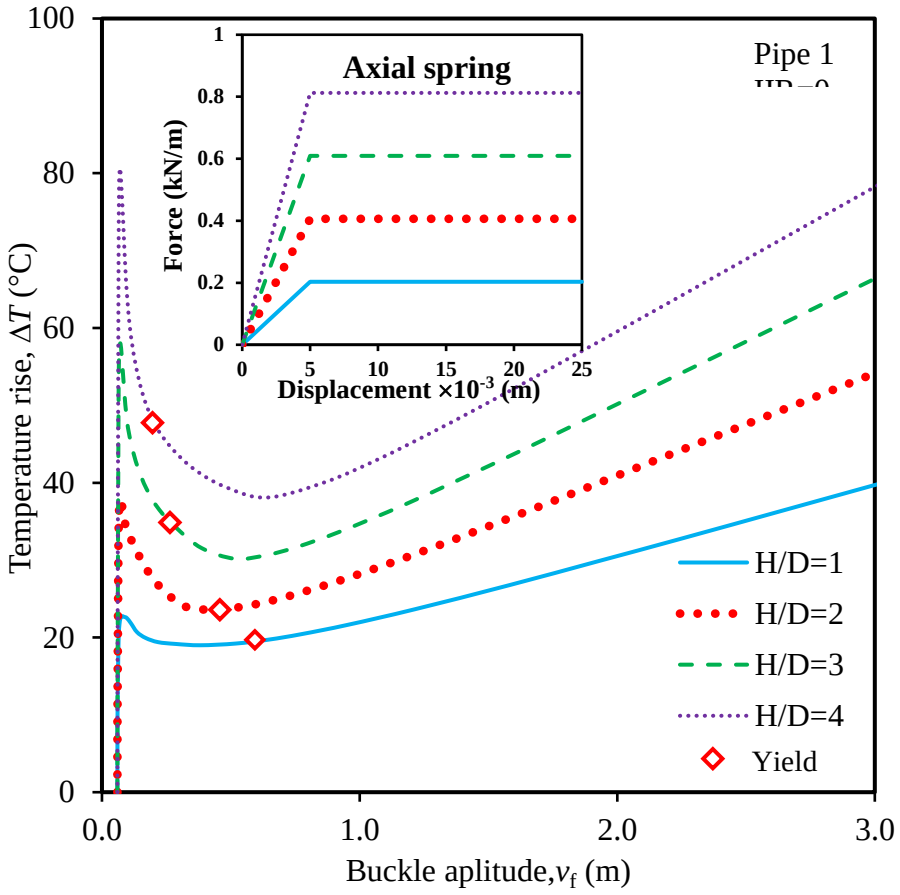
Pipe 1
Axial spring
Force (kN/m)
Displacement ×10-3 (m)
Temperature rise, ΔT (°C)
Buckle aplitude,vf (m)
H/D=1
H/D=2
H/D=3
H/D=4
Yield

(a)

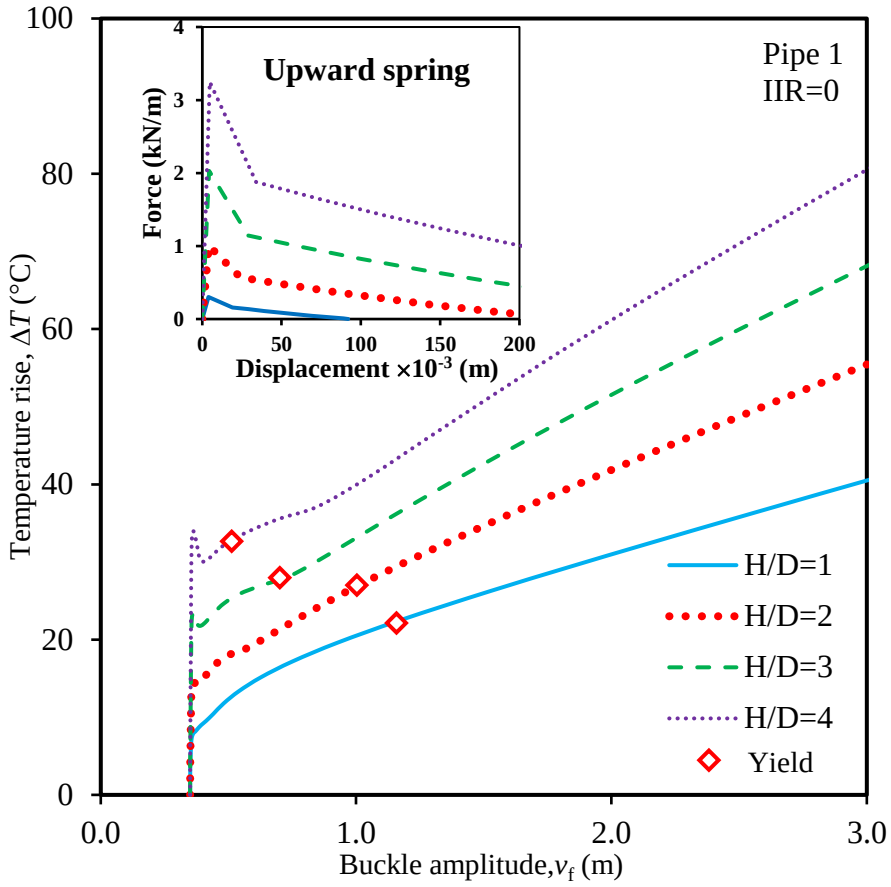

(b)

Figure 4.7: Effect of burial depth (dense sand) (a) for $\tilde{v}$ = 0.003; (b) for $\tilde{v}$ = 0.011

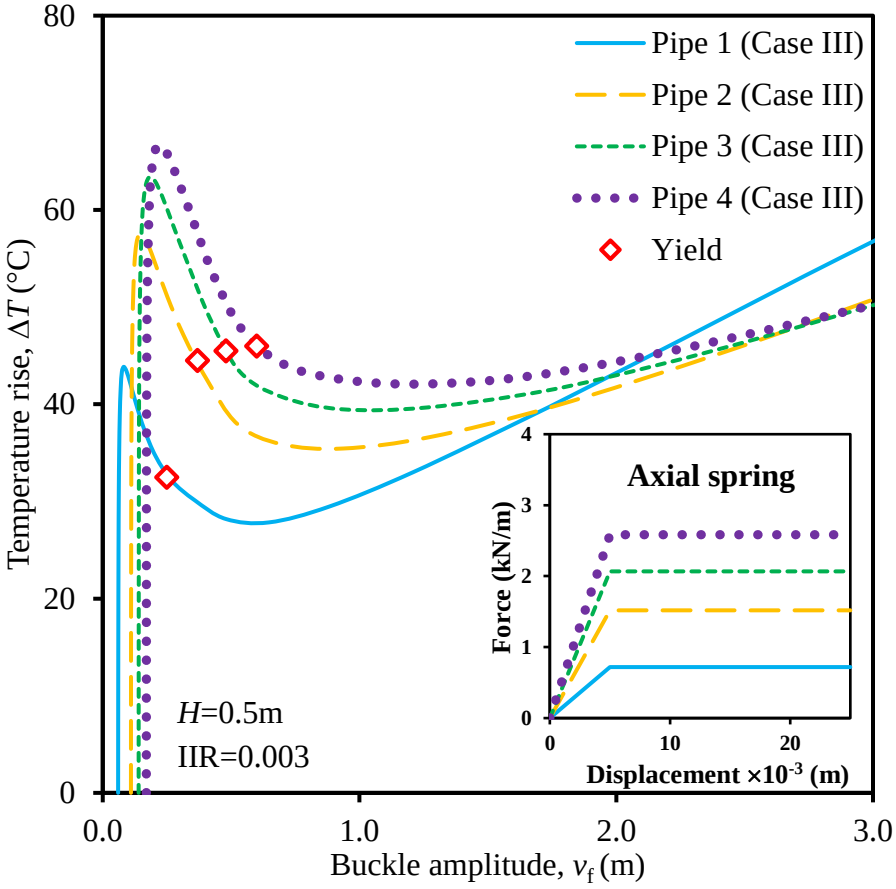
Pipe 1 (Case III)
Pipe 2 (Case III)
Pipe 3 (Case III)
Pipe 4 (Case III)
Yield
Temperature rise, ΔT (°C)
Buckle amplitude, v_f (m)
H=0.5m
IIR=0.003
Axial spring
Force (kN/m)
Displacement ×10^-3 (m)

(a)

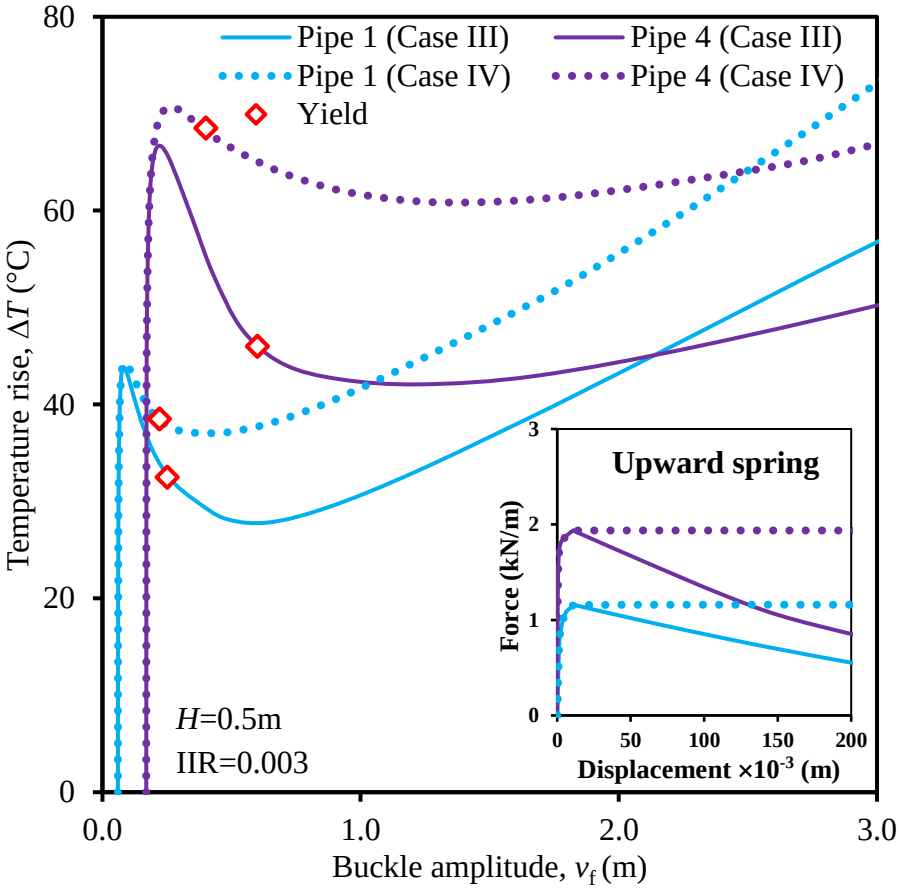
Pipe 1 (Case III)
Pipe 4 (Case III)
Pipe 1 (Case IV)
Pipe 4 (Case IV)
Yield
Temperature rise, ΔT (°C)
Buckle amplitude, v_f (m)
H=0.5m
IIR=0.003
Upward spring
Force (kN/m)
Displacement ×10^-3 (m)

(b)

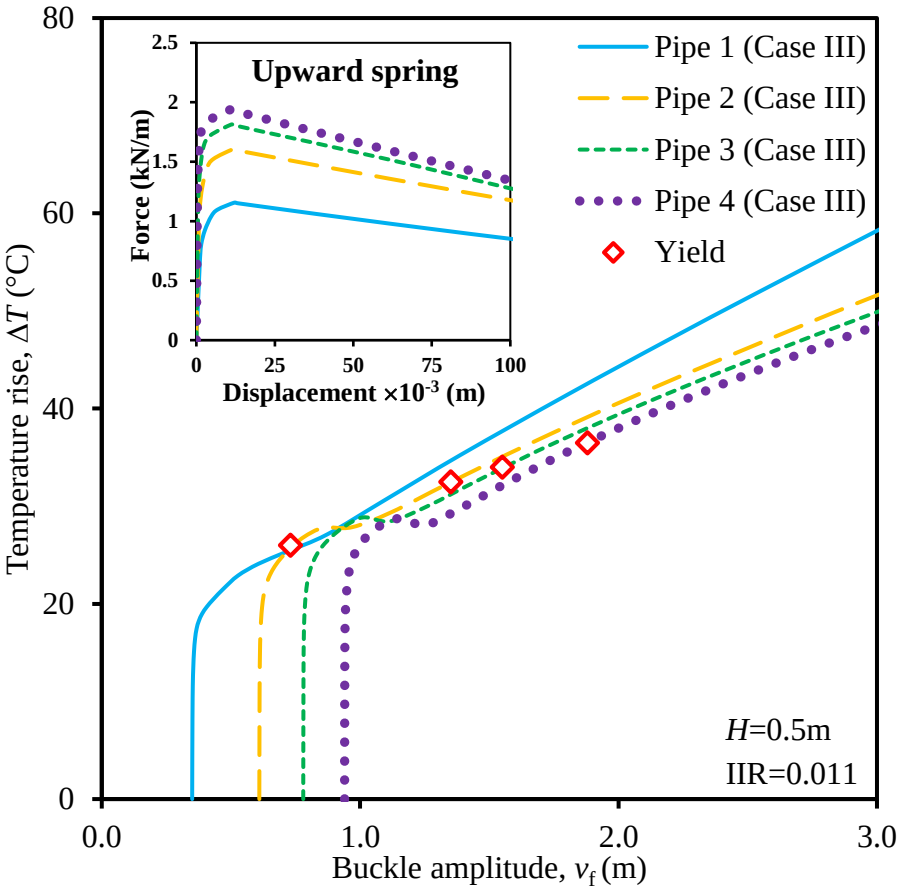
Upward spring
Force (kN/m)
Displacement ×10-3 (m)
Pipe 1 (Case III)
Pipe 2 (Case III)
Pipe 3 (Case III)
Pipe 4 (Case III)
Yield
H=0.5m
IIR=0.011
Temperature rise, ΔT (°C)
Buckle amplitude, vf (m)

(c)

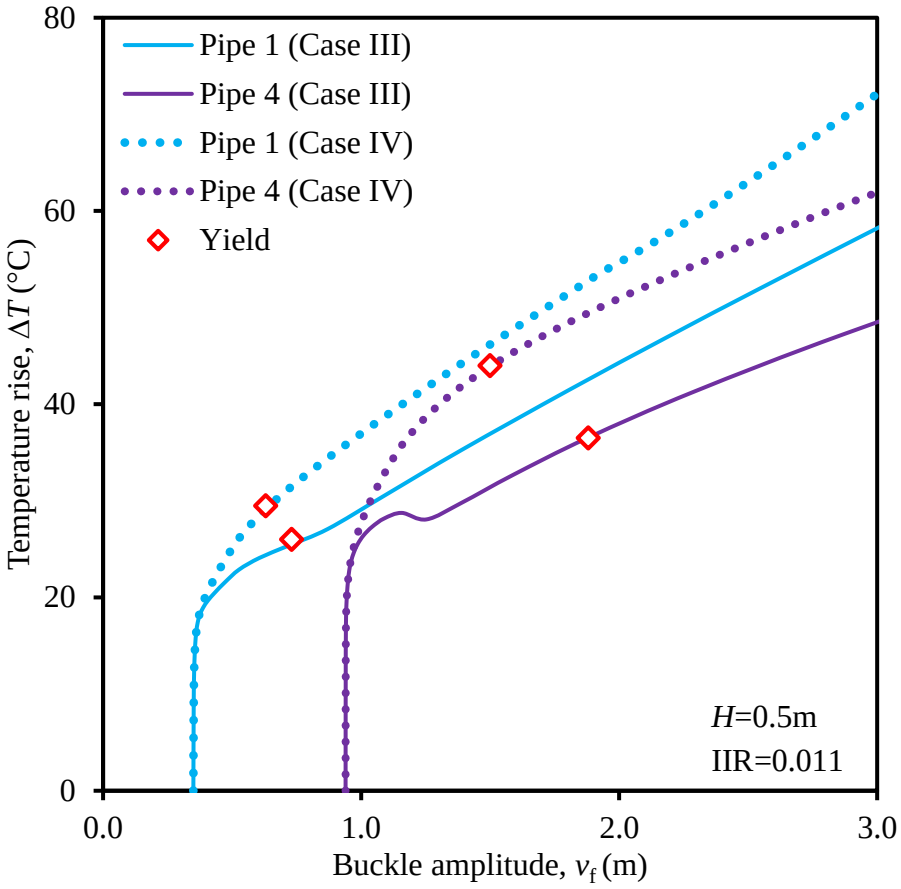

(d)

Figure 4.8: Effect of pipe diameter at 0.5m depth (loose sand) (a) for $\tilde{v}$ = 0.003 and case III; (b) comparison between case III and case IV for $\tilde{v}$ = 0.003; (c) for $\tilde{v}$ = 0.011 and case III; (d) comparison between case III and case IV for $\tilde{v}$ = 0.011

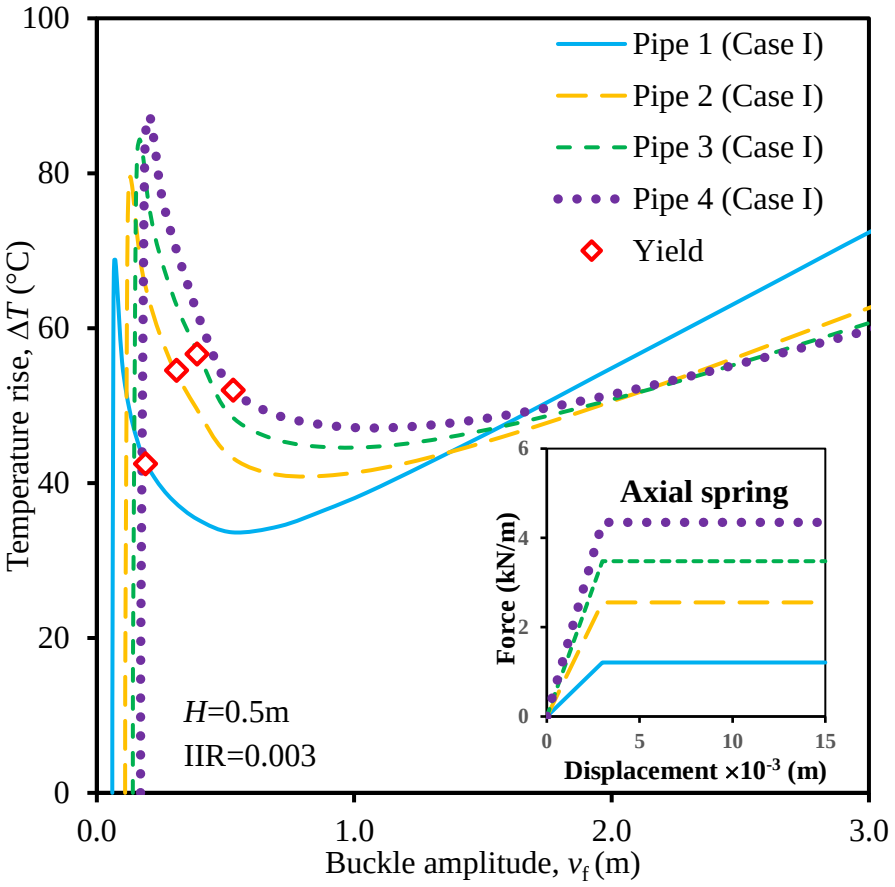
Pipe 1 (Case I)
Pipe 2 (Case I)
Pipe 3 (Case I)
Pipe 4 (Case I)
Yield
Temperature rise, ΔT (°C)
Buckle amplitude, v_f (m)
H=0.5m
IIR=0.003
Axial spring
Force (kN/m)
Displacement ×10^-3 (m)

(a)

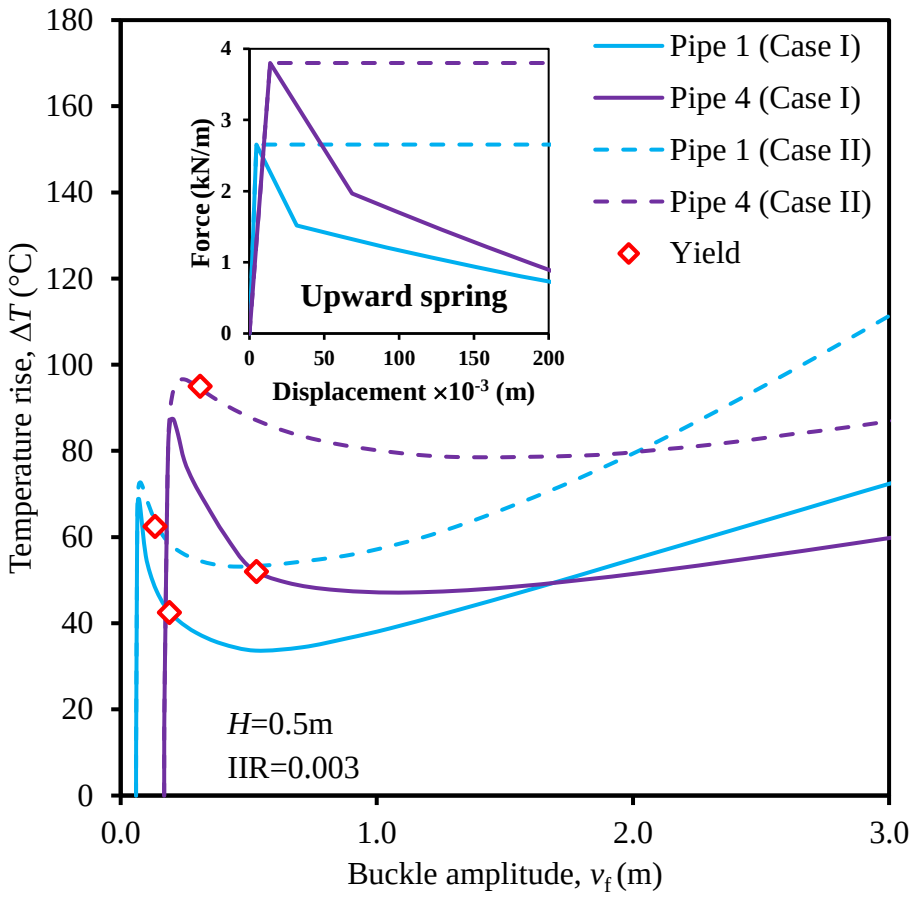
Pipe 1 (Case I)
Pipe 4 (Case I)
Pipe 1 (Case II)
Pipe 4 (Case II)
Yield
Upward spring
Force (kN/m)
Displacement ×10-3 (m)
Temperature rise, ΔT (°C)
Buckle amplitude, vf (m)
H=0.5m
IIR=0.003

(b)

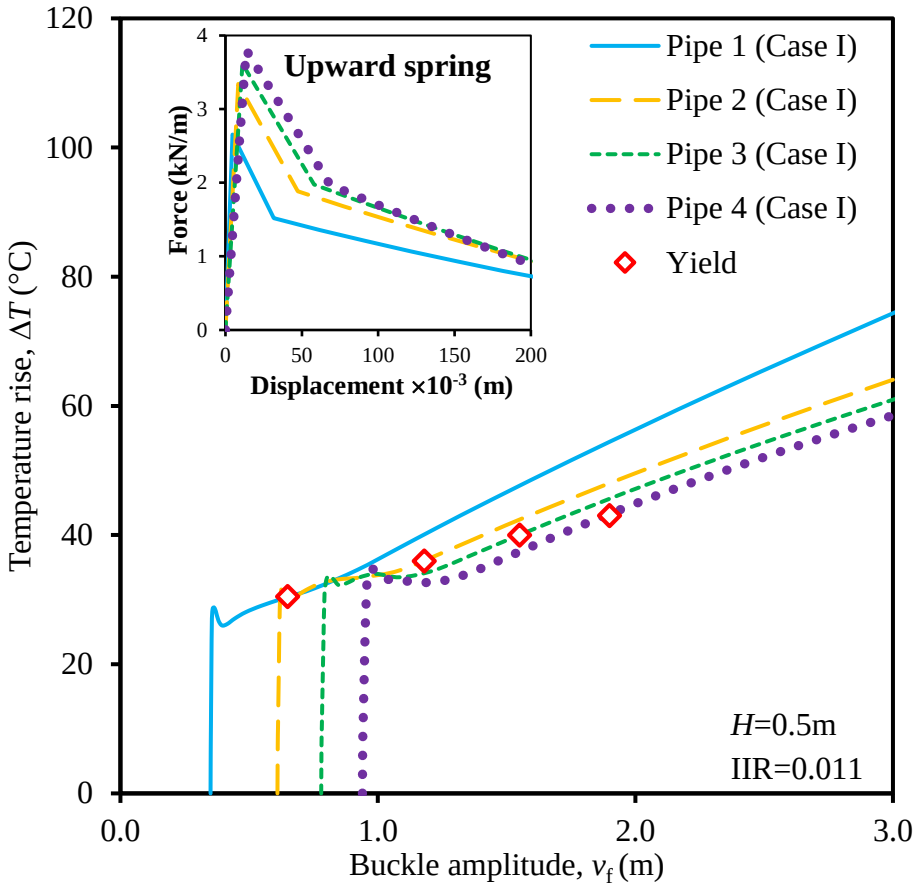
Upward spring
Force (kN/m)
Displacement ×10-3 (m)
Pipe 1 (Case I)
Pipe 2 (Case I)
Pipe 3 (Case I)
Pipe 4 (Case I)
Yield
H=0.5m
IIR=0.011
Temperature rise, ΔT (°C)
Buckle amplitude, vf (m)

(c)

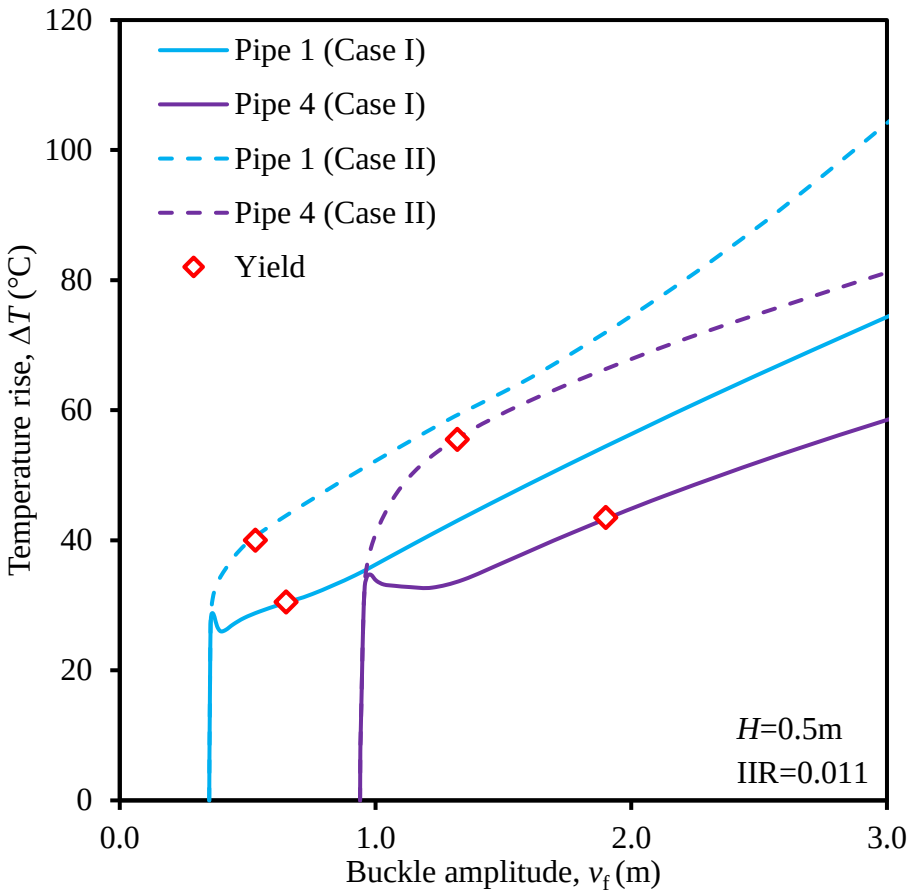

(d)

Figure 4.9: Effect of soil density at 0.5 m depth (a) for $\tilde{v}$ = 0.003 and case I; (b) comparison between case I and case II for $\tilde{v}$ = 0.003; (c) for $\tilde{v}$ = 0.011 and case I; (d) comparison between case I and case II for $\tilde{v}$ = 0.011

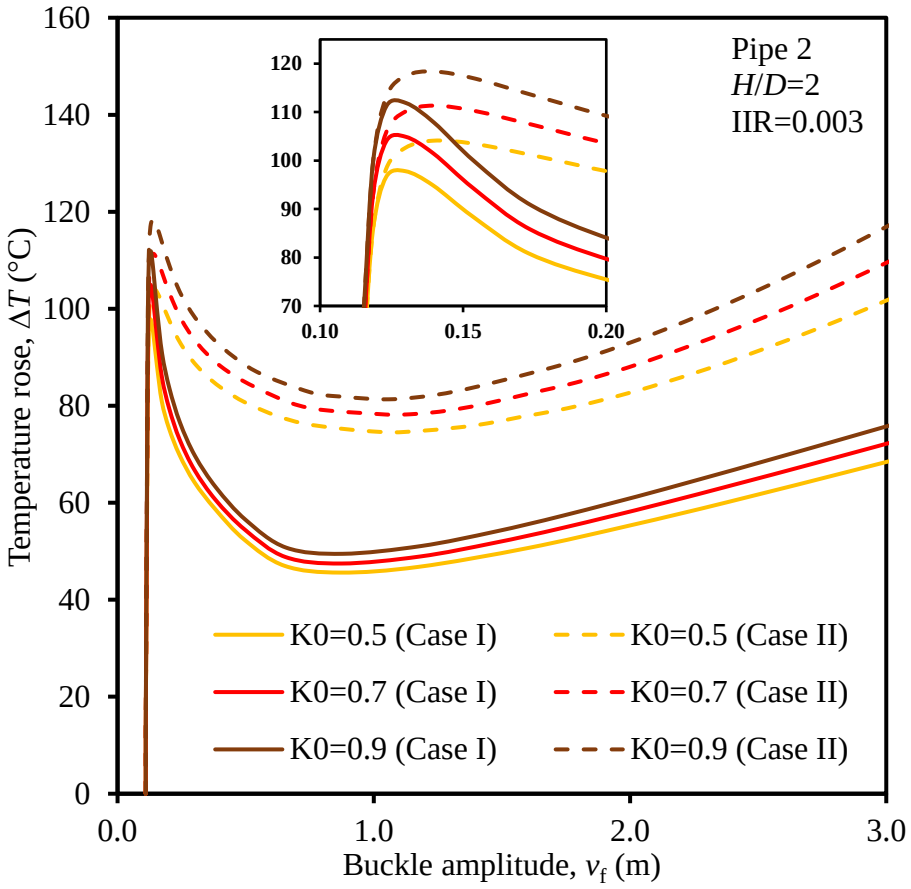

Figure 4.10: Effect of coefficient of earth pressure at rest (dense sand)

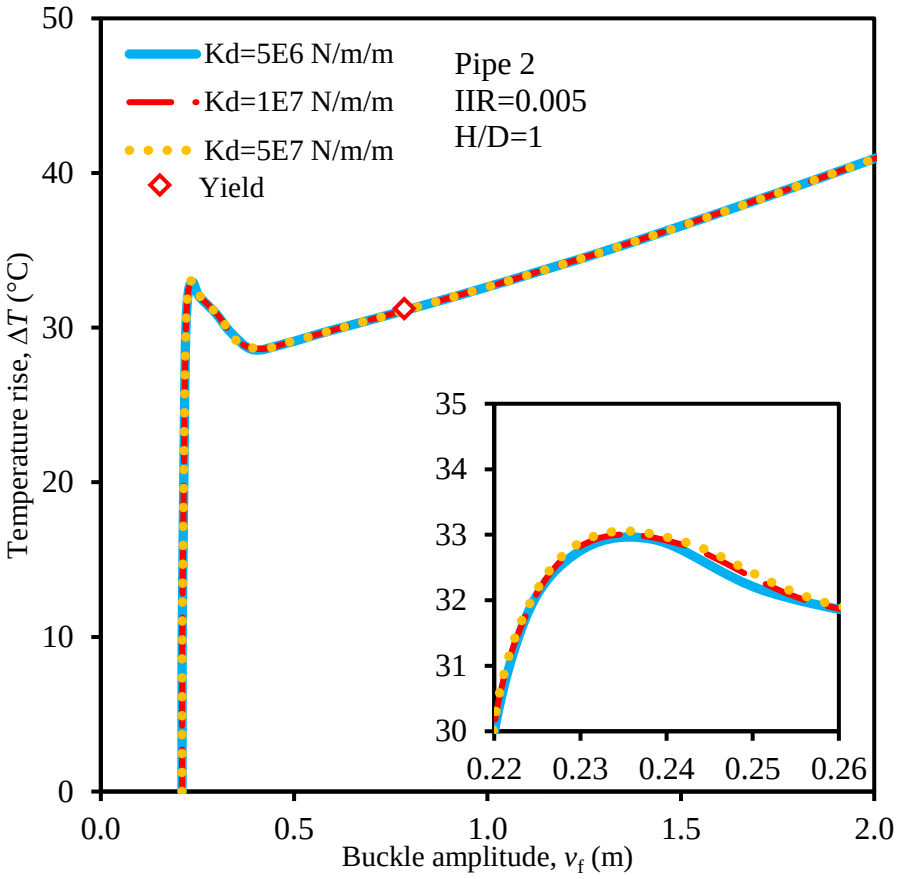
Kd=5E6 N/m/m
Kd=1E7 N/m/m
Kd=5E7 N/m/m
Yield
Pipe 2
IIR=0.005
H/D=1
Temperature rise, ΔT (°C)
Buckle amplitude, v_f (m)
0
10
20
30
40
50
0.0
0.5
1.0
1.5
2.0
30
31
32
33
34
35
0.22
0.23
0.24
0.25
0.26

(a)

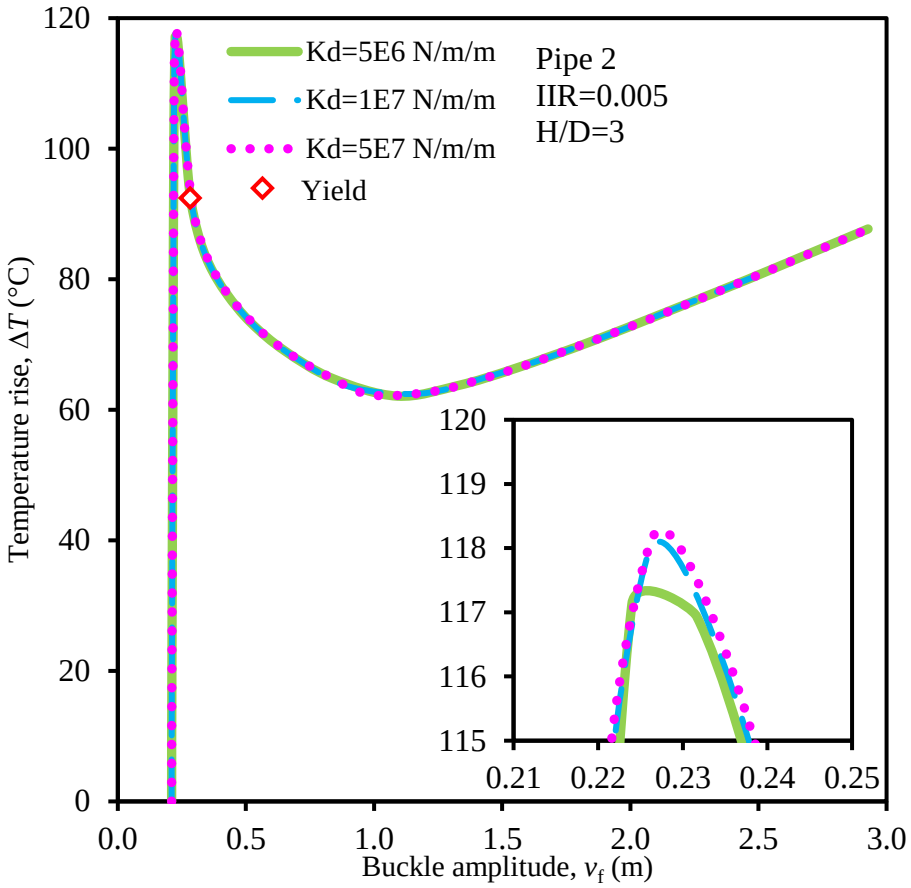

(b)

Figure 4.11: Effect of downward soil stiffness (case I) (a) *H*/*D* = 1; (b) *H*/*D* = 3

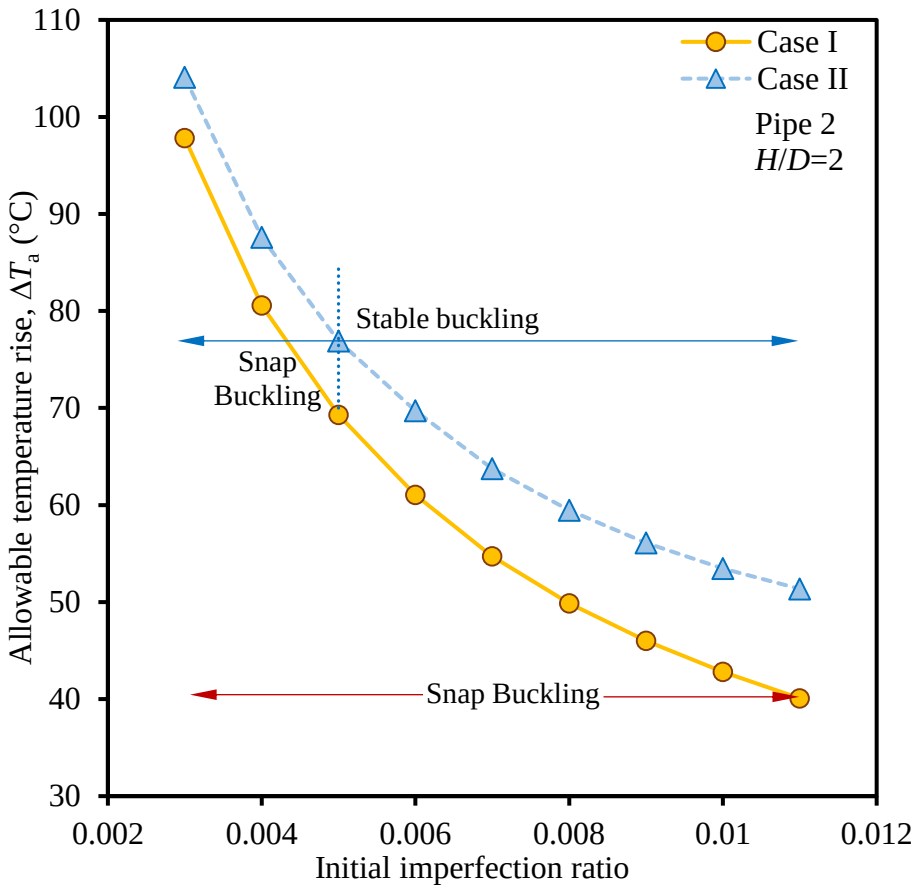

Figure 4.12: Effect of soil softening on buckling characteristics

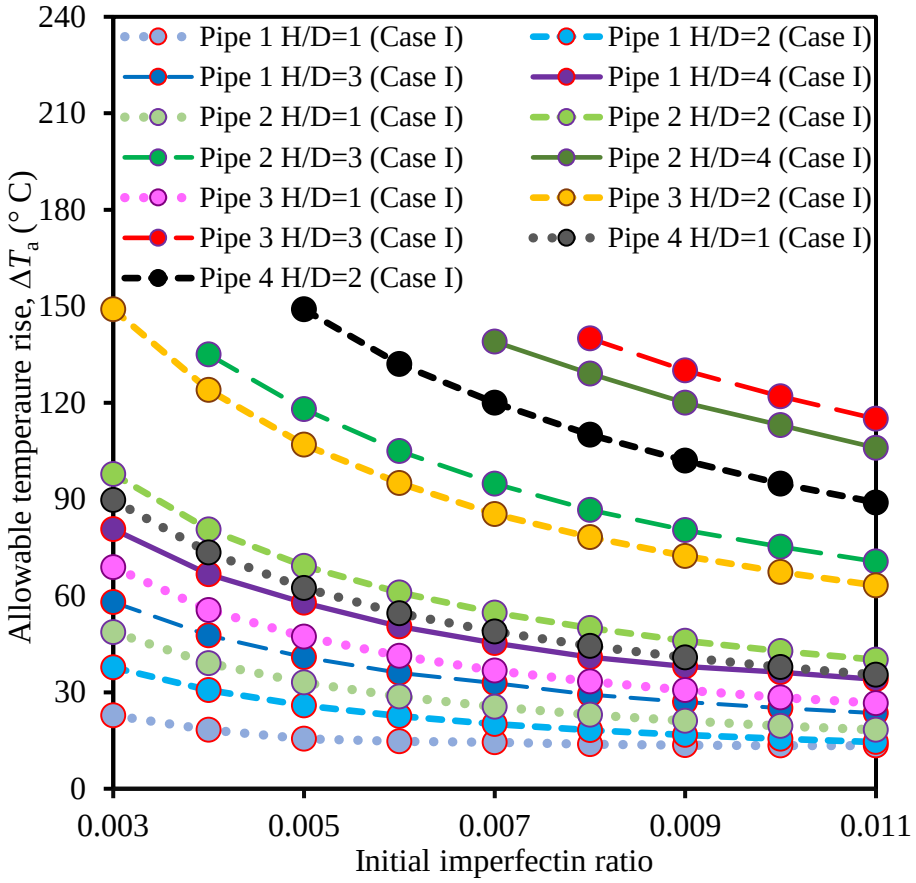
Pipe 1 H/D=1 (Case I)
Pipe 1 H/D=2 (Case I)
Pipe 1 H/D=3 (Case I)
Pipe 1 H/D=4 (Case I)
Pipe 2 H/D=1 (Case I)
Pipe 2 H/D=2 (Case I)
Pipe 2 H/D=3 (Case I)
Pipe 2 H/D=4 (Case I)
Pipe 3 H/D=1 (Case I)
Pipe 3 H/D=2 (Case I)
Pipe 3 H/D=3 (Case I)
Pipe 4 H/D=1 (Case I)
Pipe 4 H/D=2 (Case I)
Allowable temperaure rise, ΔTa (° C)
240
210
180
150
120
90
60
30
0
0.003
0.005
0.007
0.009
0.011
Initial imperfectin ratio

(a)

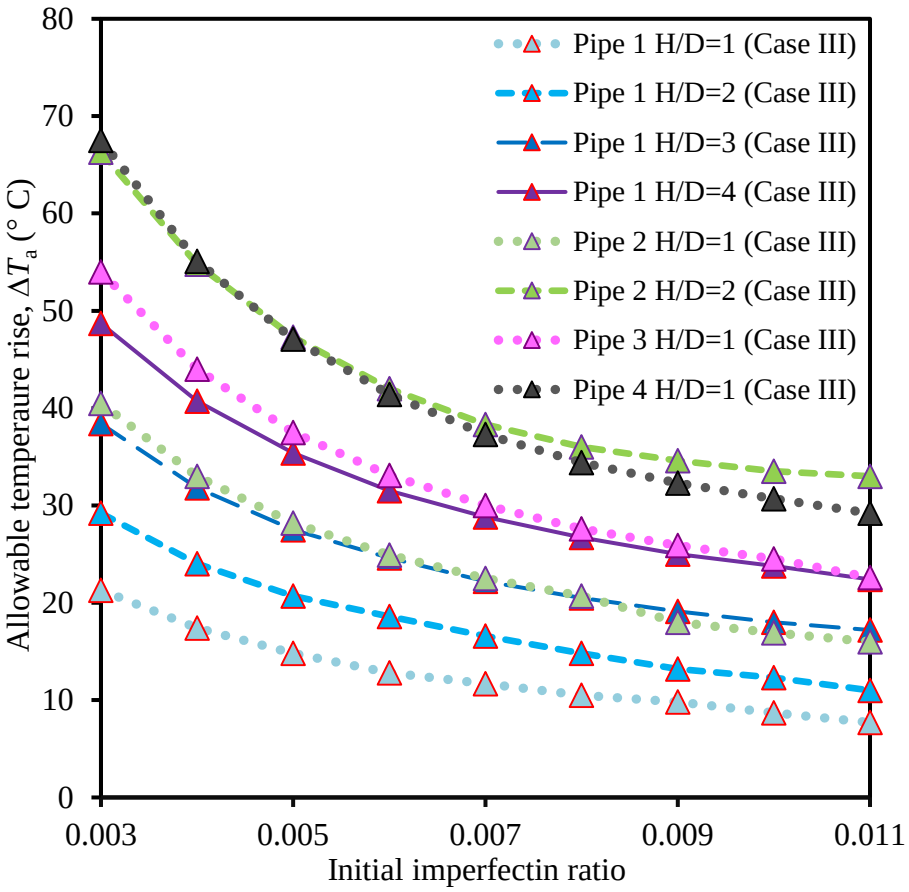

(b)

Figure 4.13: Allowable temperature rise for different initial imperfection ratio, pipe diameter and burial depth (a) dense sand, (b) loose sand

Table 4.1 Parameters used in FE analysis for different pipe sizes

Parameters	**Pipe 1**	**Pipe 2**	**Pipe 3**	**Pipe 4**
External diameter, D (m)	0.1413	0.2985	0.4064	0.508
Wall thickness, t (m)	0.0127			
Cross sectional area, A (m^2)	5.13×10^{-3}	1.14×10^{-2}	1.57×10^{-2}	1.98×10^{-2}
Young's modulus of pipe, E (GPa)	206			
Sectional moment, I (m^4)	1.07×10^{-5}	1.17×10^{-4}	3.05×10^{-4}	6.06×10^{-4}
Submerged self-weight, q (N/m)	320.25	634.17	800.05	919.35
Yield stress of pipe, σ_y (MPa)	448			
Thermal expansion coefficient, α ($°C^{-1}$)	11×10^{-6}			

Table 4.2 Critical and safe temperature for different initial imperfection ratios, burial depths (Case I, Pipe 1)

Initial imperfection ratio ($\tilde{v}$)		**0.003**	**0.004**	**0.005**	**0.006**	**0.007**	**0.008**	**0.009**	**0.010**	**0.011**
***H*/*D* = 1**	T_{cr} (°C)	22.8[a]	18.3[a]	15.5[a]	-	-	-	-	-	-
	T_s (°C)	19	17.5	15.4	14.7[b]	14.4[b]	13.8[b]	13.5[b]	13.4[b]	13.4[b]
***H*/*D* = 2**	T_{cr} (°C)	37.7[a]	30.6[a]	25.9[a]	22.6[a]	20.1[a]	18.2[a]	16.7[a]	15.5[a]	14.5[a]
	T_s (°C)	23.6	23.1	22.3	21.4	18.9	17.7	16.3	15.3	14.2
***H*/*D* = 3**	T_{cr} (°C)	58[a]	47.7[a]	40.9[a]	36[a]	33.1[a]	29.3[a]	27[a]	25.1[a]	23.5[a]
	T_s (°C)	30.2	29.9	29.9	29.1	28.4	26.3	24.6	23	21.8
***H*/*D* = 4**	T_{cr} (°C)	80.7[a]	66.7[a]	57.8[a]	50.4[a]	45.3[a]	40.9[a]	38.9[a]	36.2[a]	34[a]
	T_s (°C)	38.4	38.2	37.9	37.6	36.5	35.4	33.4	31.7	30.1

[a]snap buckling; [b] stable buckling

Table 4.3 Critical and safe temperature for different initial imperfection ratios, burial depths (Case I, Pipe 2)

Initial imperfection ratio ($\tilde{v}$)		**0.003**	**0.004**	**0.005**	**0.006**	**0.007**	**0.008**	**0.009**	**0.010**	**0.011**
***H*/*D* = 1**	T_{cr} (°C)	48.7[a]	39[a]	33[a]	28.7[a]	25.5[a]	23[a]	21.1[a]	19.5[a]	18.3[a]
	T_s (°C)	32.7	31.3	28.7	26.2	24.5	22.7	20.9	19.4	18.2
***H*/*D* = 2**	T_{cr} (°C)	97.8[a]	80.6[a]	69.3[a]	61[a]	54.7[a]	49.9[a]	46[a]	42.8[a]	40.1[a]
	T_s (°C)	45.6	45	44.2	43.4	42.2	41.4	41	39.1	37
***H*/*D* = 3**	T_{cr} (°C)	-	135[a]	118[a]	105[a]	94.8[a]	86.7[a]	80.4[a]	75.2[a]	70.6[a]
	T_s (°C)	-	62.9	62.5	61.7	61.3	60.5	60.2	59.8	59
***H*/*D* = 4**	T_{cr} (°C)	-	-	-	-	139[a]	130[a]	120[a]	113[a]	106[a]
	T_s (°C)	-	-	-	-	82	81.3	81	80.3	79.2

[a]snap buckling;

Table 4.4 Critical and safe temperature for different initial imperfection ratios, burial depths (Case I, Pipe 3)

Initial imperfection ratio ($\tilde{v}$)		**0.003**	**0.004**	**0.005**	**0.006**	**0.007**	**0.008**	**0.009**	**0.010**	**0.011**
***H*/*D* = 1**	T_{cr} (°C)	68.9[a]	55.5[a]	47.3[a]	41.3[a]	36.7[a]	33.3[a]	30.6[a]	28.4[a]	26.6[a]
	T_s (°C)	40.5	39	36.5	34	31.7	30	28.7	27.3	26
***H*/*D* = 2**	T_{cr} (°C)	149[a]	124[a]	107[a]	95[a]	85.4[a]	78.2[a]	72.3[a]	67.4[a]	63.2[a]
	T_s (°C)	60.4	59.9	59	57.8	57.1	55.8	55	54.8	53.9
***H*/*D* = 3**	T_{cr} (°C)	-	-	-	-	-	140[a]	130[a]	122[a]	115[a]
	T_s (°C)	-	-	-	-	-	83.7	82.8	82.7	82.1
***H*/*D* = 4**	T_{cr} (°C)	-	-	-	-	-	-	-	-	-
	T_s (°C)	-	-	-	-	-	-	-	-	-

[a] snap buckling

Table 4.5 Critical and safe temperature for different initial imperfection ratios, burial depths (Case I, Pipe 4)

Initial imperfection ratio ($\tilde{v}$)		**0.003**	**0.004**	**0.005**	**0.006**	**0.007**	**0.008**	**0.009**	**0.010**	**0.011**
***H*/*D* = 1**	T_{cr} (°C)	89.7a	73.4a	62.4a	54.5a	48.9a	44.4a	40.8a	37.8a	35.4a
	T_s (°C)	47.1	45.5	43.1	40.4	38.2	36.3	35	33.4	32.3
***H*/*D* = 2**	T_{cr} (°C)	-	-	149a	132a	120a	110a	102a	94.8a	89a
	T_s (°C)	-	-	72.8	71.4	70.8	69.5	68.5	68.3	67.6
***H*/*D* = 3**	T_{cr} (°C)	-	-	-	-	-	-	-	-	-
	T_s (°C)	-	-	-	-	-	-	-	-	-
***H*/*D* = 4**	T_{cr} (°C)	-	-	-	-	-	-	-	-	-
	T_s (°C)	-	-	-	-	-	-	-	-	-

[a] snap buckling

Table 4.6 Critical and safe temperature for different initial imperfection ratios, burial depths (Case III, Pipe 1)

Initial imperfection ratio ($\tilde{v}$)		**0.003**	**0.004**	**0.005**	**0.006**	**0.007**	**0.008**	**0.009**	**0.010**	**0.011**
***H*/*D* = 1**	T_{cr} (°C)	21.3[a]	17.4[a]	14.8[a]	-	-	-	-	-	-
	T_s (°C)	17.3	16.5	14.6	12.8[b]	11.7[b]	10.5[b]	9.8[b]	8.7[b]	7.7[b]
***H*/*D* = 2**	T_{cr} (°C)	29.2[a]	24[a]	20.7[a]	18.6[a]	-	-	-	-	-
	T_s (°C)	20.5	20.1	19.3	18.4	16.6[b]	14.8[b]	13.2[b]	12.3[b]	11[b]
***H*/*D* = 3**	T_{cr} (°C)	38.4[a]	31.8[a]	27.5[a]	24.6[a]	-	-	-	-	-
	T_s (°C)	25	24.7	24.6	23.9	22.2[b]	20.5[b]	19.1[b]	18[b]	17.2[b]
***H*/*D* = 4**	T_{cr} (°C)	48.7[a]	40.7[a]	35.4[a]	31.5[a]	28.8[a]	-	-	-	-
	T_s (°C)	30.3	30.2	30.2	29.8	28.6	26.7[b]	25.5[b]	23.8[b]	22[b]

[a] snap buckling; [b] stable buckling

Table 4.7 Critical and safe temperature for different initial imperfection ratios, burial depths (Case III, Pipe 2)

Initial imperfection ratio ($\tilde{v}$)		**0.003**	**0.004**	**0.005**	**0.006**	**0.007**	**0.008**	**0.009**	**0.010**	**0.011**
***H*/*D* = 1**	T_{cr} (°C)	40.5[a]	33[a]	28.2[a]	24.9[a]	22.5[a]	20.7[a]	-	-	-
	T_s (°C)	29.6	28.8	26.3	23.9	22	20.4	18[b]	16.9[b]	16[b]
***H*/*D* = 2**	T_{cr} (°C)	66.3[a]	54.8[a]	47.3[a]	42[a]	38.3[a]	36[a]	34.6[a]	33.5[a]	-
	T_s (°C)	38.8	38.3	37.6	36.7	35.5	34.9	34.1	33.1	32b

[a] snap buckling; [b] stable buckling

Table 4.8 Critical and safe temperature for different initial imperfection ratios, burial depths (Case III, Pipe 3)

Initial imperfection ratio ($\tilde{v}$)		**0.003**	**0.004**	**0.005**	**0.006**	**0.007**	**0.008**	**0.009**	**0.010**	**0.011**
***H*/*D* = 1**	T_{cr} (°C)	54[a]	44[a]	37.5[a]	33.1[a]	30[a]	27.6[a]	25.9[a]	24.5[a]	-
	T_s (°C)	36.5	35.5	33.1	30.6	28.5	26.9	25.2	24.1	22.6[b]

[a] snap buckling; [b] stable buckling

Table 4.9 Critical and safe temperature for different initial imperfection ratios, burial depths (Case III, Pipe 4)

Initial imperfection ratio ($\tilde{v}$)		**0.003**	**0.004**	**0.005**	**0.006**	**0.007**	**0.008**	**0.009**	**0.010**	**0.011**
***H*/*D* = 1**	T_{cr} (°C)	67.5[a]	55.1[a]	47.1[a]	41.4[a]	37.3[a]	34.4[a]	32.3[a]	30.7[a]	29.2[a]
	T_s (°C)	42.3	41.2	39	36.5	34.1	32.4	30.7	29.3	28.4

[a] snap buckling

Chapter 5

Conclusions and Future Recommendations

5.1 Conclusions

This study shows that in FE analyses nonlinear soil spring can be employed to simulate the soil behavior during the pipeline movement. For modeling uplift resistance of the soil, a force-displacement curve with post-peak reduction of uplift soil resistance is recommended. Along the pipeline, axial direction soil resistance can be modeled by elastic-perfectly plastic spring. For a pipeline subjected to axial compression, the snap buckling and the stable buckling are analyzed. The effects of initial imperfection, post-peak reduction of uplift soil resistance, burial depth, pipe diameter, soil density, the coefficient of earth pressure at rest and downward soil stiffness are discussed.

Based on the finite element analyses the following conclusions can be drawn:

- The present FE modeling technique can successfully capture both the snap and the stable buckling. The current study confirms that the amplitude of the initial imperfection has a significant effect on the pipeline thermal UHB. The larger the initial imperfection ratio, the smaller the temperature required to induce the UHB of the pipeline. That means the capacity of pipeline against thermal buckling decreases with increase in the amplitude of initial imperfection. Moreover, a pipeline with a small initial imperfection ratio will suffer a dynamic snap after critical temperature. With an increasing initial imperfection ratio, a stable buckling will develop instead of snap buckling.
- With the increase in burial depth, upward soil restraint on pipe increases. Thus, the critical buckling temperature and safe temperature increases with burial depth (H/D) for both snap

and stable buckling. This indicates that to prevent UHB, the depth of backfill cover can be increased in practice.

- Force–displacement curve plays a major role in UHB phenomenon. The critical buckling temperature as well as the safe temperature significantly decreases with an increase in post-peak reduction of uplift soil resistance. The effect of post-peak reduction of uplift soil resistance becomes more prominent for higher burial depth.
- It is evident that the critical buckling temperature and the safe temperature increase with the increase in the pipe diameter at the same burial depth. This is mainly due to the fact that for a certain burial depth a larger diameter pipe has wider soil column on it than a smaller diameter pipe.
- Analyses results suggest that the critical buckling temperature and the safe temperature increase with the increase in soil density and coefficient of earth pressure at rest. For a given burial depth, the uplift resistance of the soil is higher for higher soil density and lager K_0 which eventually increases the capacity of the pipeline against UHB.
- Downward soil stiffness has minimal effect on the critical buckling temperature and the safe temperature for shallowly buried pipeline. However, with is increase in burial depth the influence of downward soil stiffness may become important.
- Current design guidelines overpredict the pipeline resistance against UHB. It is noteworthy that for the model with soil softening, the pipeline tends to undergo snap through at a higher initial imperfection height. This finding can be very helpful for choosing pipeline protection measure in practice.
- Finally, a simple design chart for use in thermal offshore pipeline buckling is produced. Considering the pipeline initial imperfection and operation conditions, the covered depth

can be determined. However, such a chart could be prepared for other pipeline and soil parameters.

5.2 Future recommendations

The UHB of a pipeline is a complex phenomenon. Numerical modeling of UHB can be a viable alternative to the simplified analytical solution. Moreover, DNV 2007 suggests not to employ analytical methods for analyzing the UHB of a pipeline. In this study, 2-D FE analyses are carried out. Current study can be extended to 3-D FE analyses to simulate the field condition better. While adopting the vertical springs in the upward direction, it is assumed that soil resistance is same throughout the pipeline, which might not be the case in reality since burial depth varies because of the initial imperfection of the pipeline. Thus, to obtain more accurate result variable soil resistance should be used throughout the pipeline depending on the burial depth. Though only empathetic model is considered in this study, similar FE modeling technique can be used for other imperfection types. Moreover, local deformation of the cross-section of the beam is ignored. Beam theory does not consider beam cross-section deformations. It is entirely possible that some of these scenarios would include local pipeline failures. Finally, it must be noted that the effects of residual stresses are ignored. Further, the effect of eccentricity of axial friction forces with respect to the centerline of the pipeline is not considered. These features require being considered in the future study.

References

Allan, T, 1968. One-way Buckling of a Compressed Strip under Lateral Loading. Journal of Mechanical Engineering Science, 10(2), pp.175–181.

American Lifelines Alliance (ALA) 2005. Guidelines for the Design of Buried Steel Pipe. <https://www.americanlifelinesalliance.com/pdf/Updat e061305.pdf > (Mar. 13, 2017).

Anand, S., & Aganwal, S. L, 1980. Field and Laboratory Studies for Evaluating Submarine Pipeline Frictional Resistance. In Offshore Technology Conference, Houston.

Arman, R., Roy, K., Hawlader, B., & Dhar, A, 2017. Finite Element Analysis of Upheaval Buckling of Submarine Pipelines with Initial Imperfection. In the 70th Canadian Geotechnical Conference, Ottawa.

Bai, Q., & Bai, Y, 2014. Upheaval Buckling. Chapter 11, Subsea Pipeline Design, Analysis, and Installation. Gulf Professional Publishing.

Bai, Y., & Bai, Q, 2005. Soil and Pipe Interaction. Chapter 5, Subsea Pipelines and Risers. Elsevier.

Baldry, J. A. S, 1973. The Buckling of Axially Loaded Buried Pipelines. Doctoral dissertation, University of Cambridge.

Ballet, J. P. and Hobbs, R. E, 1992. Asymmetric Effects of Prop Imperfections on the Upheaval Buckling of Pipelines. Thin-Walled Structures, 13(5), pp.355–373.

Bransby, M. F., Newson, T. A., Brunning, P., & Davies, M. C. R, 2001. Numerical and Centrifuge Modeling of the Upheaval Resistance of Buried Pipelines. In Proceedings of the OMAE Pipeline Symposium, Rio de Janeiro.

Bransby, M. F., Newson, T. A., Davies, M. C. R., & Brunning, P, 2002. Physical Modelling of the Upheaval Resistance of Buried Offshore Pipelines. In the 4th International Conference on Physical Modelling in Geomechanics, St. John's.

Bransby, M. F., White, D. J., Low, H. E., & Rodriguez, A. B, 2013. The Use of Centrifuge Model Testing to Provide Geotechnical Input Parameters for Pipeline Engineering. In the 32nd International Conference on Ocean, Offshore and Arctic Engineering, ASME.

Cathie D.N., Jaeck C., Ballard J-C and Wintgens J-F, 2005. Pipeline Geotechnics – State-of-the-Art. In Proceedings of the International Symposium on Frontiers in Offshore Geotechnics, Perth.

Cheuk, C. Y., White, D. J. and Bolton, M. D, 2008. Uplift Mechanisms of Pipes Buried in Sand. Journal of Geotechnical and Geoenvironmental Engineering, 134(2), pp.154–163.

Chin, E. L., Craig, W. H. and Cruickshank, M, 2006. Uplift Resistance of Pipelines Buried in Cohesionless Soil. In 6th International Conference on Physical Modelling in Geotechnics, London.

Clukey, E.C., Haustermans, L. and Dyvik, R, 2005. Model Tests to Simulate Riser-soil Interaction Effects in Touchdown Point Region. In International Symposium on Frontiers in Offshore Geotechnics, Perth.

Collberg, L., Mørk, K. J., Levold, E., & Vitali, L. 2005. Hotpipe JIP: Design Guidelines for HP/HT Pipelines. In the 24th International Conference on Offshore Mechanics and Arctic Engineering, Halkidiki.

Croll, J. G. A, 1997. A Simplified Model of Upheaval Thermal Buckling of Subsea Pipelines. Thin-Walled Structures, 29(1–4), pp.59–78.

Dassault Systèmes 2014. Abaqus [Computer Program]. Dassault Systèmes, Inc., Providence, R.I.

Det Norske Veritas (DNV) 2007. Global Buckling of Submarine Pipelines—Structural Design due to High Temperature/High Pressure, DNV-RP-F110, Det Norske Veritas, Baerum, Norway.

Dickin, E. A, 1994. Uplift Resistance of Buried Pipelines in Sand. Soils and Foundations, 34(2), pp.41–48.

Finch, M, 1999. Upheaval Buckling and Floatation of Rigid Pipelines: The Influence of Recent Geotechnical Research on the Current State of the Art. In Offshore Technology conference. Offshore Technology Conference, Houston.

Friedmann, Y, 1986. Some Aspects of the Design of Hot Buried Pipelines. In the Offshore Oil and Gas Line Technology Conference, Richardson.

Friedmann, Y., & Debouvry, B, 1993. Analytical Design Method Helps Prevent Buried Pipe Upheaval. Pipe Line Industry, 75(11), pp.63-68.

Gao, X. F., Liu, R. and Yan, S. W, 2011. Model Test Based Soil Spring Model and Application in Pipeline Thermal Buckling Analysis. China Ocean Engineering, 25(3), pp.507–518.

Goplen, S., Strøm, P., Levold, E., & Mørk, K. J, 2005. Hotpipe JIP: HP/HT Buried Pipelines. In 24th International Conference on Offshore Mechanics and Arctic Engineering, Halkidiki.

Guijt, J, 1990. Upheaval Buckling of Offshore Pipeline: Overview and Introduction. In Proceedings of the 22nd Annual Offshore Technology Conference, Richardson.

Hobbs, R. E, 1981. Pipeline Buckling Caused by Axial Loads. Journal of Constructional Steel Research, 1(2), pp.2–10.

Hobbs, R. E, 1984. In-service Buckling of Heated Pipelines. Journal of Transportation Engineering, ASCE, 110(2), pp.175–189.

Hobbs, R. E. 1981. Pipeline Buckling Caused by Axial Loads, Journal of Constructional Steel Research, 1(2): 2–10.

Hunt, G. W. and Blackmore, A, 1997. Homoclinic and Heteroclinic Solutions of Upheaval Buckling. Philosophical Transactions of the Royal Society of London A: Mathematical, Physical and Engineering Sciences, 355(4), pp.2185–2195.

Jin, J., Audibert, J. M., & Kan, W. C, 2010. Practical Design Process for Flowlines with Lateral Buckling. In Proceedings of the 29th International Conference on Ocean, Offshore and Arctic Engineering, Shanghai.

Jukes, P., Eltaher, A., and Sun, J, 2009. The Latest Developments in the Design and Simulation of Deepwater Subsea Oil and Gas Pipelines Using FEA. In Proceedings of the 3rd International Deep-Ocean Technology Symposium: Deepwater Challenge, International Society of Offshore and Polar Engineers, Cupertino.

Jung, J. K., O'Rourke, T. D., & Argyrou, C, 2016. Multi-directional Force–displacement Response of Underground Pipe in Sand. Canadian Geotechnical Journal, 53(11): pp.1763-1781.

Jung, J.K., O'Rourke, T.D. and Olson, N.A. 2013. Uplift Soil–Pipe Interaction in Granular Soil, Canadian Geotechnical Journal, 50(7): 744–753.

Karampour, H., Albermani, F., Gross, J., 2013. On Lateral and Upheaval Buckling of Subsea Pipelines. Engineering Structures, 52, pp.317–330.

Kerr, A. D, 1972. On the Stability of the Railroad Track in the Vertical Plane, National Technical Information Service, No. NYU-AA-72-35.

Kerr, A. D, 1978. Lateral Buckling of Railroad Tracks due to Constrained Thermal Expansions—A Critical Survey. In Proceedings of the Symposium on Railroad Track Mechanics, New Jersey.

Klever, F. J., Van Helvoirt, L. C., and Sluyterman, A. C, 1990. A Dedicated Finite-element Model for Analyzing Upheaval Bucking Response of Submarine Pipelines. In Proceedings of the 22nd Annual Offshore Technology Conference, Houston.

Lim, Y. M., Kim, M. K., Kim, T. W., & Jang, J. W, 2001. The Behavior Analysis of Buried Pipeline: Considering Longitudinal Permanent Ground Deformation. In Pipelines 2001: Advances in Pipelines Engineering and Construction, San Diego.

Liu, R., & Yan, S, 2012. Brief History of Upheaval Buckling Studies for Subsea Buried Pipeline. Journal of Pipeline Systems Engineering and Practice, 4(3), pp.170–183.

Liu, R., Basu, P., & Xiong, H, 2015. Laboratory Tests and Thermal Buckling Analysis for Pipes Buried in Bohai Soft Clay. Marine Structures, 43, pp.44–60.

Liu, R., Wang, W.G., Yan, S., 2013. Finite Element Analysis on Thermal Upheaval Buckling of Submarine Burial Pipelines with Initial Imperfection. Journal of Central South University, 20(1), pp.236–245.

Liu, R., Xiong, H., Wu, X.L., Yan, S.W., 2014. Numerical Studies on Global Buckling of Subsea Pipelines. Ocean Engineering, 78, pp.62–72.

Lyons, C. G, 1973. Soil Resistance to Lateral Sliding of Marine Pipelines. In Offshore Technology Conference, Houston.

Maltby, T. C. and Calladine, C. R, 1995a. An Investigation into Upheaval Buckling of Buried Pipelines—I. Experimental Apparatus and Some Observations. International Journal of Mechanical Sciences, 37(9), pp.943–963.

Maltby, T. C. and Calladine, C. R, 1995b. An Investigation into Upheaval Buckling of Buried Pipelines—II. Theory and Analysis of Experimental Observations, International Journal of Mechanical Sciences, 37(9), pp.965–983.

Mandolini, A., Minutolo, V., & Ruocco, E, 2001. Coupling of Underground Pipelines and Slowly Moving Landslides by BEM Analysis. Computer Modeling in Engineering and Sciences, 2(1), pp.39-48.

Martinet, A, 1936. A Flembement des Voies Sans Joints sur Ballast et Rails de Grande Longueur. Revue Generale des Chemins de Fer, 55(2), pp. 212-230.

Newson, T. and Deljoui, P, 2006. Finite Element Modeling of Upheaval Buckling of Buried Offshore Pipelines in Clayey Soils. In GeoShanghai International Conference, Shanghai.

Nielsen, N. J. R., Pedersen, P. T., Grundy, A. K., and Lyngberg, B. S, 1990. Design Criteria of Upheaval Creep of Buried Sub-Sea Pipelines. Journal of Offshore Mechanics and Arctic Engineering, 112(4), pp.290–296.

Nielson, N.J.R, Lyngberg, B. and Pedersen, P.T, 1990. Upheaval Buckling Failures of Insulated Pipelines: A Case Story. In the Offshore Technology Conference, Houston.

Palmer, A. C., Ellinas, C. P., Richards, D. M., and Guijt, J, 1990. Design of Submarine Pipelines against Upheaval Buckling. In Proceedings of the 22nd Offshore Technology Conference, Richardson.

Palmer, A.C., White, D.J., Baumgard, A.J., Bolton, M.D., Barefoot, A.J., Finch, M., Powell, T., Faranski, A.S. and Baldry, J.A.S, 2003. Uplift Resistance of Buried Submarine Pipelines:

Comparison between Centrifuge Modelling and Full-Scale Tests. Géotechnique, 53(10), pp.877-883.

Pedersen, P. T., & Jensen, J. J, 1988. Upheaval Creep of Buried Heated Pipelines with Initial Imperfections. Marine Structures, 1(1), pp.11–22.

Raoof, M., and Maschner, E, 1993. Thermal Buckling of Subsea Pipelines. In Proceedings of the International Conference on Offshore Mechanics and Arctic Engineering, New York.

Roy, K., Hawlader, B.C., Kenny, S. and Moore, I, 2017a. Upward Pipe-Soil Interaction for Shallowly Buried Pipelines in Dense Sand. [Under review].

Roy, K., Hawlader, B.C., Kenny, S. and Moore, I, 2017b. Uplift Failure Mechanism of Pipes Buried in Dense Sand. [Under review].

Rubio, N., Roehl, D., & Romanel, C, 2007. A Three-Dimensional Contact Model for Soil-pipe Interaction. Journal of Mechanics of Materials and Structures, 2(8), pp.1501-1513.

Saboya Jr, F. A., Santiago, P. D. A. C., Martins, R. R., Tibana, S., Ramires, R. S., & Araruna Jr, J. T, 2012. Centrifuge Test to Evaluate the Geotechnical Performance of Anchored Buried Pipelines in Sand. Journal of Pipeline Systems Engineering and Practice, 3(3), pp.84–97.

Schaminee, P. E. L., Zorn, N. F., and Schotman, G. J. M, 1990. Soil Response for Pipeline Upheaval Buckling Analyses: Full-scale Laboratory Tests and Modeling. In the 22nd Annual Offshore Technology Conference, Houston.

Schupp, J, 2009. Upheaval Buckling and Flotation of Buried Offshore Pipelines. Doctoral dissertation, University of Oxford.

Selvadurai, A. P. S., & Pang, S, 1988. Non-linear Effects in Soil-pipeline Interaction in the Ground Subsidence Zone. In Proceedings of the 6th International Conference on Numerical Methods in Geomechanics, Innsbruck.

Shaw, P. K. and Bomba, J. G, 1994. Finite-element Analysis of Pipeline Upheaval Buckling. International Conference on Offshore Mechanics and Arctic Engineering (OMAE), New York.

Taylor, N. and Gan, A.B, 1986. Submarine Pipeline Buckling-Imperfection Studies. Thin-Walled Structures, 4(4), pp.295–323.

Taylor, N. and Tran, V, 1993. Prop-imperfection Subsea Pipeline Buckling. Marine Structures, 6(4), pp.325–358.

Taylor, N. and Tran, V, 1996. Experimental and Theoretical Studies in Subsea Pipeline Buckling. Marine Structures, 9(2), pp.211–257.

Taylor, N., Richardson, D., & Gan, A. B, 1985. On Submarine Pipeline Frictional Characteristics in the Presence of Buckling. In Proceedings of the 4th International Offshore Mechanics and Arctic Engineering Symposium.

Trautmann, C, 1983. Behavior of Pipe in Dry Sand under Lateral and Uplift Loading. Doctoral dissertation, Cornell University.

Trautmann, C. H., O'Rourfce, T. D., & Kulhawy, F. H, 1985. Uplift Force–displacement Response of Buried Pipe. Journal of Geotechnical Engineering, 111(9), pp.1061–1076.

Vanden Berghe, J. F., Cathie, D., & Ballard, J. C, 2005. Pipeline Uplift Mechanisms Using Finite Element Analysis. In Proceedings of the 16th International Conference on Soil Mechanics and Foundation Engineering, Brussels.

Villarraga, J. A., Rodríguez, J. F. and Martínez, C, 2004. Buried Pipe Modeling with Initial Imperfections. Journal of Pressure Vessel Technology, 126(2), pp.250–257.

Wang, J., Ahmed, R., Haigh, S. K., Thusyanthan, I., & Mesmar, S, 2010. Uplift Resistance of Buried Pipelines at Low Cover-diameter Ratios. In Offshore Technology Conference, Houston.

Wang, J., Eltaher, A., Jukes, P., Sun, J., and Wang, F. S, 2009. Latest Developments in Upheaval Buckling Analysis for Buried Pipelines. In Proceedings of the International Offshore and Polar Engineering Conference, California.

Wang, J., Haigh, S. K., Forrest, G., & Thusyanthan, N. I, 2011. Mobilization Distance for Upheaval Buckling of Shallowly Buried Pipelines. Journal of Pipeline Systems Engineering and Practice, 3(4), pp.106–114.

Wang, W., Liu, R., Yan, S., Xu, Y., 2011. Vertical Upheaval Buckling of Submarine Buried Heated Pipelines with Initial Imperfection. Transactions of Tianjin University, 17(2), pp.138–145.

Wang, Z., Huachen, Z., Liu, H., & Bu, Y, 2015. Static and Dynamic Analysis on Upheaval Buckling of Unburied Subsea Pipelines. Ocean Engineering, 104, pp.249–256.

Wijewickreme, D., Karimian, H., & Honegger, D, 2009. Response of Buried Steel Pipelines Subjected to Relative Axial Soil Movement. Canadian Geotechnical Journal, 46(7), pp.735–752.

Williams, E.S., 2014. Upheaval Buckling of Offshore Pipelines Buried in Loose and Liquefiable Soils. Doctoral dissertation, University of Oxford.

Yimsiri, S., Soga, K., Yoshizaki, K., Dasari, G. and O'Rourke, T, 2004. Lateral and Upward Soil-Pipeline Interactions in Sand for Deep Embedment Conditions. Journal of Geotechnical and Geoenvironmental Engineering, 130(8), pp.830−842.

Zeng, X.G., Duan, M.L., Che, X.Y, 2014. Critical Upheaval Buckling Forces of Imperfect Pipelines. Applied Ocean Research, 45, pp.33–39.

Zhang, W. and Tuohy, J, 2002. A Three-dimensional Finite Element Analysis of Unburied Flexible Flowline—A Case Study. In the International Conference on Offshore Mechanics and Arctic Engineering, New York.

Zhang, X., & Duan, M, 2015. Prediction of the Upheaval Buckling Critical Force for Imperfect Submarine Pipelines. Ocean Engineering, 109, pp.330–343.

Zhou, Z., & Murray, D. W, 1993. Behavior of Buried Pipelines Subjected to Imposed Deformations. In Proceedings of the International Conference on Offshore Mechanics and Arctic Engineering, American Society of Mechanical Engineers.

Zhou, Z., & Murray, D. W, 1996. Pipeline Beam Models Using Stiffness Property Deformation Relations. Journal of Transportation Engineering, 122(2), pp.164–172.